ISSN 2226-3659
VOL # 91-96 July 2016 to Dec 2017

IEEEP NEW HORIZONS

HEC Approved
Z-Category

IEEEP
Journal of The Institution of
Electrical and Electronics Engineers Pakistan

Editorial

I feel immense pleasure to present before you another issue of "New Horizons" Journal of the Institution of Electrical and Electronics Engineers Pakistan. Continuing the tradition of disseminating latest technical knowledge, IEEEP editorial team has taken all their efforts to bring this issue of IEEEP Journal covering emerging topics and novel aspects of technology, application and service development within the multidisciplinary framework of Electrical, Electronics, Computer, and Telecommunication Engineering.

In this issue total 10 research papers are included covering diverse fields. Considering the important of FACTS devices, dynamic modelling of shunt FACTS devices such as SVC, STATCOM in congested QESCO network is investigated to alleviate the issues of congestion. The comparative study between SVC and STATCOM suggest that STATCOM is more superior to SVC for congestion management. Another paper analysis the transient stability of 11 Bus Systems where the faults are created on different buses and are analyzed by bus admittance matrix. It was observed that in case of any fault or disturbance on the system, the rotor angle of the generator changes and its frequency also changes. In third paper, the issue of congestion is mitigated by improving the transient and dynamic stability of voltage, frequency and rotor angle profiles and damped the power oscillations. Various control methods such as PID controllers, fuzzy logic controllers and multi-agent control systems are discussed for optimization of electrical energy and comfort features in modern near-zero energy buildings in fourth paper. In another paper, the comparative analysis of GSM and internet based home automation systems is made on the basis of cost, security, real time monitoring, status, user friendly environment, GUI. The paper titled as Multi-Agent Surveillance and Threat Evaluation for Indoor Environment discusses a hierarchical multi-agent architecture for implementing semi-automated surveillance in the indoor environment and a three-layered multi-agent architecture of the surveillance system is presented with local intelligence, global intelligence, and human supervision. Another paper focuses on Radius Stability of Inverted Pendulum on a Cart System where a design guideline for inverted pendulum mass to length ratio has been derived. For the vehicle monitoring, the Automatic Number Plate Recognition System Based on Discrete Wavelet Transform and Bounding Box Technique is used as a unique approach in another paper. In next paper for Millimeter Wave Applications using Dielectric Lens the gain of Membrane Antenna is enhanced. In final paper, to enhance the directivity in patch antennas a rectangular micro strip patch antenna operating at 5GHz that has slots cut over the patch are proposed.

I am extremely grateful to the National advisory board of experts and senior faculty members for their valuable input to improve the quality of journal. However, due to unforeseen circumstances, several volumes have combined together as vol. 91 to vol.96. In future, all the efforts will be made to bring out the issue in time.

Finally, On behalf of IEEEP journal management committee, I welcome the submission for the upcoming issue and look forward to receive your valuable feedback.

Chief Editor
Engr. Prof. Dr. Bhawani Shankar Chowdhry

"New Horizons"

Journal of
The Institution of
Electrical and Electronics
Engineers Pakistan

VOL # 91-96 July, 2016 to Dec 2017

4-Lawrence Road, Lahore. Ph:(042) 36305289
Fax: (042) 36360287 Email:ieeep1969@gmail.com
Website:www.ieeep.org.pk

Disseminate Technical Knowledge

Conserve Electricity

CONTENTS

NATIONAL ADVISORY MEMBER/EDITORIAL BOARD FOR IEEEP JOURNAL

Steady State and Dynamic Performance of Shunt FACTS Devices

Zaira Anwar[1], Tahir Nadeem Malik[2], Tahir Abbas[3], Hassan Jaffar Zaidi[4],

[1,2] UET Lahore [3,4] Power Planer International (PVT.) Ltd. 95-H2 Wapda Town Lahore.

Abstract

Nowadays, the electronic switches are the emergent technology to control the power flow and line losses. In this way, the steady state and dynamic stability of the system is enhanced. In this paper, we have considered the Pakistan National Grid network which has a lot of congestion management issues that leads to enrichment in power operational cost. These issues are becoming frequent due to integration of renewable energy resources. This integration is significantly raised because of increased load demand in the system. However, one of the cost-effective solution to this problem is shunt compensation in transmission lines. It increases the transfer capability of transmission lines of existing transmission lines instead of installing new lines in the network. It significantly enhances the stability performances at a lower cost and has shorter installation time. This paper deals with the dynamic modelling of shunt FACTS devices such as SVC, STATCOM in congested QESCO network to alleviate the issues of congestion in this network. This study is carried out in PSS/E tool and comparison of SVC and STATCOM is presented. The simulation results dictated that STATCOM is prior to SVC and it provides the reliable and encouraging results.

Keywords

Flexible AC transmission systems (FACTS), Power system simulation for engineers (PSS/E) tool, Static volt-ampere reactive (VAR) compensator (SVC), Static compensator (STATCOM)

I. Introduction

In an economically stressed situation of the world, the cost-effective methodology of the system is required. In this perspective of electrical industry, uninterruptable power supply to the consumers is today era need so, the new emerging techniques are developed which are economic as well as environment friendly. For this purpose, the renewable energy sources are introduced in the conventional networks such as wind and solar technologies. These emerging technologies played a superficial effect in the existing network according to need. In Pakistan, the environment is very feasible for these wind and solar energy technologies. The coastal area is used for the wind power generation and the desert is used for the solar power generation. Some mega projects of power generation are under construction using these technologies. Due to the old ones conventional networks, the issues of congestion and power stability in transmission lines is raised.

Network or transmission congestion is one of the technical challenges in context of power system operation. The transmission congestion occurs when there is insufficient transmission capacity of simultaneously accommodate all constraints. The constraints such as these limits of lines, voltage profile, thermal limits, overloading and generation integration reduces the quality of transmission.

The literature review revealed that many methodologies are adopted to meet the challenges of congestion. These methods are cost and not cost free means, given in table.

Table1. Remedies of Congestion

Cost-Free Means	•Removal of old lines •Operation of transformer taps / phase shifter •FACTS [1]
Not Cost-Free Means	•Re-dispatching of generation amounts •Prioritization and curtailment of load [2]

Due to the emergent technology of electronic switches, in this paper, we have focused on Flexible AC Transmission System (FACTS) devices for the congestion management and power stability of the network. It controls the power flow by compensating the reactive power and provides the steady state and dynamic stability to the network.

II. Facts Devices

Basic types of FACTS devices

Flexible AC transmission systems are used to control the power system by changing voltage, impedance and angle of the network. The technology developments of FACTS are classified into three generation [3];

1st Generation

The function of the FACTS devices is controlled by the mechanically switched components. The response time of these devices are breaker delay. It gives slow VARs in the system.

2nd Generation

The function of the FACTS devices is controlled by the thyristor-controlled components. The response time of these devices are 2-3 cycles. It provides fast VARs in the system.

3rd Generation

The function of the FACTS devices is controlled by the voltage source convertor (VSC) technology, gate turn off (GTO), insulator gate bipolar transistor (IGBT) and

integrated gate commutated transistor (IGCT) switches. The response time of these devices are 1-2 cycles. It delivers fast VARs in the system.

Applications of FACTS Controllers

These controllers are mainly classified into four categories of series, shunt, series-series and series-shunt controllers. It has numerous applications in the power system e.g.;

- Control of power flow
- Increase the loading capacity of lines
- Improve transient stability limit during contingencies
- Reduce the short-circuit power level
- Compensate the reactive power
- Improve dynamic voltage stability
- Control loop power flow
- Damp power oscillation
- Mitigate voltage unbalance due to single-phase loads

III. Basic Mechanism Of Shunt Facts Controller

Shunt FACTS controllers (SVC and STATCOM) are used to control the reactive power according to requirement of the network. It is installed in parallel midway of transmission lines to provide the VAR compensation which is being used as voltage regulation to prevent from voltage instability. In this way, loading capacity, the dynamic and transient stability and power flow of the network is increased.

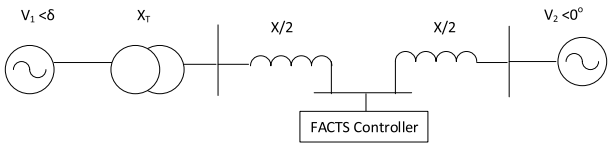

Fig 1. Power system model with shunt FACTS controller [4]

1. Reactive compensation by Shunt FACTS Controller

In usual approximation, power transfer equation becomes;

$$P(t) = \frac{V_1 V_2}{X_d + X_T + X_E} \sin\delta\,(t) \qquad (1)$$

where P is power, V_1 is sending end voltages, V_2 is receiving end voltages, X_d is generator reactance, X_T is transformer reactance, X_E is effective line reactance, δ is angle between sending and receiving ends.

When the controller is added in the line then the effective line reactance is modulated by susceptance of controller and effective voltage (V_E) becomes;

$$V_E = \frac{V_1}{\frac{X}{2}(B_L(t) - B_C) + 1} \qquad (2)$$

$$V_E = \frac{X}{2} + \frac{\frac{X}{2}}{\frac{X}{2}(B_L(t) - B_C) + 1} \qquad (3)$$

Where $B_L(t)$ is susceptance of inductor while B_C is susceptance of capacitor in the controller.
Thus, the power transfer equation becomes;

$$P(t) = \frac{V_1 V_2}{X_{ds}\,(1-K)} \sin\delta\,(t) \qquad (4)$$

where X_{ds} is the total reactance and the coefficient k defined the degree of compensation.

$$K = \frac{B(t)}{X}\left\{\frac{X}{2}\left(X_a + X_T + \frac{X}{2}\right)\right\} \qquad (5)$$

It has direct relationship to power-angle (P-δ) curve which is controlled by voltage (V), angle between voltages (δ) and impedance (Z). These variables have direct impact on power system performance which is illustrated by given Fig.

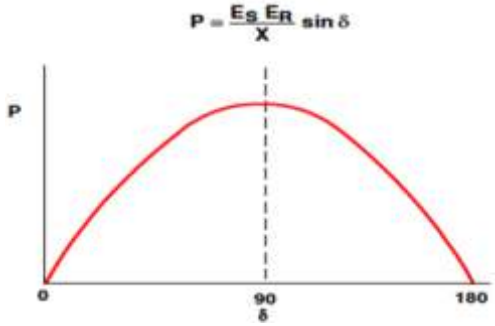

Fig 2. Controllability of power system [5]

From the above relationship, there are two cases;

i. k > 0 if B(t) > 0

In this case, the effective line reactance is reduced then P-δ curve is enlarged. In this way, the stability margin is improved.

ii. k < 0 if B(t) < 0

In this case, the effective line reactance is increased then P-δ curve is reduced. In this way, the stability margin is reduced.

In case of SVC, $B(t) = B_{SVC}(t)$, and in case of STATCOM, $B(t) = B_Q(t)$.

2. Midpoint Regulation

When the controller is added at the midway point, the reactance of line is distributed. In this way, the reactive power exchanges within transmission lines while the real power remains same in the line. Thus, the real and reactive powers are;

$$P = 2\frac{V^2}{X}\sin\frac{\delta}{4} \qquad (6)$$

$$Q = VI\sin\frac{\delta}{4} = 4\frac{V^2}{x}\,(1 - \cos\frac{\delta}{4}) \qquad (7)$$

3. Voltage Stability at the End of Line

Reactive shunt compensation is used to provide the voltage regulation at load ends in case of generation, line outage and impaired voltage system. It contributes the voltage support in the system and prevent from voltage instability.

4. Transient Stability Improvement

Shunt compensation is used to control the power flow and enhances the transient stability which is evaluated by equal area criterion. This criterion is illustrated by the power-angle (P-δ) curve that is disturbed by the fault in the system.

5. Power Damping Oscillations

In an undamped system, the minor disturbance can cause a machine angle to oscillate its steady state value. Thus, the shunt compensation is provided to counteract the accelerating and deaccelerating swings in the disturbed system [6].

I. Dynamic Modelling of Shunt Facts Controller

Dynamic Modelling of SVC and STATCOM is illustrated in this section.

1. Dynamic Modelling of SVC

Static VAR compensator is an electrical device to control the voltage by controlling reactive power of the transmission network. It is consisted of FC that acts as harmonic filter to provide the reactive power supply and TCR which is thyristor-controlled reactor series to inductor without gate turn off capability.

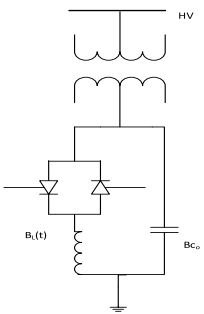

Fig 3. Basic configuration of SVC [8]

The dynamic model can be expressed as [7];

$$B_L(t) = \frac{1}{TB}(-B_L(t)+B_{LO}+K_B\mu_L(t)) \quad (8)$$

$$B_{SVC}(t) = B_c(t) - B_L(t) \quad (9)$$

$$\nabla B(t) = B_L(t) - B_{LO}(t) \quad (10)$$

$$B_{SVC}(t) = B_c(t) - (B_{LO})\Delta B_L(t)) \quad (11)$$

where $B_L(t)$ is susceptance of TCR, T_B is time constant, K_B is gain of control system, μ_B is input of control system, B_{Lo} is susceptance of TCR at operating point, while the B_{Co} is susceptance of FC and $B_{SVC}(t)$ is the susceptance of SVC.

If the reactive load of the power system is capacitive (leading), SVC consumes the reactive load from the system and lowers the voltage. In case of inductive (lagging) condition, SVC produces the reactive power by switching of capacitor banks and higher the voltage. In this way, the P-δ curve improves.

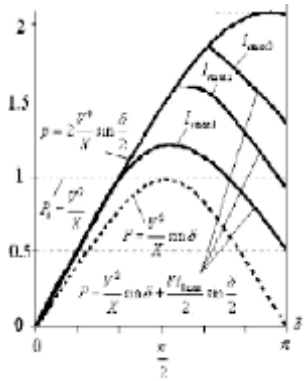

Fig 4. P-δ curve of SVC [8]

SVC are cheaper, reliable and higher capacity. It has no gate turn-off capability. It is used to control the voltage, voltage stability, VAR compensation, damping oscillation, transient and dynamic stabilities.

2. Dynamic Modelling of STATCOM

A shunt connected device to compensate the capacitive or inductive load based on voltage sourced or current sourced converter. It is consisted of thyristor-controlled reactor parallel to capacitor or inductor independent of ac voltages. It has fast switching time due to IGBTs and provides better reactive power support at low ac voltages.

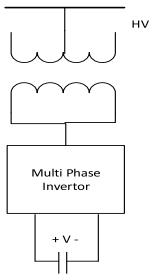

Fig 5. Basic configuration of STATCOM [8]

The dynamic model of STATCOM is expressed as [7];

$$B_Q(t) = \frac{i_Q(t)}{V_Q(t)} \quad (12)$$

$$i_Q(t) = \frac{1}{T_Q}(-i_Q(t)+i_{QO}+K_Q\mu_Q(t)) \quad (13)$$

Where $B_Q(t)$ is susceptance of STATCOM, $I_Q(t)$ is reactive current, $V_Q(t)$ is the voltage to which STATCOM is connected, K_Q is gain of control system, μ_Q is input of control system, $I_{Qo}(t)$ reactive output current at operating point of STATCOM.

The reactive power from the STATCOM is deceases linearly with the ac voltage due to direct proportions. The

reactive current is possibly controlled by δ, by which convertor output voltage leads by bus voltage. The positive value of δ leads to inductive region while the negative value leads to capacitive region. In this way, the P-δ curve improves.

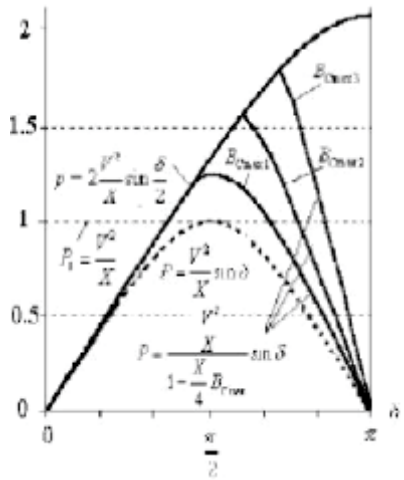

Fig 6. P-δ curve of STATCOM [8]

It have higher losses and expansive device. It is used to control the voltage, voltage stability, VAR compensation, damping oscillation.

V. Dynamic Modelling of Shunt Facts Controller In PSS/E

Dynamic modelling of SVC and STATCOM in PSS/E tool is expressed as;

1. Dynamic Modelling of SVC in PSS/E

SVC is the shunt controller without any controlling switch. In this paper, CSVGN1 model of SVC is implemented which has 300 MVAR rating. It provides the reactive power in case of inductive load and consumes reactive power in case of capacitive load. The SCR switch is controlled by the auxiliary signal. It controls the voltage and provides transient and dynamic stability [9-10].

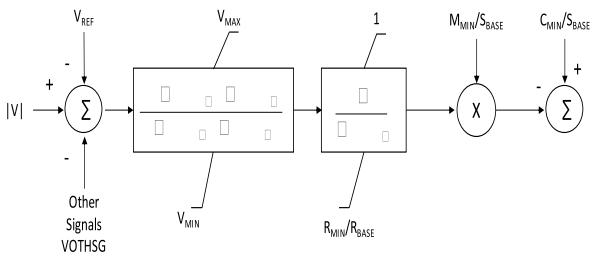

Fig 7. Control diagram of SVC [11]

The description of constants, used in control diagram, are given in Table 2.

Table 2. Parameters of SVC

No.	Value	Parameters
1	0	PGEN
2	0	QGEN
3	-9999	PMAX
4	450	PMIN
5	450	QMAX
6	-50	QMIN
7	500	MBASE
8	9999	XSOURSE

2. Dynamic Modelling of STATCOM in PSS/E

Static condenser (STATCON) or static compensator (STATCOM) is a shunt capacitor that is voltage source convertor with thyristor-controlled switch. It is used to control the reactive power that has direct relation with the voltage. The voltage is synthesized behind the convertor transformer reactance. For the reactive control, the synthesized voltage is kept in phase with the terminal voltage. In ideal condition, the capacitor remains charged because there is no exchange of active power with the network. In practical network, the convertor has losses and a trend of discharging of capacitor is followed. For charging of capacitor, the voltage is controlled and lag by the terminal voltage, thus the active power flow between the system and condenser is maintained. In this way, the voltage of the capacitor is controlled which determine the internal voltage that control the reactive power exchange with the network.

In this paper, CSTCNT models of STATCOM is modeled which has 150 MVAR rating. It delivers the reactive power whereas the active power is considered as negligible. STATCOM is modeled as FACTS device and has no active output power. [9-10].

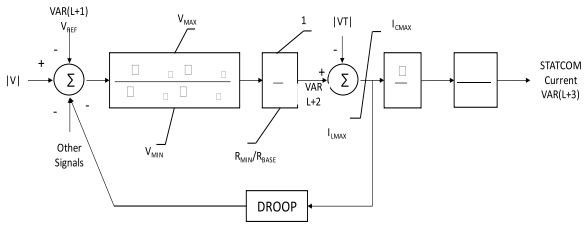

Fig 8. Control diagram of STATCOM (CSTCNT) [11]

The description of constants, used in control diagram, re given in Table 3.

Table 3. Parameters of STATCOM

No.	Value	Parameters
1	1	DEVIE MODLE
2	0	TERMINAL BUS
3	NORMAL	CONTROL MODE
4	0	P SET-POINT
5	0	Q SET-POINT
6	1.02	VS END-SETPOINT
7	64	SHUNT MAX
8	100	RMPCT
9	0	BRIDGE MAX
10	1.1	V TERM MAX
11	0.9	V TERM MIN
12	1	V SERIES MAX
13	64	I SERIES MAX
14	0.05	DUMMY SERIES X
15	VS ENDING	V SERIES REFERENCE

VI.Test Case Scenerio

Pakistan National Grid network is comprised of numerous generators, busses, lines, transformers, and variety of loads. As the old existing network, the system becomes more overloaded due to generation integration and increased demand of power. In this way, the issues of stability, loss and congestion are raised. For this purpose, new transmission lines are needed to meet the criteria of demanded power. The proposed strategies of new transmission lines are not the right way to meet this challenge. Thus, many methodologies are adopted to mitigate these issues. In this paper, we have focused on FACTS devices to address these issues of stability and congestion.

For a test case, the network of National Grid of Pakistan is modeled in PSS/E tool considering all parameters of the system. This network has large integration of renewable energy sources such as 784 MW of wind energy and 400 MW of solar energy. These renewable energy sources are also modelled, to see the impact of these energy sources in the network which are shown in Figs. 9-10.

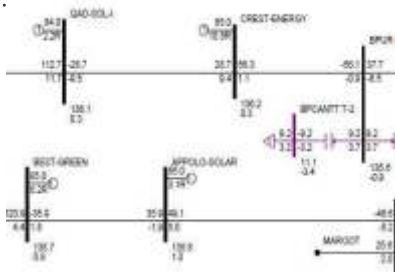

Fig 9. Solar power plants in Pakistan National Grid

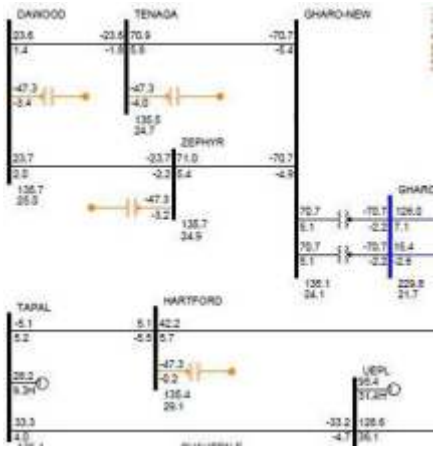

Fig 10. Wind power plants in Pakistan National Grid

This above generation integration as well as load demand and disturbed stability profiles made the high ration congestion issues in the system. The stability analysis is analyzed using PSS/E tool and identified the most critical regions in the network. So, after the critical observations, QESCO network is selected as a test case in this paper. We have observed that the lines of this region are over loaded which are clearly viewed in PSS/E tool, as shown in red and pink color which showed the heavily loaded lines and highly unstable busses respectively.

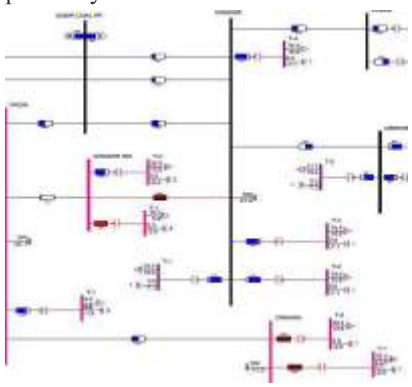

Fig 11. Loading of lines

In case of contingency, when the line is tripped due to fault or switching from Gwadar to Gwadar Coal then the lines are more heavily loaded and does not maintain their stable state as shown in red color.

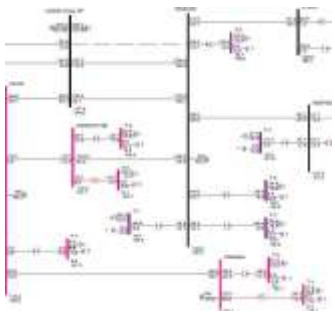

Fig 12. Loading of lines in case of line tripping

VII. Stability Studies

The condition of being stable even after the disturbance in the network is the major need of the power system. The disturbance is due to the switching, faults and outage of the lines or equipment. These disturbances have a great impact on the voltage, frequency, and rotor angle profiles. Power system stability is mainly classified into rotor angle, frequency and voltage stability and further classified into short and long-term phenomenon.

Methodology of Stability Study

The system of being stable even after the disturbance, the following disturbances is studied;

- The severe three-phase balanced fault as per Grid Code of National Electric Power Regulatory Authority (NEPRA) is occurred on the bus bar at critical locations. It remains for the 5 cycles.
- The three-phase fault will be backed up in 9 cycles after fault initiation.
- Contingency is applied for unbalancing of system and remains for 20 cycles.

In this scenario, the waveforms of voltage, frequency, power flows and rotor angle of given bus and nearby busses are plotted against the time axis in PSS/E to perceive the effect of disturbance in the network.

- The voltage waveforms of Gwadar bus bar and nearby busses are plotted in red, green, blue and pink colors.
- The frequency waveform of Gwadar bus bar is plotted in red color.
- The power flows waveform of Gwadar bus bars are plotted in red and green colors.
- The rotor angle waveform of Gwadar bus bar is plotted in red color compared to rotor angle of Tarbela generator.

a. Voltage Waveform

At the time of fault, the reactive power of the system becomes unbalanced and results in disturbed voltage profile of the bus bars. This disturbed voltage profile does not maintain the stable state even after the fault clearance.

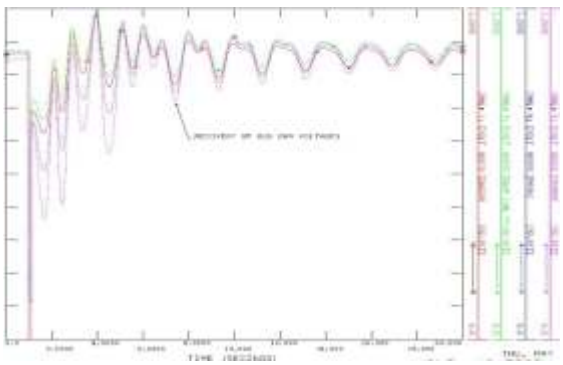

b. Frequency Waveform

At the time of fault, the frequency of Gwadar bus bar has more excursions in the system and exceed the rated boundary of plot book due to no restoration in system generation and load in the system. It does not approach the stable state in 20 cycles after the fault clearance.

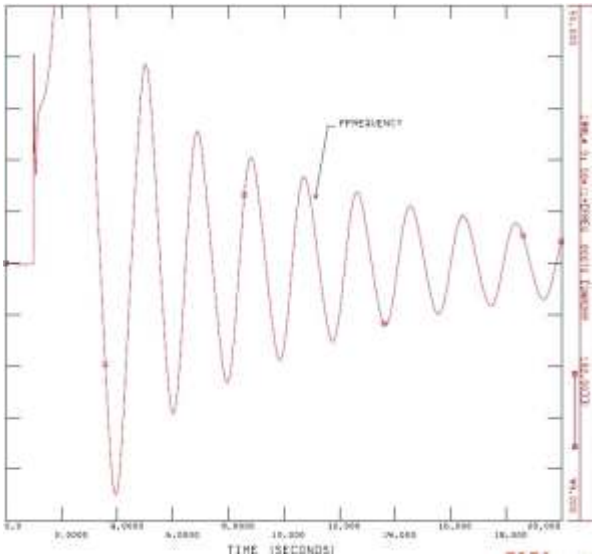

Fig 13 (b). Frequency waveform

c. Power Flow Waveform

The one circuit of Gwadar to Gwadar Coal is switched thus the flow is carried out from the another circuit that is parallel to it. At the time of fault, the loss in active power causes of drooping MW flow whereas increase in reactive power causes of increasing MVAR flow. Both MW and MVAR power flows do not approach the stable state within the 20 cycles.

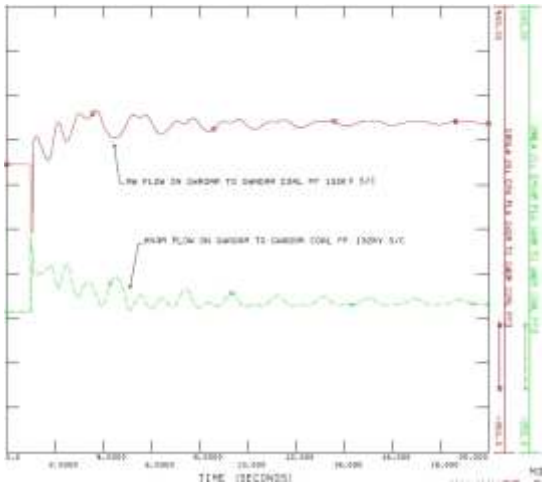

Fig 13 (c). Power flow waveform

d. Angle Waveform

At the time of fault, the loss of synchronism between electromagnetic and mechanical torques causes of

disturbed rotor angle profile of generator. It does not approach the stable state even after the fault clearance.

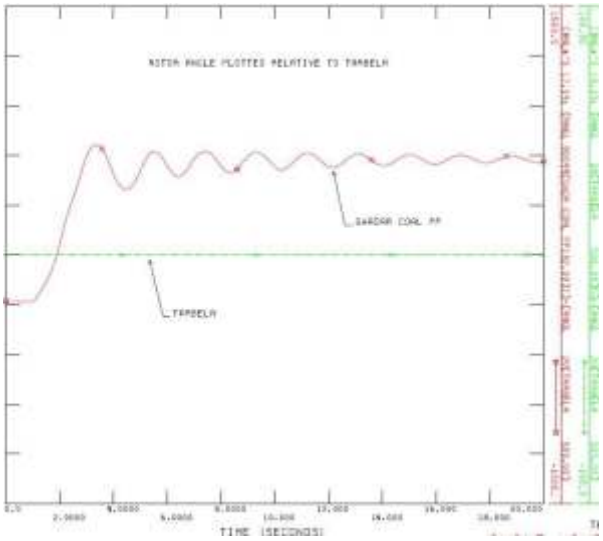

Fig 13 (d). Angle waveform

VII. Implementation of Facts Devices

Congestion includes both MW and MVAR loading. The traditional solution to MW loading is the installation of a new circuit while the solution to MVAR loading is usually installation of capacitors. However, these are not feasible or reliable solutions due to either high cost (in case of stringing new circuits) or due to nonexistent support during fault conditions (in case adding capacitors).

In the selected critical region, Gwadar is located in a remote region as far as the electrical network is concerned. There is no local generation, so it needs to draw power from the National Grid, which passes hundreds of kilometers away from Gwadar. The long transmission lines needed to transport this power need to carry high amounts of reactive power, which causes significant MVAR loading in the network. Again, the traditional solution to this scenario is the addition of transmission lines. However, this is an expensive solution, especially since hundreds of kilometers worth of transmission towers, insulators and conductors are involved. So, SVC and STATCOM are proposed for providing MVARs in the system.

In case of poor damping or oscillations in system recovery after the disturbance is cleared in the simulations. The remedial solutions are proposed to install the FACTS devices and establish the proposed solutions through simulations.

In this paper, we have selected the Gwadar bus bar of QESCO network for the implementation of shunt compensation in the system which is the most significant and critical bus bar of the network.

A. Stability Studies with SVC

The loading of the lines are relieved by installation of SVC. Therefore, no one line is presented in red color which is shown in given figure.

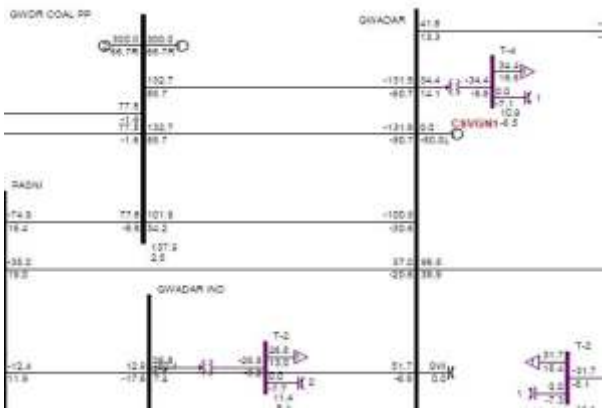

Fig 14. QESCO network with SVC

a. Voltage Waveform with SVC

With the installation of SVC, the reactive power of the system comes to be balanced state, results in the voltages of Gwadar, Pasni, Turbat and Gwadar Coal bus bars are collapse at the time of fault but they are recovered sooner in 8 cycles.

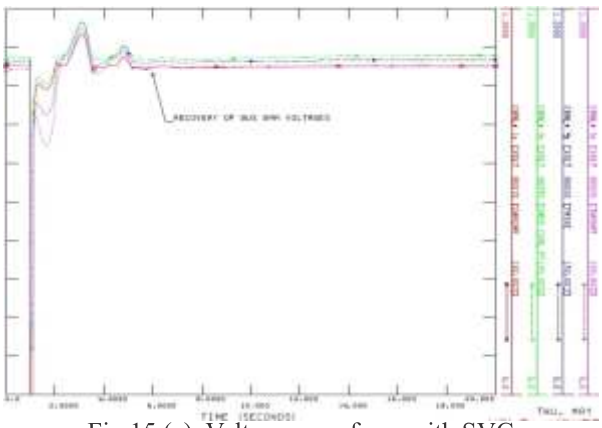

Fig 15 (a). Voltage waveform with SVC

b. Frequency Waveform with SVC

With the installation of SVC, the frequency reaches its peak value within its plot book, at the time of fault. Then it is recovered after 4 peaks within 8 cycles due to restoration in system generation and load.

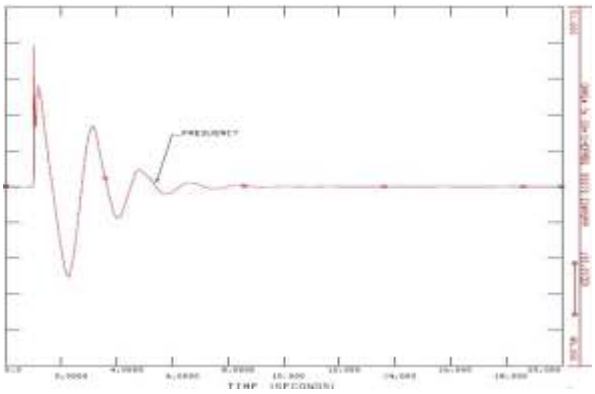

Fig 15 (b). Frequency waveform with SVC

c. Power Flow Waveform with SVC

The one circuit of Gwadar to Gwadar Coal is switched thus the flow is carried out from the another circuit that is parallel to it. At the time of fault, the MW flow is drops out and its oscillation remains for 6 cycles whereas the MVAR flow reaches its peak value and approached the stable state within the 8 cycles.

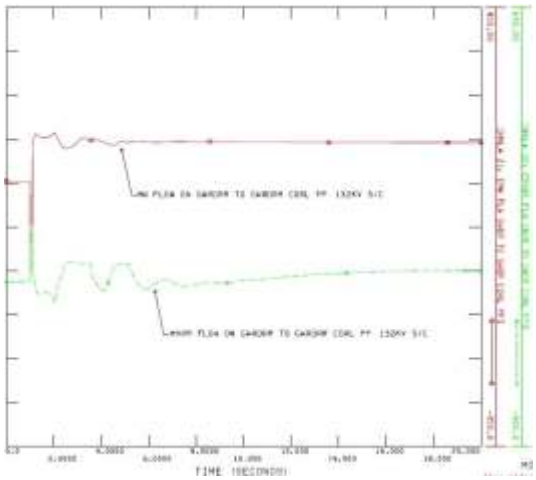

Fig 15 (c). Power flow waveform with SVC

d. Angle Waveform with SVC

With the installation of SVC, rotor angle reaches its maximum peak and being synchronized within 8 cycles after the fault clearance.

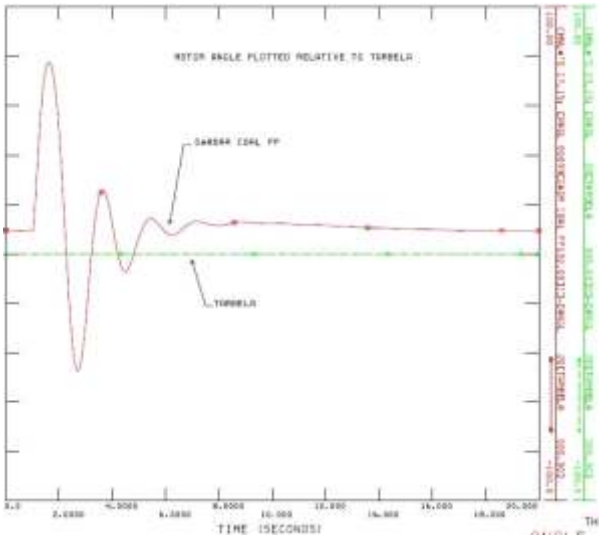

Fig 15 (d). Angle waveform with SVC

e. SVC Output Waveform

SVC provides the current when the system stability drops due to fault occurrence. At the time of fault, SVC delivers current in the system until the system achieved its stable state.

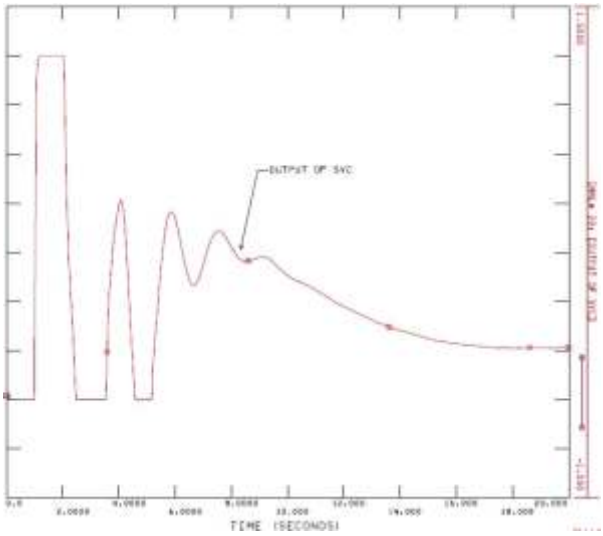

Fig 15 (e). Output waveform of SVC

B. Stability Studies with STATCOM

The loading of the lines are relieved by installation of STATCOM which is shown in given figure.

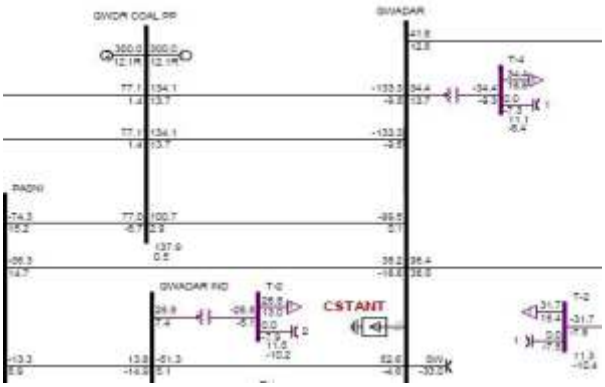

Fig 16. QESCO Network with STATCOM(CSTCNT)

a. Voltage Waveform with STATCOM

The voltages of all bus bars near the faulted bus recover soon after fault clearance with the help of STATCOM, it provides reactive power balancing in the network within 6.5 cycles.

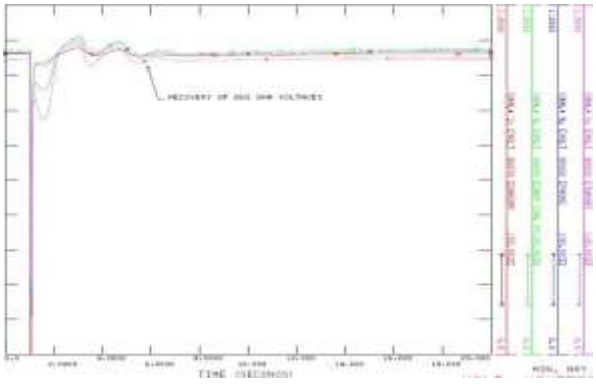

Fig 17 (a). Voltage waveform with STATCOM

b. Frequency Waveform with STATCOM

With the installation of STATCOM, the frequency reaches its peak value within its plot book, at the time of fault. Then it is recovered after 4 peaks within 6.5 cycles due to restoration of system generation and load.

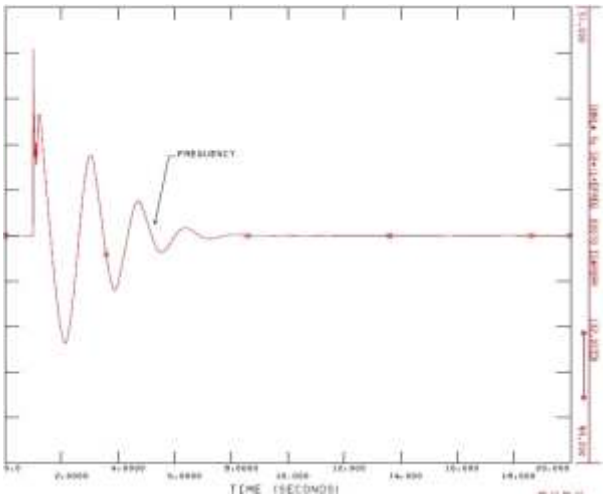

Fig17 (b). Frequency waveform with STATCOM

c. Power FlowWaveform with STATCOM

At the time of fault, the MW flow is drops out and its oscillation remains for 4 cycles whereas the MVAR flow reaches its peak value and approached the stable state within the 6 cycles.

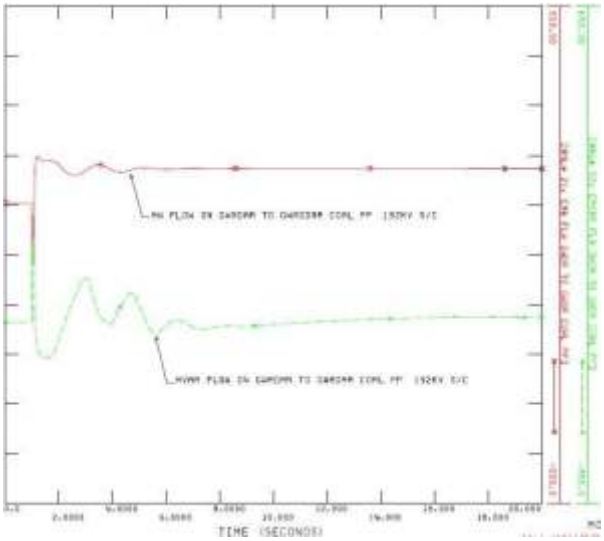

Fig 17 (c). Power Flow waveform with STATCOM

d. Angle Waveform with STATCOM

The first swing has a value within the boundry of plot area. With the installation of STATCOM, the synchronism between electromagnetic and mechanical torques attained within the 8 cycles.

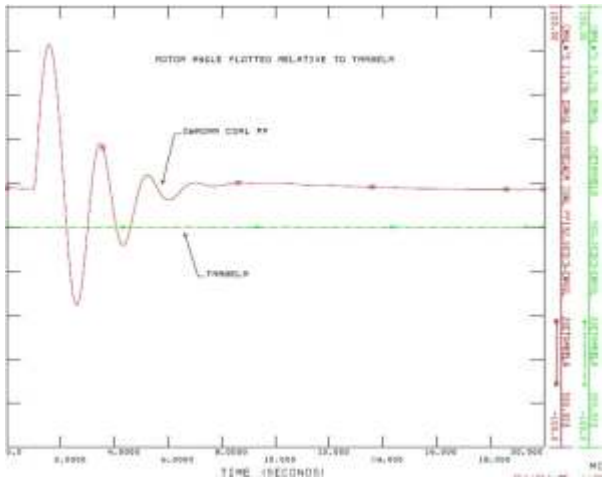

Fig 17 (d). Angle waveform with STATCOM

e. STATCOM Output current waveform

STATCOM provides the current when the sytem stability drops due to fault occurrence. After the fault cleraence, STATCOM delivers current untill the system achieved its stable state.

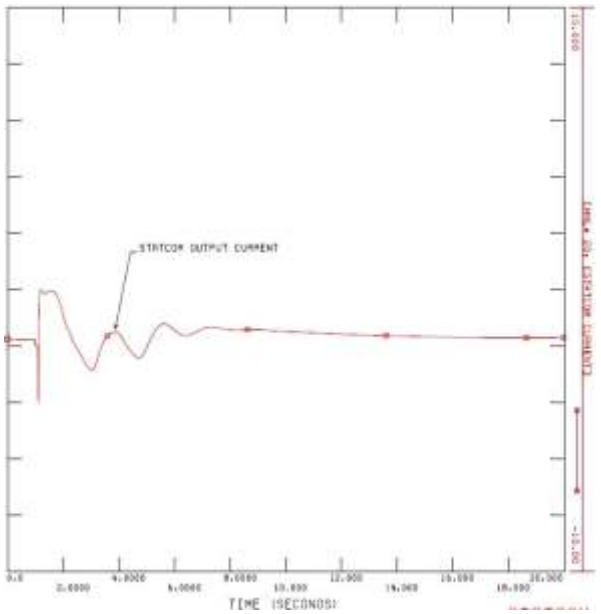

Fig 17 (e). Output waveform of STATCOM

IX. Comparison of SVC and STATCOM

In this paper, two shunt FACTS devices are presented which has its own pros and cons. The dynamic modelling and simulation result that STATCOM is prior to SVC.

STATCOM provides the first swing stability enhancement by controlling the reactive power in the transmission lines.
It has fast switching time due to IGBTs switches.
It improved the phase angle and voltage magnitude.
It has reduced size and need low MVAR rating.
It is slightly costly [12-13].

Table 4. Comparison of SVC and STATCOM

FACTS	Load Flow Control	Voltage Control	Transient Stability	Dynamic Stability	Cost / Kvar ($)
SVC	✓	✓✓✓	✓	✓✓	40-70
STAT-COM	✓✓	✓✓✓	✓✓	✓✓✓	55-70

X. Results and Discussion

The issues of congestion become more frequent due to disturbed voltage profile, generation integration and load demand. These issues are generally observed in QESCO which is selected after the critical study of Pakistan National Grid in PSS/E tool that is highly unstable and over loaded. In PSS/E tool, the simulations are performed which showed that without the insertion of FACTS, voltage, frequency, load flows and angle profiles are disturbed due to unbalanced reactive power, sub-synchronous reactance and loss of synchronism.

As a remedial solution to these disturbed profiles is to insert the shunt FACTS device on Gwadar bus bar. In this paper, SVC and STATCOM is installed in the network. It provides the reactive power compensation and causes of reactive power balancing, restoration between generation and load with less losses, load balancing and synchronism between electromagnetic and mechanical torque. Thus, the voltage, frequency, load flows and angle profiles are maintained and in this way, the capability of transmission lines is increased. The steady state, dynamic and transient stability of the system is enhanced and losses are reduced in the network. It also provides the cost effective solution as compared to laid a new transmission line in the network. When a new transmission line is laid, it includes the material cost (tower, conductor, insulator strings, overhead line and spacers), installation cost (tower, conductor, insulator strings, overhead line and spacers), right of way cost, line bay cost, civil works cost and engineering cost for constructing the lines. These costs are much larger than the cost of FACTS devices. That is why, we preferred these devices specially STATCOM due to superior quality as compared to SVC, for relieving the issues of stability and congestion.

XI. Conclusions

In this paper, power flow and dynamic stability enhancement using shunt FACTS devices is presented. For an analysis, QESCO network of Pakistan National Grid is selected for the installation of FACTS devices. This system is modelled in PSS/E tool and simulation results indicated that system is not being stable without the reactive line compensation. Therefore, the reactive compensation has been applied using shunt devices to support the system. The plotted results show that the voltage, frequency, and power flows of the circuit settled within the rated capacities and enhanced the transfer capability of lines. Significantly, the dynamic stability analysis shows that the reliability of existing National Grid is enhanced with the shunt compensation using SVC and STATCOM. It improves the dynamic stability by providing the reactance in lines and also increases the power flow capacity of TLs. In this way, it provides the reactive power support to the system.

References

[1] L. Rajalakshami, M. V. Suganyadevi, S. Parameswari, "Congestion management in deregulated power system by locating series FACTS devices", *International Journal of Computer Applications*, vol. 13, n0. 8, pp. 19-22, Jan 2011.

[2] R. S. Fang and A. K. David, "Transmission congestion management in an electricity market", *IEEE Transactions on Power Systems*, vol. 14, no. 3, pp. 877-883, Aug. 1999.

[3] G. Beck, W. Breure, D. Povh and D. Retzmann, "Use of FACTS for System Performance Improvement" CEPSI Electric Power Supply Industry, pp. 1-23, Nov 2006.

[4] Y. L. Tan, Y. Wang, Effects of FACTS Controller Line Compensation on Power System Stability, IEEE Power Engineering Review, vol. 18, n0. 8, pp. 55-56, Aug 1998.

[5] A. K. Mohanty and A. K. Barik, "Power System Stability Improvement using FACTS Devices", International Journal of Modern Engineering Research, vol. 1, no. 2, pp. 666-672.

[6] N. G. Hingorani, L. Gyugyi, "Understanding FACTS: Concepts and Technologies of Flexible AC Transmission Systems", IEEE Press Marketing, 1999.

[7] Y. L. Tan, "Analysis of Line Compensation by Shunt-Connected FACTS Controllers: A Comparison between SVC and STATCOM" IEEE Power Engineering Review, pp. 57-58, Aug 1999.

[8] P. Gopi, I. P. Reedy and P. S. Hari, "Shunt FACTS Devices for First-Swing Stability Enhancement in Inter-area Power System", Sustainable Energy and Intelligent System, Dec 2012.

[9] PSS/E 33.5 Program Applications Guide Volume II October 2013, Siemens Power Technologies International.

[10] P. DAS, H. S. Dee, A. Chakarbarti and T. Datta, "A Comparative Study in Improvement of Voltage Security in A Multi-Bus Power System using STATCOM and SVC", IEEE, pp. 1-6, 2011.

[11] PSS/E 33.5 Model Library, October 2013, Siemens Power Technologies International.

[12] N. Acharya, FACTS and Figures", Training Workshop of FACTS Application, EPSM Energy, Dec 2004.

[13] J. Kueck, B. Kirby, T. Rizy, F. Li and N. Fall, "Reactive Power from Distributed Energy", Electricity Journal, Dec 2006.

Transient Stability Analysis of 11 Bus Systems

Muhammad Danyal Zahid[1], Muhammad Irfan Yousaf[1], Muhammad Sufyan Zafar[2]

[1,2]Electrical Engineering Department, University of Central Punjab,Lahore, Pakistan

Abstract

Stability of the system is the important parameter for the stable, profitable and proper operation of the power system. The main aim of this research project is to implement the transient stability of the 11 bus power system in power word simulator. Two generators are modeled with different MW ratings. Our system is interconnected system of 11 Buses. The fault is created on different buses and analyzed by bus admittance matrix. Furthermore, the modelling of this system is done on power word simulator. The designing of the electric power system is mandatory to study the small and transient disturbance. The rotor angle variation and bus faults at different buses are studied and also studied its impact on the load. When there is fault or any kind of disturbance on the system, the rotor angle of the generator changes and its frequency also changes. These rotor angle variations can be simulated in the power word simulator. In this research work, it is clearly observed in the simulated graphs that when there is disturbance or fault in the system then the system cannot come back to stability position. As the fault or disturbance is removed then the power system comes to stability. The system that is proposed is universal and generalized system than any other power system. This system has proposed in the aspect that it can be applicable to any power network irrespective of the power generation that how fault affects the stability and rotor angle, how bus admittance matrix changes with the instability of the system. In this system it can be easily analyzed that how voltages vary on different phases when fault occurs on the system.

***Key Words**:*

Transient stability, Fault analysis, Y-Bus, Rotor angle.

1. Introduction

Power system stability is the important parameter for the smooth working of the power system network,When the load on the generator suddenly changes, or disturbance occurs then the rotor angle of the generator changes due to the change in rotor angle the frequency also changes. This research project emphasizes on the importance of the rotor angle and different types of fault in the power system network. When there is fault or disturbance in the power system network then the rotor angle changes, and the system goes to instability. When the fault is removed from the system then rotor angle changes and system comes to stability position.This paper focuses on different types of unsymmetrical faults i-e Line to ground fault, line to line fault and double line to ground fault. These unsymmetrical faults are analyzing through Y-bus.The diagram of the 11 bus power system network is shown in figure 1.

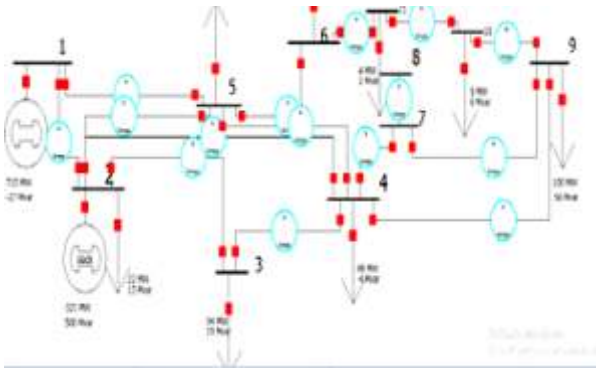

Figure 1: One Line Diagram of 11 Bus Power System

2. Problem Establishment

Power Transient stability deals with the disturbance occur in the system, which occurs due to sudden change in load and generation parameters. Due to sudden change in load and other parameters the system undergoes to instability condition. If this instability goes to long duration the system undergoes a transient instability. In this paper different faults are created (i-e symmetrical and unsymmetrical faults) at different bus to check the instability of the system. When the system undergoes disturbance or fault then the admittance matrix also changes which gives useful information about the data which is useful to study the load flow analysis or load changes, so the admittance matrix for different fault condition can be observed and also the rotor angle under steady state and fault conditions can be analyzed.

In the previous papers the transient stability analysis is done using power flow study methods (i-e Newton Raphson method) and the previously proposed systems are limited to specific generation system but in this paper problem is analyzed by creating faults at different buses and check the admittance matrix and rotor angle stability using power world simulator. This system is universal

that can be applied to any power network for transient stability analysis.In this research work transient stability can be improved by using FACT devices (i-e STATCOM and SVC devices). The remaining papers that are discussed in the literature review explains the fault analysis or transient stability analysis about the specific power system like wind power system, micro grids, diesel generators and renewable energy resources.

Some research works focus on the wind energy system that is wind causes different electrical and mechanical distrubance due to the change in size of wind turbines and other factors. This is more related with the control system in which pole zero study is done for the transient and steady state analysis.[1].Some research papers discuss about the fault that occurs in the micro grids and the micro grid stability using electrical transient analyzer program(ETAP). Micro grids are connected with the grids, for the proper operation of the micro grid during fault in grid an islanding operation is adopted. Islanding is a technique in which grid continues to supply power.[2]. Another research shows that different fault calculations like three phase fault, line to ground fault and the fault occur due to sudden removal of generator are discussed in the combined cycle power plant that include conventional and non- convention energy sources, using the ETAP software.[3]. Some research papers discuss about the transient stability i-e when there is variation in wind pressure or frequency varies then instability occurs and the system is no more stable during peak and off peak hours.[4]

The drawback of the above discussed research works and the systems is that they are limited to specific power system. Therefore, a generalized and universal system about the transient stability analysis is proposed that covers the all types of generation systems.

Sr. No	Time	Gen 1#1 Rotor Angle	Gen2#1 Rotor Angle
1	0	96.928	-24.65
2	0.008	96.928	-24.65
3	0.017	96.928	-24.65
4	0.025	96.928	-24.65
5	0.033	96.928	-24.65
6	0.042	96.928	-24.65
7	0.05	96.928	-24.65
8	0.058	96.928	-24.65
9	0.067	96.928	-24.65
10	0.075	96.928	-24.65
11	0.083	96.928	-24.65
12	0.092	96.928	-24.65
13	0.1	96.928	-24.65
14	0.108	96.928	-24.65
15	0.117	96.928	-24.65
16	0.125	96.928	-24.65
17	0.133	96.928	-24.65

Table 1: Rotor angle Gen 1 and Gen 2

In the table 1 it is shown that after simulation in power word simulator, two different rotor angles at generator 1 and generator 2 are obtained at different time intervals. After simulation process, the graph of rotor angle Gen 1 is obtained. In the graph shown in figure 2 it can be seen that the system is stable up to 1.5 time scale axis and after that there is disturbance in the system and graph is going towards instability.

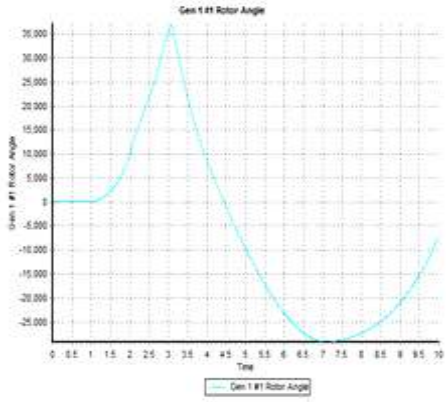

Figure 2: Rotor angle of Gen 1

In the Second graph which is shown in figure 3, it is shown that after simulation process when there is disturbance at rotor angle Gen 1 then there is also effect on rotor angle Gen 2. So the instability at Gen rotor angle 2 also occurs.

Figure 3: Rotor angle of Gen 2

3. Importance of Y-bus and Sequence components

Y-bus is also called admittance matrix, Y-bus is useful in load flow studies and fault calculations. In any power system network there are different number of buses that are link with each other through transmission lines. In any admittance matrix the diagonal elements are positive and off diagonal elements are negative. When fault occurs i-e unsymmetrical faults in the power network then the voltage and current values in the three phase network do not remain same. To solve these kind of faults, symmetrical components are used. The phenomena of symmetrical components are to resolve the phasor vectors into three sets of balanced phasors. One has positive rotation, negative rotation and zero rotation. When data is simulated in the software, Y-bus matrix of the overall network of 11 bus system is obtained and then resolve the network into positive, negative and zero sequence bus admittance matrix as shown in following tables 2,3,4 and 5.

Sr.No	Number	Name	Bus 1	Bus 2	Bus 3	Bus 4	Bus 5	Bus 6	Bus 7	Bus 8	Bus 9
1	1	1	6.03-j2.500	-5+j15.26			1.03+j4.23				
2	2	2	-5+j15.26	9.74-j35.95	-1.14+j4.74	-1.69+j5.12	-1.70+j5.19				
3	3	3		-1.14+j4.74	4.42-j10.08	-1.99+j5.07					
4	4	4		-1.69+j5.12	-1.99+j5.07	11.22-j38.26	-6.84+j21.58				
5	5	5	1.03+j4.23	-1.70+j5.19		-6.84+j21.58	9.64-j34.95	-0.00+j3.97			
6	6	6					-0.00+j3.97	2.16-j8.20			
7	7	7				-0.00+j4.78			0.00-j19.55	-0.00+j5.68	-0.00+j9.09
8	8	8							-0.00+j5.68	0.00-j5.68	
9	9	9				-0.00+j1.80			-0.00+j9.09		6.93-j22.96
10	10	10									-3.90+j10.37
11	11	11						-1.96+j4.09			

Table 2: Y-Bus Matrix of overall Power system

	Number	Name	Bus 1	Bus 2	Bus 3	Bus 4	Bus 5	Bus 6	Bus 7	Bus 8	Bus 9
1	1	1	6.03-j25.00	-5.00+j15.26			-1.03+j4.23				
2	2	2	-5.00+j15.26	9.74-j35.95	-1.14+j4.78	-1.69+j5.12	-1.70+j5.19				
3	3	3		-1.14+j4.78	4.42-j10.08	-1.99+j5.07					
4	4	4		-1.69+j5.12	-1.99+j5.07	11.22-j38.26	-6.84+j21.58		-0.00+j4.78		-0.00+j1.80
5	5	5	-1.03+j4.23	-1.70+j5.19		-6.84+j21.58	9.67-j34.95	-0.00+j3.97			
6	6	6					-0.00+j3.97	2.16-j8.20			
7	7	7				-0.00+j4.78			0.00-j19.55	-0.00+j5.68	-0.00+j9.09
8	8	8							-0.00+j5.68	0.00-j5.68	
9	9	9				-0.00+j1.80			-0.00+j9.09		6.93-j22.96
10	10	10									-3.90+j10.37
11	11	11						-1.96+j4.09			

Table 3: Positive Sequence Y-bus Matrix

Sr.No	Number	Name	Bus 1	Bus 2	Bus 3	Bus 4	Bus 5	Bus 6	Bus 7	Bus 8	Bus 9
1	1	1	6.03-j25.00	-5.00+j15.26			-1.03+j4.23				
2	2	2	-5.00+j15.26	9.74-j35.95	-1.14+j4.78	-1.69+j5.12	-1.70+j5.19				
3	3	3		-1.14+j4.78	4.42-j10.08	-1.99+j5.07					
4	4	4		-1.69+j5.12	-1.99+j5.07	11.22-j38.26	-6.84+j21.58		-0.00+j4.78		-0.00+j1.80
5	5	5	-1.03+j4.23	-1.70+j5.19		-6.84+j21.58	9.67-j34.95	-0.00+j3.97			
6	6	6					-0.00+j3.97	2.16-j8.20			
7	7	7				-0.00+j4.78			0.00-j19.55	-0.00+j5.68	-0.00+j9.09
8	8	8							-0.00+j5.68	0.00-j5.68	
9	9	9				-0.00+j1.80			-0.00+j9.09		6.93-j22.96
10	10	10									-3.90+j10.37
11	11	11						-1.96+j4.09			

Table 4: Negative Sequence Y-Bus Matrix

Sr.No	Number	Name	Bus 1	Bus 2	Bus 3	Bus 4	Bus 5	Bus 6	Bus 7	Bus 8	Bus 9
1	1	1	6.03-j25.00	-5.00+j15.26			-1.03+j4.23				
2	2	2	-5.00+j15.26	9.74-j35.95	-1.14+j4.78	-1.69+j5.12	-1.70+j5.19				
3	3	3		-1.14+j4.78	4.42-j10.08	-1.99+j5.07					
4	4	4		-1.69+j5.12	-1.99+j5.07	11.22-j38.26	-6.84+j21.58		-0.00+j4.78		-0.00+j1.80
5	5	5	-1.03+j4.23	-1.70+j5.19		-6.84+j21.58	9.67-j34.95	-0.00+j3.97			
6	6	6					-0.00+j3.97	2.16-j8.20			
7	7	7				-0.00+j4.78			0.00-j19.55	-0.00+j5.68	-0.00+j9.09
8	8	8							-0.00+j5.68	0.00-j5.68	
9	9	9				-0.00+j1.80			-0.00+j9.09		6.93-j22.96
10	10	10									-3.90+j10.37
11	11	11						-1.96+j4.09			

***Table 5**: Zero Sequence Y-Bus Matrix*

4. Fault Analysis and Calculations

Fault analysis is an important parameter in the power system network for the selection of circuit breaker, setting of digital relays. When Fault occurs in the power network the rotor angle of the generator changes and frequency also changes. In studying the load flow studies, it is important that the system is working under balanced conditions. There are symmetrical and unsymmetrical faults in the power network. Unsymmetrical faults include line to line fault, line to ground fault and double line to ground fault. Fault on different buses and lines are created and then analyze the admittance matrix. When the fault occurs on the phase "A" of bus 1 then the phase "A" voltages and the phase "A" angle goes to zero as shown in table 6.

Sr.No	Number	Name	Phase Volt A	Phase Volt B	Phase Volt C	Phase Angle A	Phase Angle B	Phase Angle C
1	1	1	0.00000	1.09351	1.00485	0.00	-119.52	129.22
2	2	2	0.34655	1.06342	0.94833	-9.41	-118.73	122.59
3	3	3	0.26416	0.98792	0.81584	-28.05	-127.28	117.70
4	4	4	0.21212	0.95951	0.80010	-28.52	-126.74	120.34
5	5	5	0.19804	0.98213	0.83487	-25.34	-125.21	121.69
6	6	6	0.19355	0.92582	0.71532	-48.74	-133.23	115.72
7	7	7	0.18668	0.85611	0.62453	-61.04	-136.96	114.72
8	8	8	0.18668	0.85611	0.62453	-61.04	-136.96	114.72
9	9	9	0.19999	0.81466	0.53578	-78.49	-143.27	110.30
10	10	10	0.19423	0.82173	0.55301	-75.92	-141.96	111.44
11	11	11	0.18723	0.86502	0.62581	-63.69	-137.66	113.84

Table 6: Fault at phase A of Bus 1

When the line to line fault occurs between line 11 and line 12 then the phase angle “A” and “B” goes to zero value as shown in table 7.

Sr.No	Number	Name	Phase Volt A	Phase Volt B	Phase Volt C	Phase Angle A	Phase Angle B	Phase Angle C
1	1	1	1.00001	0.77190	0.80569	3.16	-124.66	133.98
2	2	2	1.00000	0.72717	0.76587	0.00	-130.38	133.68
3	3	3	0.88001	0.44370	0.45202	-8.26	-177.42	161.09
4	4	4	0.84831	0.51844	0.55219	-6.64	-147.73	137.52
5	5	5	0.87651	0.56620	0.60968	-4.83	-141.09	135.23
6	6	6	0.78415	0.49986	0.53830	-13.79	-150.97	127.07
7	7	7	0.69741	0.42617	0.45800	-17.57	-158.00	126.09
8	8	8	0.69741	0.42617	0.45800	-17.57	-158.00	126.09
9	9	9	0.63182	0.38686	0.41280	-25.26	-165.17	118.17
10	10	10	0.64308	0.39614	0.42962	-23.55	-162.79	119.43
11	11	11	0.66683	0.40387	0.26296	0.00	180.00	180.00
12	12	Faultpt	0.86537	0.43268	0.43268	0.00	180.00	180.00

***Table** 7: Line to Line Fault Created Between Line 11 and 12*

In the table 8 it is shown that when single line to ground fault occurs at phase "A" of bus 12 then the phase angle and phase voltage of "A" and phase angle of "B" goes to zero value.

Sr.No	Number	Name	Phase Volt A	Phase Volt B	Phase Volt C	Phase Angle A	Phase Angle B	Phase Angle C
1	1	1	0.10608	1.08415	0.99300	-3.97	-118.71	128. 36
2	2	2	0.31551	1.07180	0.95930	-9.96	-119.59	123.49
3	3	3	0.24895	0.99602	0.82298	-29.62	-127.94	118.55
4	4	4	0.20948	0.96544	0.80540	-29.47	-127.22	120.95
5	5	5	0.20438	0.98651	0.83887	-25.39	-125.57	122.13
6	6	6	0.19787	0.93108	0.71894	-48.96	-133 .59	116.27
7	7	7	0.18679	0.86245	0.62887	-62.40	-137.40	115.45
8	8	8	0.18679	0.86245	0.62887	-62.40	-137.40	115.45
9	9	9	0.20166	0.82118	0.53949	-79.68	-143.67	111.14
10	10	10	0.19611	0.82801	0.55674	-76.91	-142.36	112.22
11	11	11	0.08260	0.64754	0.26 102	0.00	180.00	180.00
12	12	Faultpt	0.00000	0.57162	064785	0.00	180.00	180.00

***Table 8** : Single Line to Ground Fault at Phase A of bus 12*

Table 9 describes when the double line to ground fault occurs at phase A, B and C of bus 12 then it is clear that all three phase voltages and phase angles of bus 12 are zero

Sr.No	Number	Name	Phase Volt A	Phase Volt B	Phase Volt C	Phase Angle A	Phase Angle B	Phase Angle C
1	1	1	0.70472	0.70472	0.70472	5.66	-114.34	125.66
2	2	2	0.64049	0.64049	0.64049	2.99	-117.01	122.99
3	3	3	0.09655	0.09655	0.09655	-5.36	-125.36	114.64
4	4	4	0.37434	0.37434	0.37434	-2.49	-122.49	117.51
5	5	5	0.45325	0.45325	0.45325	-0.56	-120.56	119.44
6	6	6	0.39344	0.39344	0.39344	-9.51	-129.51	110.49
7	7	7	0.31431	0.31431	0.31431	-13.32	-133.32	106.68
8	8	8	0.31431	0.31431	0.31431	-13.32	-133.32	106.68
9	9	9	0.28862	0.28862	0.28862	-20.68	-140.68	99.32
10	10	10	0.29970	0.29970	0.29970	-18.80	-138.80	101.20
11	11	11	0.33148	0.33148	0.33148	0.00	180.00	180.00
12	12	Faultpt	0.00000	0.00000	0.00000	0.00	0.00	0.00

***Table 9**: Double Line to Ground Fault at phase A,B and C of Bus 12*

5. Conclusion

In this research work,the transient stability of 11 bus system in electric power system is analyzed using power world simulator.This is clarifying from the graph of the rotor angles that is shown in figure 4that the rotor angle of generator 1 is unstable up-to 4.5 times scale value. When system becomes normal which means there is no fault in the power network, then rotor angle become stable after 5 times scale value. The figure 5 clarifies that when there is fault on power network, the rotor angle of generator 2 becomes unstable up-to 4.5 times scale value and system becomes stable (no fault in system) after 5 times scale value. This research paper clearly explains how the proposed system is more universal and generalized than the remaining system that have been studied for the reference.

Transient stability analysis of 11 bus system focuses on the fault calculations, rotor angle, Admittance matrix of any power system network, irrespective of the power generation mechanism because this system emphasizes on the universal power system network. The research work proposes a system that is easier to understand, reliable and generalized method that can be applied on any kind of power system. Such kind of proposal is not discussed using the Power word simulator. In this research work, faults at different buses and transmission lines can be calculated and the bus admittance matrix under normal and fault conditions can be analyzed. Moreover rotor angles are analyzed in the software under normal and transient conditions.In future, transient stability problem can also be improved by using Fact devices (i-e STATCOM and SVC devices)

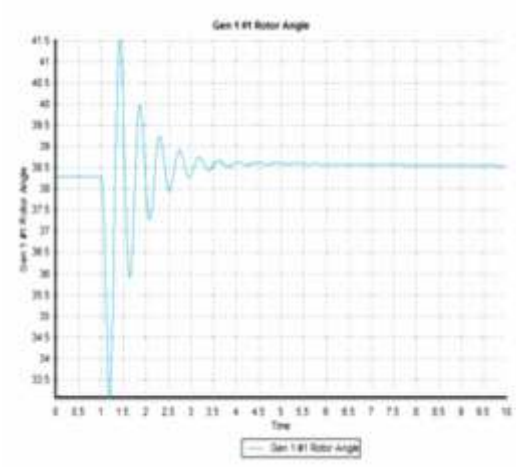

Figure 4: Rotor angle of Gen 1 after stability

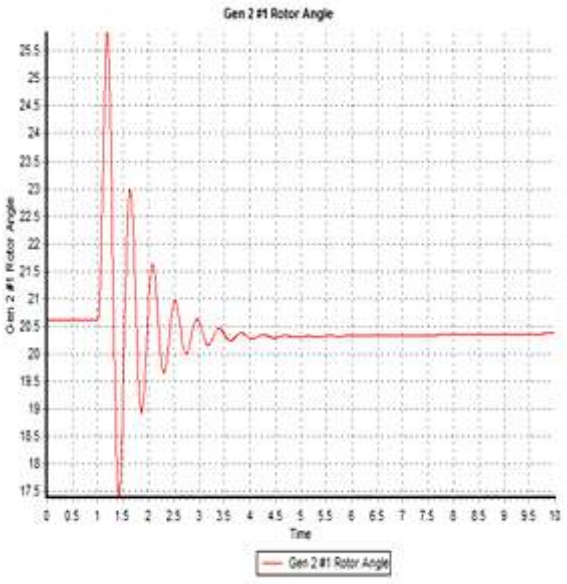

Figure 5: Rotor angle of Gen 2 after stability

1. References:

[1] A. Patil, "Steady State and Transient Stability Analysis of Wind Energy System," pp. 250-254, 2016.

[2] R. Singh and M. Kirar, "Transient stability analysis and improvement in microgrid," Electr. Power Energy Syst. (…, no. i, pp. 239-245, 2016.

[3] D. S. Reddy, "Transient Stability Analysis of a Combined Cycle Power Plant Using Etap Software," 2017.

[4] C. C. Yeh, C. S. Chen, C. T. Hsu, and T. J. Cheng, "Transient stability analysis for an island with diesel generators and wind generators," 2017 IEEE 3rd Int. Futur. Energy Electron. Conf. ECCE Asia, IFEEC - ECCE Asia 2017, pp. 2106-2110, 2017.

Steady State and Dynamic Analysis of Congested Regions using D-SMES

Zaira Anwar[1], Tahir Nadeem Malik[2], Tahir Abbas[3], Hassan Jaffar Zaidi[4],

[1,2]UET Lahore[3,4]Power Planer International (PVT.) Ltd. 95-H2 Wapda Town Lahore.

Abstract

This study presented the steady state and dynamic analysis to enhance the power flow and transient enhancements through D-SMES. In this paper, congested regions are observed using the steady state analysis in PSS/E software. The test case is analyzed with worst case scenario, at that time the responses of the system with or without D-SMES are compared. It stored the energy of the existing system and damped the oscillations in the network and enhanced the system stability. In this way, the issue of congestion is mitigated by improving the transient and dynamic stability of voltage, frequency and rotor angle profiles and damped the power oscillations. It also compensated the reactive power and controlled the power factor which increased the loading capacity of transmission lines. The economic analysis is also presented which provided the most economical way to transmit power.

Keywords:

Distributed super-conducting magnetic energy storage (D-SMES), power system simulator for engineers (PSS/E)

I. Introduction

Electrical Power system is a critical infrastructure having a dominant role in every walk of life. It deals with generation, transmission and distribution of electric power. The power transmission lines in power system are like arteritis, as power carrying from generating-stations to load centers. It is the natural tendency that electric load is increasing depending upon the socioeconomic and industrial trait of a particular country. As per energy requirement of a country, additional energy sources are needed in the network. Thus, due to less availability of coal, oil and other nonrenewable energy sources, the renewable energy sources are introduced in the network. These renewable energy sources such as wind or solar energy is now becoming the emergent technologies. These sources are integrated in the existing network cause of intermittence and congestion in the transmission lines. There are several methods to tackle these issues. The most efficient and cost effective method is to install the FACTS and ESS devices in the congested location of network.

In this paper, we represented the steady state and dynamic analysis of Pakistan National Grid network in the PSS/E environment. This tool is the graphical user interface and has versatile nature in simulations. All the network is modelled and analysis are carried out which showed the critical location in the network. One of the most critical location is selected for the implementation of FACTS & ESS devices. Although, in this paper, we have focused on the distributed super conducting magnetic storage system (D-SMES) device. It is the combination of SMES with IGBTs controller to give the active and reactive power according to system need. It allows the generation integration and demand response requirements and solves the issue of intermittency by aligning the power along with grid. It provides transient stability during faults, supports the voltage and frequency at critical loads and improves the power factor and power quality.

II. Distributed Superconducting Magnetic Energy Storage System (D-SMES)

Superconductor has the zero-electrical resistance when cooled below a certain critical temperature. D-SMES provides the two significant competences of active power storage and instantaneous response. One is an energy storage device which stores energy in dc magnetic field by passing the current through a coil and gives current even after the removal of voltage source. Other is IGBTs system that detects the fluctuations in the system and provide precise stability in the system. D-SMES is mainly consisted of superconducting coil with magnet, power conditioning system, cryogenic system (formation of superconductor) and control unit. During the charging, the current flows in one direction containing positive charge across the coil to store energy. The current flows through the load containing negative charge causing of discharging phenomenon. It is used to reduce the low frequency oscillations and power quality applications. It has fastest response time, rapidly switching, efficient and reliable system.

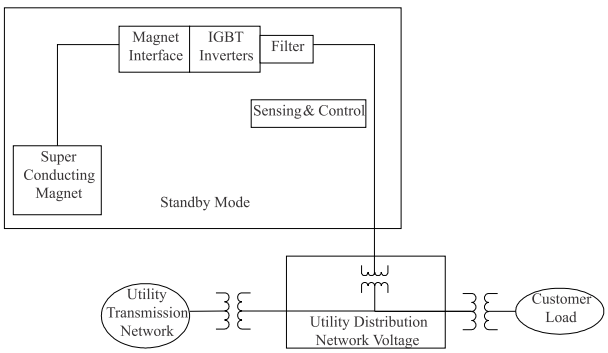

Fig 1: D-SMES

III. Power System Stability

The condition of being stable even after the disturbance in the network is the major need of the power system. The disturbance is basically due to the switching, faults and outage of the lines or equipment. These disturbances have a great impact of the voltage, frequency, and rotor angle profiles. Power system stability is mainly classified into rotor angle, frequency and voltage stability and further classified into short and long-term phenomenon.

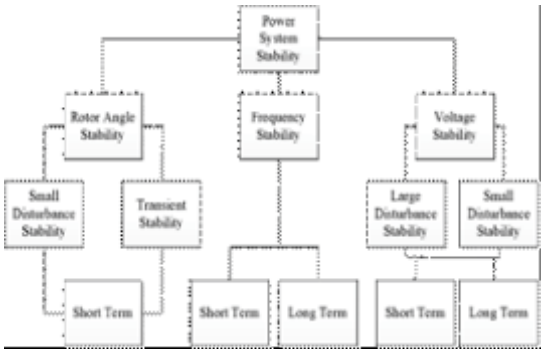

Fig 2: Power System Stability

IV. Test Case Scenario

National Grid of Pakistan is a radial network in which Northern side has Hydel power plants whereas Southern side has thermal and renewable power plants. In summer season, due to replenish of water, the hydro power plants run at their peak level. While in winter season, thermal power plants run at their maximum level. The renewable energy sources are also integrated in the network to meet the maximum demand.

We have observed that in summer season, the flow of electric power is from Northern to Southern areas whereas in winter season, the electric power flow is from southern to northern areas. Due to long radial network, the line losses are maximum in the network. It has disturbed voltage profile, reliability and stability issues so, the new lines are proposed to meet these issues. The implementation of new lines is most expensive to curtail the over loading of lines.

After the critical observation, we have observed that QESCO network is highly unstable and heavily loaded. These networks has many issues related to congestion such as voltage stability, frequency stability and angle stability. When the system of Pakistan National Grid is modelled in PSS/E then steady state analysis is studied using the Newton Raphson method. In steady state analysis, steady state performance of the system under normal (N-0) and under one-line-out (N-1) contingency conditions for on-peak and off-peak conditions for the system is observed. Circuit overloads and under/over voltages judged against the transmission design and operational criteria is highlighted to justify the need of reinforcements going to be proposed accordingly.

In accordance with the requirements of the reliability criteria, the Normal Case and N-1 Contingency Analysis is simulated throughout the system. Normal Case means when there no circuit is out of service, and Contingency means One-Circuit-Out or One-Transformer-Out as the case may be.

In Normal Case, the steady state analysis of QESCO network is studied using Newton Raphson method, which showed the critical locations of congested area. One of the critical location of congested area is Gwadar Coal PP busbar.

In given figure, QESCO network has stability issues in which current ratings are shown in boxes. The red color showed the heavily loaded branches and pink color showed the highly unstable buses.

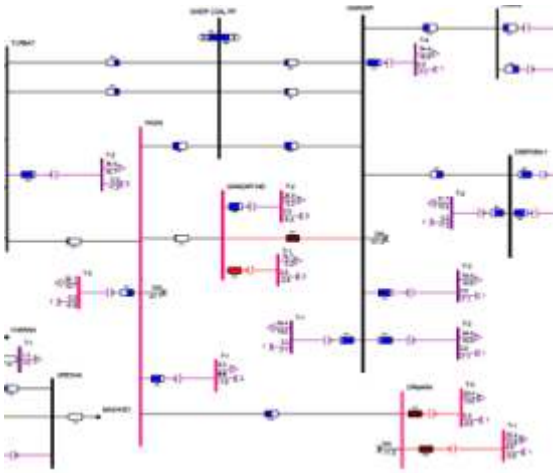

Fig 3. Loading of QESCO Network

In N-1 Contingency Case, QESCO network is more heavily loaded which is shown in pink and red color.

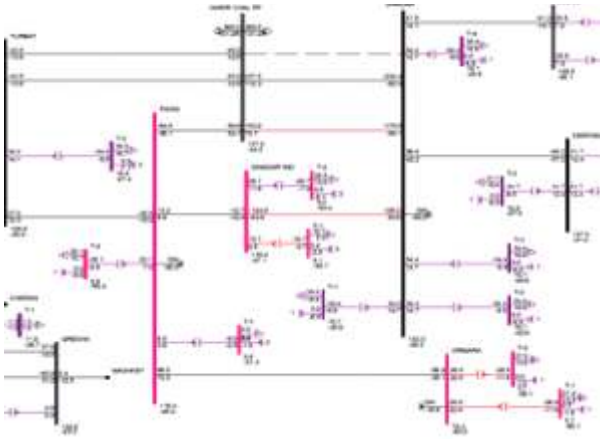

Fig 4. Loading of Congested QESCO Network

At this congested region, the stability study is carried out which showed the stability after the disturbance in the network. The stability study is investigated by following the given steps;

- Run the system for one cycle
- 3-phase (severest) bus fault is created for five cycles and then it is cleared in nine cycles
- Line is tripped from Gwadar to Gwadar Coal for twenty cycles.

The congested state under faulty situation is plotted in PSS/E by following given quantities;

1. Bus bar voltages such as Gwadar near the faulted buses
2. System frequency during and after fault conditions
3. Line power flows (MW/MVAR) through Gwadar to Gwadar Coal circuit
4. Rotor angles near the faulted transmission line, relative to the rotor angle of Tarbela

In PSS/E tool, voltage, frequency, power flows and angle waveforms are plotted against the time.

- In voltage waveform, Gwadar, Gwadar Coal PP, Pasni and Turbat are shown in red, green, blue and pink colors.
- In frequency waveform, Gwadar is shown in red color.
- In power flows waveform, the MW and MVAR of Gwadar bus bar shown in red and green colors.
- In angle waveform, Gwadar is shown in red color.

Dynamic faulty period becomes unstable and the results in the given figures showed that system voltage, frequency, line flows and rotor angle stability are not in the declared limits. Consequently the system gets unstable.

1. Voltage Waveform

At the time of fault, voltages of the bus bars are suddenly collapses and have severe oscillations unbalancing of reactive power in the system. So, it does not maintain the stable state even after the fault clearance.

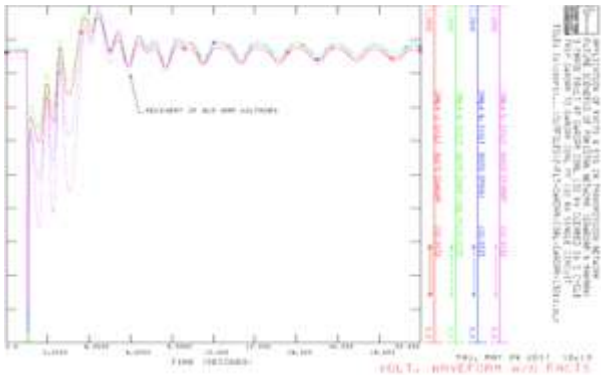

Fig 5(a): Voltage Waveform of QESCO Network

2. Frequency Waveform

At the time of fault, the frequency of Gwadar Coal bus bar has more excirsions in the system and exceed the rated limit of the frequency. It does not approach the stable state in 20 cycles after the fault clearance.

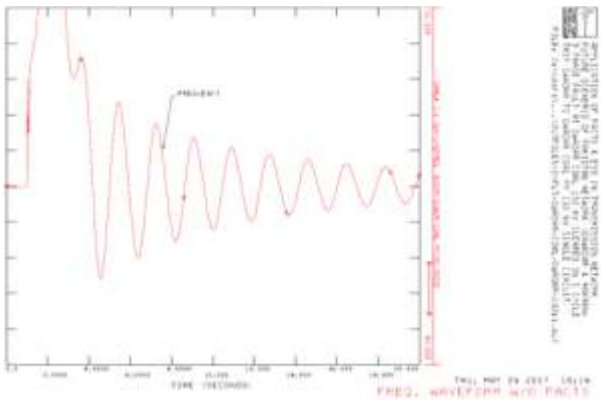

Fig 5(b): Frequency Waveform of QESCO Network

3. Power Flow Waveform

The one circuit of Gwadar to Gwadar Coal is switched thus the flow is carried out from the another circuit that is parallel to it. At the time of fault, the MW flow is drops out and its oscillation remains after the recovery of the system whereas the MVAR flow reaches its peak value and does not approach the stable state within the 20 cycles.

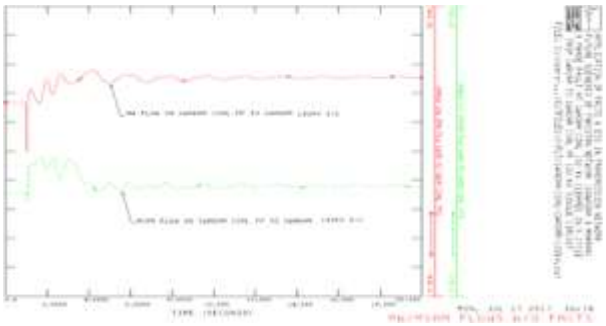

Fig 5(c): Power Flow Waveform of QESCO Network

4. Angle Waveform

At the time of fault, rotor angle reaches its maximum peak due to loss in synchronism caused by unbalancing between electromagnetic torque and mechanical torque.It does not approach the stable state even after the fault clearance.

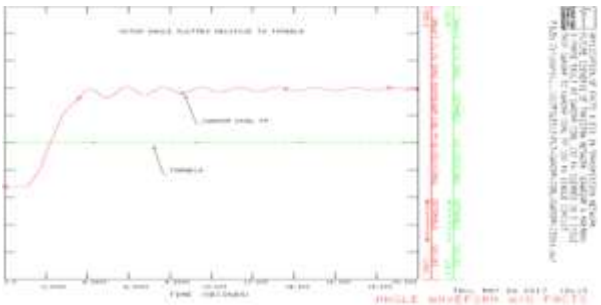

Fig 5(d): Angle Waveform of QESCO Network

These figures showed that at the time of 3-phase fault, the system voltage, frequency and rotor angle of the generator suddenly collapse too much and does not maintain their values even after the disturbance. As we have seen that congestion includes MW loading and MVAR loading. The traditional solution to MW loading is the installation of a new circuit while the solution to MVAR loading is usually installation of capacitors. However, these are not feasible or reliable solutions due to either high cost (in case of stringing new circuits) or due to nonexistent support during fault conditions (in case adding capacitors).

In the selected critical region, Gwadar is located in a remote region as far as the electrical network is concerned. There is no local generation, so it needs to draw power from the National Grid, which passes hundreds of kilometers away from Gwadar. The long transmission lines needed to transport this power need to carry high amounts of reactive power, which causes significant MVAR loading in the network. Again, the traditional solution to this scenario is the addition of transmission lines. However, this is an expensive solution, especially since hundreds of kilometers worth of transmission towers, insulators and conductors are involved. So, D-SMES is proposed for providing MWs and MVARs in the system.

V. D-SMES Modeling in PSS/E

D-SMES is the combination of SMES with IGBTs controller. It provides fast and effective control by injecting both active and reactive powers in the system. It has benefits in generation, transmission and distribution systems by improving the voltage, angular and frequency stability, damping oscillations and transmission capacity of existing system.

CDSMS1 model of D-SMES is used in this system. It is installed on 132 kV bus bar having rating of 100 MW. It provided the initial coil current of 1.05 kA and thus maintained at 0.4 kA. The magnet discharge time is 0.6 seconds which is represented in graphs. It indicated that uninterrupted and repetitive discharge according to need of system.

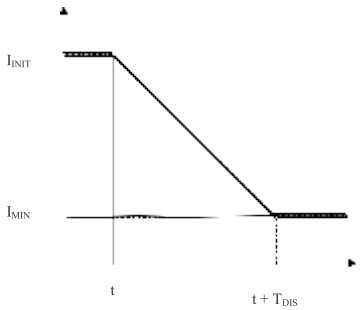

Fig 6(a) Uninterrupted Discharge

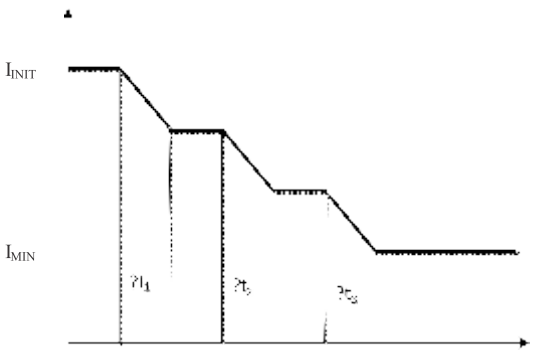

Fig 6(b): Repetitive Discharge

It injects and consumes both active and reactive power to control the voltage up to desired value in the network. It injects active power in the system by discharging the D-SMES while the reactive power injects by the IGBTs voltage source convertor.

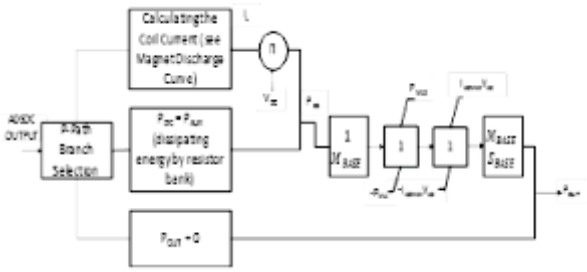

Fig 7(a): Control Diagram of D-SMES (MW Output)

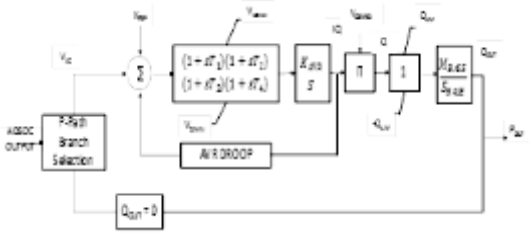

Fig 7(b): Control Diagram of D-SMES (MVAR Output)

When D-SMES is modeled in the QESCO network, the stability and quality of the system is improved which is shown in given figure.

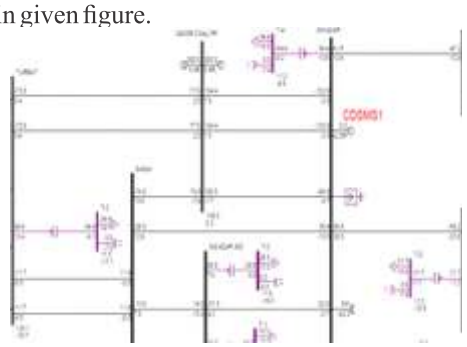

Fig 8: SLD of QESCO Network with D-SMES

These stabilities are further studied by the voltage, frequency, angle and power flow graphs.

1. Voltage Waveform with D-SMES

The voltage waveforms of nearby buses of Gwadar Coal bus bar are collapses at the time of fault. With the installation of D-SMES, the voltages of the bus bars are recovered after the fault clearance within the 6 cycles.

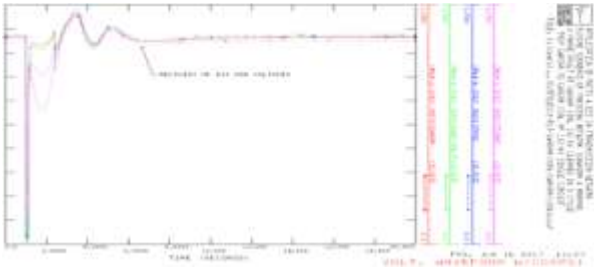

Fig 9(a): Volatge Waveform of QESCO Network

2. Frequency Waveform with D-SMES

With the installation of D-SMES, the frequency of Gwadar Coal bus bar reaches its maximum value but within its range of plot area at the time of fault due to restoration between generation and load in the network. After the fault clearance, it maintained the stable state after some oscillations within the 5 cycles.

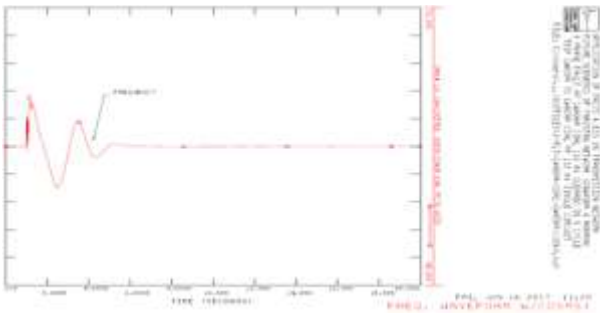

Fig 9(b): Frequency Waveform of QESCO Network

3. Power Flow Waveform with D-SMES

At the time of fault, the MW flow is drops out and its oscillation remains for 4 cycles whereas the MVAR flow reaches its peak value and approached the stable state within the 4 cycles.

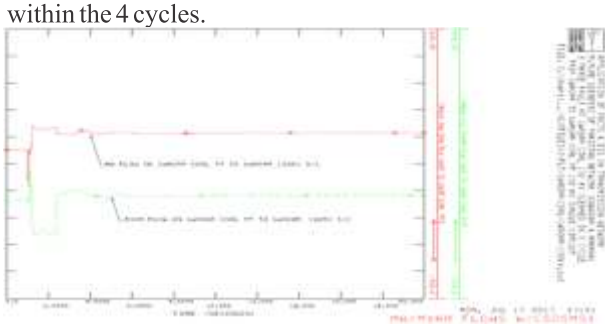

Fig 9(c): Power Flow Waveform of QESCO Network

4. Angle Waveform with D-SMES

With the installation of D-SMES, the first swing has value within the limit of plot area due to synchronism between electromagnetic and mechanical torques. After the fault clearance, the system attained the stable state within the 6 cycles.

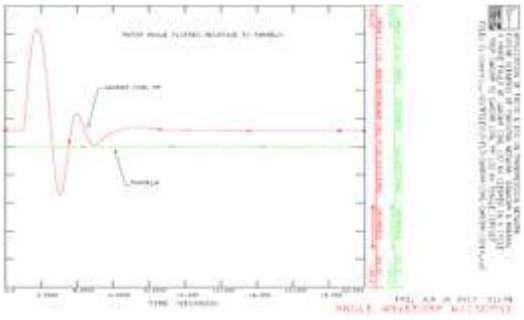

Fig 9(d): Angle Waveform of QESCO Network

5. Output Current Waveform with D-SMES

D-SMES provides the current when the sytem stability drops due to fault occurrence. After the fault clearance, D-SMES gives current untill the system achieved its stable state.

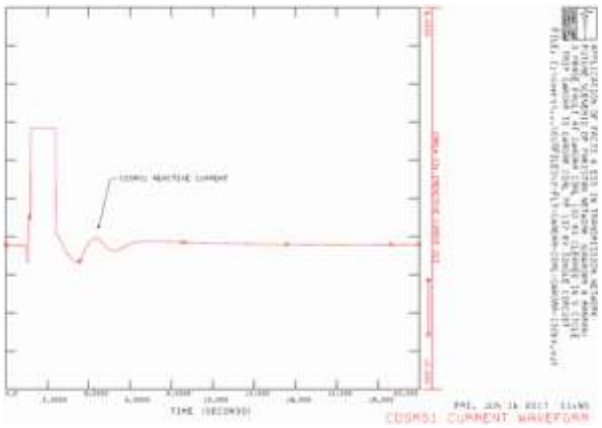

Fig 9(e): Output Waveform of QESCO Network

The dynamic stability of the network is shown by the figures of voltage recovery, frequency and angle in which they are recovered within the 10 cycles. The load flow graph showed that MW flow increases and MVAR flow decreases on the time of disturbance. The reactive output current graph showed the reactive current of the system that provides at first swing and improves the system. The output MW graph showed that CDSMS1 provides MW at the time of disturbance for transient stability.

VI. Economic Analysis

As the new line is needed for relieving the issue of congestion. It could be very expensive due to material and installation cost of tower, conductor, overhead lines, insulator strings and spacers. It also includes the right of way, line bay, civil, engineering and commissioning costs for laying the transmission lines in the network. When we calculate these costs for new transmission line, it reaches to billions. Thus by evaluating the cost of D-SMES and new transmission lines, it has a huge difference which will be pay-backed to Pakistan Nation Grid within month.

Conclusions

The issue of congestion in transmission lines is observed due to voltage, thermal limits, generation integration and load demand. It mainly deals with the active and reactive powers loadings in the lines which disturbed the voltage, frequency and rotor angle profiles. For this purpose, Pakistan National Grid is modelled in PSS/E environment in which steady state analysis showed the critical congested regions of the system. The most critical region QESCO is selected which is highly congested. In this paper, D-SMES is introduced in the congested network for mitigating the congestion issue in QESCO. It provides the active and reactive power support to the system and increases the reliability of existing system. In this way, the capability of transmission lines are enhanced and also provide the cost-effective solution.

References

[1] PSS/E 33.5 Model Library, Siemens Power Technologies International, October 2013.

[2] PSS/E 33.5 Application Program Interface, Siemens Power Technologies International, October 2013.

[3] PSS/E 33.5 Program Applications Guide, Siemens Power Technologies International, vol. 2, October 2013,

[4] PSS/E 33.5 Program Operation Manual, Siemens Power Technologies International, October 2013.

Management of Energy and Comfort Facilities in Modern Buildings using Fuzzy Logic

Muhammad Majid Gulzar[1], Bilal Sharif[1], Sajid Iqbal[2], Muhamamd Yaqoob Javed[3], Daud Sibtain[1]

[1]University of Central Punjab, Lahore, Pakistan.

[2]University of Engineering and Technology, Lahore, Pakistan.

[3]COMSATS Institute of Information Technology, Lahore, Pakistan.

Abstract

The electricity supplied by the utility grid is insufficient to meet all the load requirements due the rising trend of power utilization. For this purpose de-centralized energy generation or Micro-grid technology is used in parallel with the utility grid. Energy Management Systems (EMS) in smart buildings and homes are used to control Heating, Ventilation and Air-conditioning (HVAC) systems. Moreover, this system efficiently manage and control the usage of electricity, reduce unnecessary wastage of electrical power and at the same time provide comfort to the occupants of the building up to their desirable level. In this study, various control methods such as PID controllers, fuzzy logic controllers and multi-agent control systems are discussed for optimization of electrical energy and comfort features in modern near-zero energy buildings. In addition fuzzy logic and PID controllers for temperature regulation of airconditioning system is also presented.

***Index Terms**:*

Micro-grid, energy management system, PID controller, fuzzy logic controller, multi-agent control system, genetic algorithm, near-zero energy buildings.

I. Introduction

The demand of energy is increasing rapidly all over the world. Advancements and modernization in the power sector is the foremost important to cope with the deficit of electricity. Not only we need to generate surplus electricity but we also need to control the unnecessary wastage of energy in our everyday life. All the electricity demand cannot be fulfilled by the centralized electrical grid or macro-grid alone. We need to rely on other energy sources too, like renewable energy sources. Distributed or de-centralized energy production also known as micro-grid is a good alternative of utility grid to meet all the energy needs [1][3].

In recent decade, the residential and commercial sector is the most energy consuming sector. It is a need of the hour to optimize this energy utilization in buildings and homes besides not hampering the level of comfort of the users/occupants residing there. The factors like productivity, quality of life, health etc. of the human beings residing in a building is mainly dependent on the level of comfort that is being provided to them. The main factors or conditions of comfort of a person are related to temperature, humidity, lighting, air flow and rate of work [2]. In a broad sense, we can categorize comfort into two main classes: visual comfort and thermal comfort [3]. Thermal comfort is provided by HVAC system in buildings while lighting system is responsible for visual comfort. As the level of comfort increases, the demand of energy consumption also rises. Nowadays, when the world is facing with shortage of electricity especially in developing countries, there is a need to create a balance between utilization of electrical power and the comfort level of customers. This trade-off between energy consumption and comfort level is achieved through various intelligent control systems. These control systems include PID, fuzzy logic, multiagent etc.

According to recent policies, it is of utmost priority that all newly constructed buildings shall be energy efficient and are required to be Near Zero Energy Buildings (NZEB) [2]. This means that they shall have energy saving mechanisms in them which will prevent unwanted expenditure of electricity. Moreover, greater consumption of energy also increases the Operation and Maintenance (O&M) cost of a building. Total energy consumption of a building can be minimized by saving the surplus energy in battery storage banks. This can be achieved through proper management of electric power while at the same time ensuring the guaranteed operation of the critical loads. The energy stored by the battery storage system can be utilized later on by the essential loads [4]-[5].

This paper is organized as follows: Section II is about the literature review. Intelligent systems in building is presented in section III. Analysis and results of a fuzzy based method to control temperature of HAVC system is discussed in section IV. Discussion and future recommendation is mentioned in section V and section VI simultaneously. Section VII concludes the paper.

II. Literature Review

The major load contributors in a building are normally

associated with lighting and HVAC systems. The solar irradiation has also an indirect effect on the electricity consumption of a building. In modern buildings, dynamic shading control systems are employed to optimize the use of electricity and manage the adverse effects of sunlight, caused in terms of excess heat, in order to attain a suitable trade-off between comfort level and power consumption [6]. Change in different parameters of the room such as window size, glass transmittance, and wall reflectance can result into different configurations of the room. These different variations of the room can cause an impact on the fuzzy logic control system to achieve an optimal balance between the thermal and comfort levels in the building.

Several studies regarding various intelligent control schemes and algorithms for optimization of energy and comfort management in buildings has been conducted by different researchers. These control systems include both classical/traditional and adaptive/optimal controllers. The various types of traditional controllers are Integral (I) Controller, Proportional Integral (PI) Controller and Proportional Integral Derivative (PID) Controllers. Whereas the adaptive controllers are used where supervisory control and data acquisition system is being implemented. The optimization function of predictive controller is dependent on the value of future reference point [7][8]. Adaptive fuzzy controllers are able to change their behavior according to the external temperature, humidity and illuminance conditions and self-regulate them according to the user demand in the various buildings. The most popular adaptive controller is fuzzy adaptive controller.

Fuzzy method used to control lighting systems and it has been found to be an easy solution when optimization of lighting, thermal and comfort aspects are dealt with. It is mainly concerned about efficient improvements in energy consumptions in a room using fuzzy logic control.

An intelligent multi-agent control system for effective management of energy in commercial offices and buildings is presented in [3]. An autonomous micro-grid technology consisting of renewable wind and photo voltaic systems is used in conjunction with the conventional power supply. Airconditioning and Lighting systems being the essential entities of a building are referred to as “critical loads” while all other loads are called “non-critical loads”. The control system based on multi-layered agent topology consists of four agents: switch agent, central controller agent, local controller agents and load agent. Fuzzy logic controllers are used to control the critical loads. Fuzzy controllers tune the temperature and illumination intensities according the preferences fixed by the user. That is how energy optimization is achieved through fuzzy controllers while at the same time ensuring user's overall comfort level [9]. Furthermore, genetic algorithms are used for further energy optimization within the building, thus making it more efficient in terms of power utilization.

III. Intelligent Systems In Buildings

There are several different variations and applications of intelligent controllers in smart buildings including fuzzy logic based controllers, neuro-fuzzy logic controllers, adaptive fuzzy PD and adaptive fuzzy based PID logic controllers [10]. The block diagram of fuzzy logic controller is shown in Figure-1.

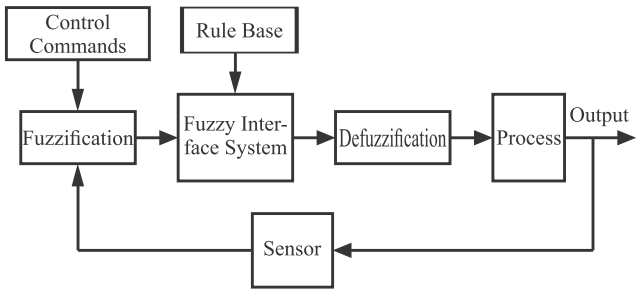

Fig. 1 Block diagram of fuzzy logic controller

A. Fuzzy Logic Based Controllers

Fuzzy control logic is actually an algorithm based on mathematical modeling. It is used to deal with uncertain conditions [1]. In fuzzy logic, the values of variables range between 0 and 1 in comparison with the crisp digital logic. Control systems based on fuzzy logic are efficient in governing complex systems, which cannot be represented in a systematic way. They are capable of taking input from the user or human operators and convert them into a linguistic, rule-based engine: the operation and control philosophy is generally governed by a set of “if-then” rules [11]-[12]. These rules allow programming of fuzzy control process based upon past knowledge and understanding, without having know-how of the involved phenomena.

B. Neuro-Fuzzy Logic Controllers

These hybrid systems arise when neural systems are used in fuzzy logic control methods. Such systems find great applications in optimization of energy in modern buildings [13].

Moreover, genetic algorithm is an optimization technique that is based on human biological genetic system and natural selection. This technique is utilized to

further optimize the energy consumption is buildings, hence reducing the total energy consumed by the critical loads in a building. This is achieved by choosing the optimized desired values of temperature and illumination instead of the values defined by the customers or building users [3]. The user's set values are adjusted for the minimum power utilization with the available power as the constraint.

C. Adaptive Fuzzy PD and Adaptive Fuzzy Based PID Logic Controllers

Such systems have replaced the conventional PD and PID controllers. Adaptive fuzzy based PD controller uses a 2nd degree equation as a reference model to determine the gains values of the controller [14]. The output of a precisely designed adaptive fuzzy PD controller is much closer to behavior of the desired model of the building. By using adaptive fuzzy PID controllers, the controller gains are selected much more accurately; so optimization results are achieved closer to the desired results.

IV. Analysis And Results of a Fuzzy Based Method to Control Temperature of HVAC System

The Figure 2 presents the PID and fuzzy logic control model for a typical building temperature control of HVAC system. The input to fuzzy controller is the error signal and the rate of variation in error or its derivation function. The output of fuzzy controllers is given as inputs to the HVAC system. The output of the HVAC system is given as a negative feedback to the controllers to make a closed-loop system. The fuzzy logic controller for temperature is given in Figure 3.

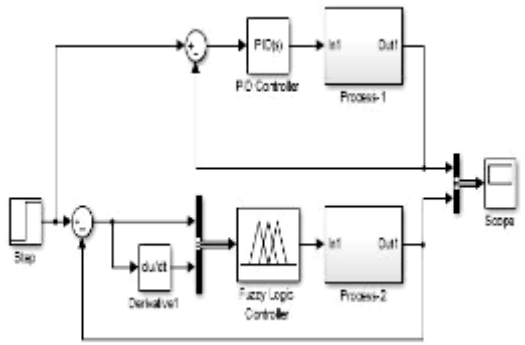

Fig. 2. MATLAB SIMULINK Model to Control Temperature of HVAC System using PID and Fuzzy Control System

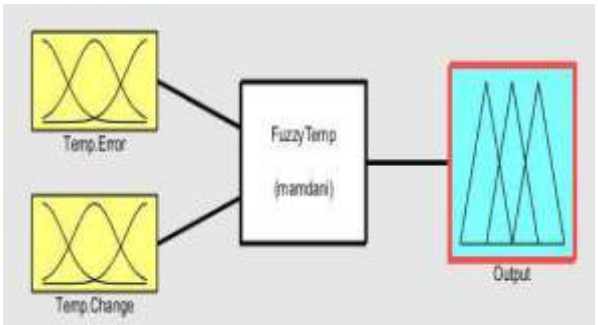

Fig. 3. Fuzzy Logic Controller for Temperature System

The input variables (temperature) in this control system are mapped into triangular membership function. The input and output variables are distributed into seven different ranges: Negative Large (NL), Negative Medium (NM), Negative Small (NS), Zero (ZO), Positive Small (PS), Positive Medium (PM) and Positive Large (PL).

The triangular input membership functions for input and output are depicted in Figures 4 and Figure 5 respectively.

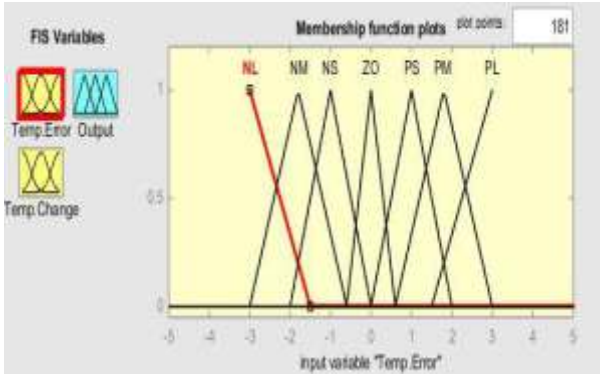

Fig. 4 Membership Function of Input

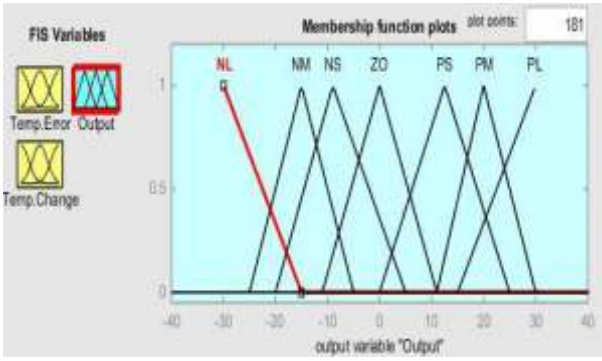

Fig. 5 Membership Function of Output

Rule development is shown in Table 1 which forms the basis of 49 fuzzy logic rules for this control system in the form of "If-Then" statements. The output of this fuzzy control system is the logical AND operation of the membership functions of two different inputs.

If the temperature error is NL and the rate of variation of error is also NL, then the output signal should be PL. According to Table 1, the rule viewer of the fuzzy logic control system is shown in Figure 6.

TABLE I. Fuzzy Logic Rules For Temperature System

Fuzzy Rules		Error In Temperature System						
		NL	NM	NS	ZO	PS	PM	PL
AE	NL	PL	PL	PM	PM	PS	PS	NS
	NM	PL	PL	PM	PS	PS	NS	NS
	ZO	PM	PM	PS	ZO	NS	NM	NM
	PS	PM	PS	PS	NS	NS	NM	NM
	PM	PS	PS	NS	NS	NM	NL	NL
	PL	PS	NS	NS	NM	NM	NL	NL

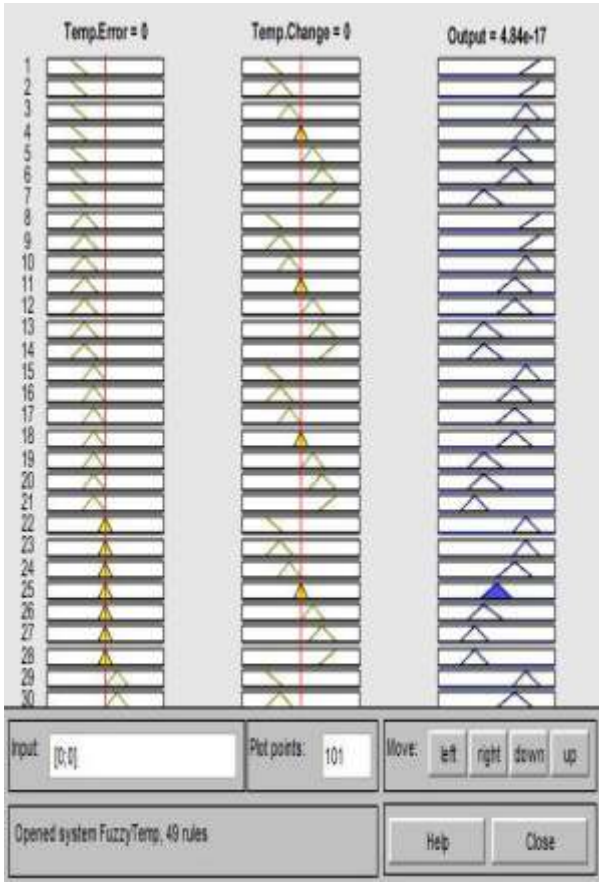

Fig. 6. Rule Viewer for Fuzzy Logic

The control surface of this fuzzy based control system is presented in Figure 7.

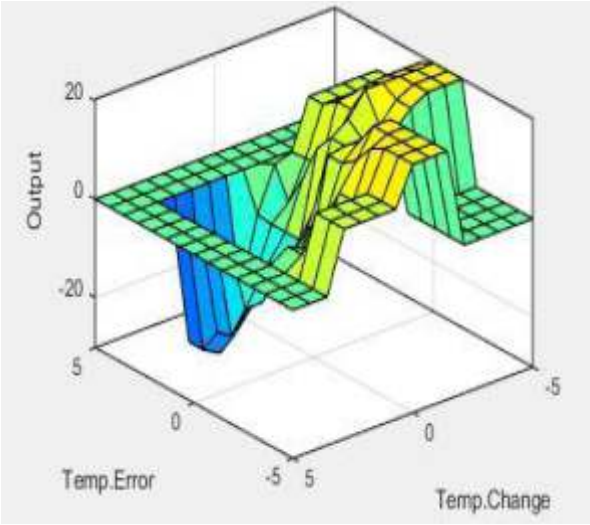

Fig. 7. Control Surface of this Fuzzy Logic Control System

Comparison of PID controller and fuzzy logic controller is shown in Figure 8. Here it can be seen that PID controller is giving more overshoot and settling time as compared to the fuzzy logic controller.

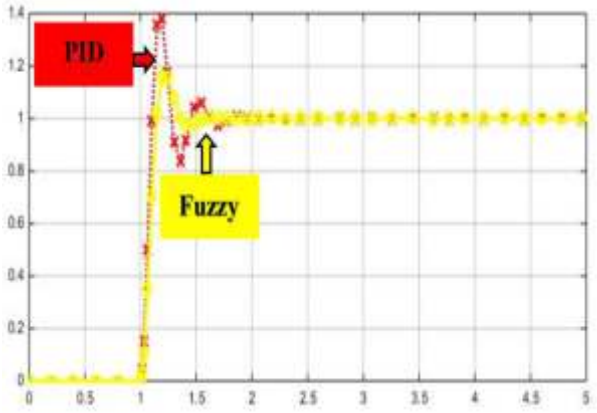

Fig. 8. Comparison of PID vs Fuzzy Logic Control System

V. Discussion

Different control methods or schemes that can be deployed for building energy and comfort management systems are discussed in this study.

Now-a-days, the controllers commonly used in buildings are based on fuzzy logic approach instead of the traditional controllers. The fuzzy controllers are based on logical reasoning which forms the basis of a rule table. Such controllers give optimal performance when the values of input and output gains are selected appropriately and the rules are defined properly. The controllers used in modern buildings are used to cut-down the increasing usage of electricity while at the same time they ensure that suitable comfort level is provided to the building occupants.

The dependence on the national grid can also be reduced by using the concept of distributed energy sources, also termed as micro-grid. Micro-grid uses renewable energy sources such as wind power or solar energy. The integration or dis-connection of micro-grid with national grid is also carried out with the help of fuzzy controllers.

Agent based control systems use more than one fuzzy logic controllers that serve different purposes. In this type of system, one is the main controller which performs the overall control actions of the whole system. The other controllers are used for controlling or switching the loads, coordinating the integration of utility grid with the micro-grid and controlling various process variables.

VI. Directions For Further Work

The work presented in this report can further be extended by the establishment of a more comprehensive and precise identification of input statistics and more precise selection of fuzzy logic rules. The system could also be tested under other climatic conditions and different orientations of lighting and shading effects to reduce emissions of carbon dioxide, increase the indoor air quality and decrease the consumption of electricity in the buildings.

Although the fuzzy controller is robust, it may not be

optimal for all operating conditions when membership functions or fuzzy rules are not properly selected. Thus, a self-tuning mechanism needs to be incorporated in the fuzzy control method in order to ensure its operability at its most optimal configuration. Self-learning or tuning can be achieved by the integration of fuzzy logic control system with the neural networks. Hence, more research in this area needs to be carried out.

VII. Conclusion

Fuzzy logic control system is a useful method to efficiently manage and control the energy consumption in a building while at the same time providing suitable comfort level to the building users. Its performance is far better as compared to the conventional PID controllers. Such a controller achieves the transient response at a faster rate and it has less overshoot, thus making its steady-state response more stable in contrast to PID controller. It design is also independent of a specific operating quiescent point as it does not require to be modeled mathematically. Such systems are based on logical decisions and artificial intelligence.

It is also worth mentioning from this study that the use of distributed energy sources can lower the dependence on the utility grid. The control and integration of the micro-grid with the main grid and overall system control is made possible through the use of intelligent fuzzy controllers.

References

[1] Soufiane Merabti, Belkacem Draoui and Fatah Bounaama, "A Review of Control Systems for Energy and Comfort Management in Buildings," in 8th International Conference on Modelling, Identification and Control (ICMIC), 2016, pp. 478-486.

[2] Tokuhashi, Kazumasa, and Yuji Ogata. "Building management device, wide area management system, data acquiring method, and program." U.S. Patent Application 15/308,881, filed March 23, 2017.

[3] Muhammad Yaqoob Javed, Muhammad Majid Gulzar, Syed Tahir Hussain Rizvi, Arslan Arif. "A Hybrid Technique to Harvest Maximum Power from PV Systems under Partial Shading Conditions", IEEE International Conference on Emerging Technologies (ICET), Islamabad, Pakistan, pp 1-5, October 2016.

[4] Fabio Bisegna, Chiara Burattini, Matteo Manganelli, Luigi Martirano, Benedetta Mattoni and Luigi Parise, "Adaptive Control for Lighting, Shading and HVAC Systems in Near Zero Energy Buildings," in 16th International Conference on Environment and Electrical Engineering (EEEIC), 2016.

[5] Muhammad Yaqoob Javed, Ali Faisal Murtaza, Qiang Ling, Shahid Qamar, Muhammad Majid Gulzar, "A Novel MPPT design using Generalized Pattern Search for Partial Shading", Energy and Buildings, Vol. # 133, pp 59-69, December 2016.

[6] Smitha S.D., Dr. J.S.Savier and Fossy Mary Chacko, "Intelligent Control System for Efficient Energy Management in Commercial Buildings," in International Conference on Microelectronics, Communication and Renewable Energy, (ICMiCR), 2013.

[7] Shahram Javadi, "Energy Management in Buildings Using MATLAB," Chapter No. 9 from the Book "MATLAB – A Ubiquitous Tool for the Practical Engineer" Edited by Clara M. Ionescu and Published by InTech, 2011.

[8] Zheng Xiaoqing, "Self-Tuning Fuzzy Controller for Air-Conditioning Systems", M.Sc. Thesis, 2002.

[9] P. Ramanathan, "Fuzzy Logic Controller for Temperature Regulation Process," Middle-East Journal of Scientific Research 20 (11), 2014, pp. 1524-1528.

[10] Drees, Kirk H. "Building management system with fault analysis." U.S. Patent 9,753,455, issued September 5, 2017.

[11] Zhang, Shengqi, Yateendra Mishra, and Mohammad Shahidehpour. "Fuzzy-logic based frequency controller for wind farms augmented with energy storage systems." IEEE Transactions on Power Systems 31, no. 2 (2016): 1595-1603.

[12] Haoran, Z. H. A. O., W. U. Qiuwei, W. A. N. G. Chengshan, Ling Cheng, and Claus Nygaard Rasmussen. "Fuzzy logic based coordinated control of battery energy storage system and dispatchable distributed generation for microgrid." Journal of Modern Power Systems and Clean Energy 3, no. 3 (2015): 422-428.

[13] Hannan, M. A., Zamre Abd Ghani, Azah Mohamed, and M. Nasir Uddin. "Real-time testing of a fuzzy-logic-controller-based grid-connected photovoltaic inverter system." IEEE Transactions on Industry Applications 51, no. 6 (2015): 4775-4784.

[14] Zhou, Qi, Lijie Wang, Chengwei Wu, Hongyi Li, and Haiping Du. "Adaptive fuzzy control for nonstrict-feedback systems with input saturation and output constraint." IEEE Transactions on Systems, Man, and Cybernetics: Systems 47, no. 1 (2017): 1-12.

Comparative Analysis of GSM and Internet Based Home Automation Systems

Rab Nawaz Maitlo[1], Nafeesa Bohra[2], Komal Memon[3], Saddar Uddin Memon[4]

[1,2,3,4] Department of Telecommunication Engineering
Mehran University of Engineering and Technology Jamshoro Sindh, Pakistan

Abstract:

Home Automation System (HAS) is gaining popularity because of its countless advantages. Home automation refers to the monitoring , controlling and automation of home appliances remotely. This paper deals with comparative analysis of GSM and Internet based HAS. The performance has been analyzed on the basis of cost, security, real time monitoring, status, user friendly environment, Graphic User Interface(GUI) etc. The Home Automated System (HAS) based on Internet not only controls but also provide real time monitoring and status of home environment through sensors whereas GSM based home automation only control home appliances but not provide real time status of appliances. The GSM based HAS is more secure as compared to Internet based Home Automation System (HAS). GSM based HAS sets a Pin code on SIM (Subscriber Identity Module) which is inserted in GSM module and also accurate AT (ATtention) commands which is given in program while Internet based system requires webpage to login through personal Gmail account. Internet based Home Automation System (HAS) has user friendly GUI which shows easy ON/OFF buttons for home appliances and real time graphs of sensors data. Whereas in GSM based HAS only define SMS format for user. GSM based system is cost efficient as compared to Internet based system. Besides all these advantages including cost efficiency, GSM based HAS lacks in providing the today's most advanced and more innovative HAS features of real time monitoring and status of home environment through PIR Motion and LM35 temperature sensors.

Keywords:

Home Automation, Arduino, Internet, GSM

I. Introduction:

Automation is the today's reality, with more things happening automatically every day, usually the basic task of turning certain appliances ON/OFF, even remotely or close proximity. When the machine completely takes over the equipment, the process of controlling, monitoring and reporting the equipment becomes more important. We are increasingly giving up the ability to do simple but routine tasks, while we need to maintain as much control over automated processes as possible. Automation reduces the possibility of human judgment but does not completely eliminate it.[1].

Home automation refers to the home that improves the quality of life of residents by promoting a flexible, relaxed, healthy and secure environment [2]. Home automation not only means reduced manpower but also increases system efficiency and save time [3]. Smart Home is an advanced technology that makes homes intelligent and automated, allowing sensors to change by adopting environmental changes [4].

Home Automation Systems (HAS) are designed to monitor and control various Home appliances can be accomplished through various communication methods, such as; wireless LAN technology, dial-up modems, private radio networks, satellite communications, Bluetooth, Zigbee, RF and more. All these system are efficient but not cost-effective. In the proposed research, the main focus is to analyze the performance of two remotely controlled Home Automation Systems (HAS) that provide efficient cost effective solution. The HAS we are focusing on are:

- Internet
- GSM

Both methods are designed for users who want to remotely access Home appliances. Therefore, the main goal of our use of the GSM network for home-to-user communications is its broad coverage, making the entire system almost always online. Another advantage of using GSM network in Home Automation is its highly secure communication that provides maximum reliability so that the information sent or received is not monitored by eavesdroppers.

Although using the GSM network has all these important advantages over other communication methods, it will be limited in real-time monitoring and in the home environment status. Real-time monitoring has always been an important function that can be used in Home Automation Systems (HAS) Therefore, we use an Internet-based home automation system that alerts the user when any changes in the Home environment state occur [5].

The proposed idea introduces the concept of comparison of two Home Automation System (HAS), which are Internet based HAS and GSM based HAS. The use of sensors in home automated system for monitoring and collecting their data on web server and alerting the owners when necessary changes should be made is the key concept for a smart Home Automation System. In this comparative analysis system, the two system's different performance parameters are compared such as: cost, security, real time monitoring, status, user friendly environment, Graphic User Interface (GUI) etc. Two systems are controlled and monitored remotely using Internet network and GSM cellular network as shown in figure 1.

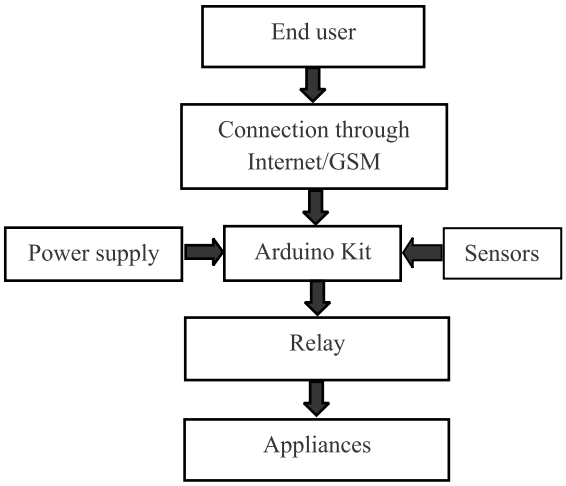

Figure 1: System block diagram [6].

The Arduino sends the collected data to the Web server. This proposed system would be able to monitor Home environment in real time and uploads data to the website. This paper is divided into the following main parts: the first part introduces the concepts, the second part describes the related work, the third part describes the prototype design and methods, and the fourth part discusses the results and comparisons. The fifth part concludes the paper and gives directions for the future.

II. Related Work:

Kotiyal et.al in [7], has developed Arduino based web server is used instead of PC based web server. Without using a computer, Idea is used to monitor and control the maximum number of home appliances or industrial equipment. Different sensors installed in the workplace helps to sense real-time environmental conditions such as temperature, light, and humidity. Web server provides a website for hosting where client can request for services.

Pawan Singh et.al in [8], has used GSM technology to solve the problem of range limitation for many technologies like Bluetooth and Zigbee. In this system, home appliances are controlled and accessed via SMS. So this technology provides a cost-effective solution for remotely controlling household appliances. The system is wireless, so it is cost-effective and easy to install.

David et.al in [9], has used Internet for communication with end user and Home appliances. In this research, it is implemented using the Arduino as a miniature web server, through which it connects hardware design, receives status updates from them, and sends control information to the microcontroller.

Shah et.al in [10], has made an approach to make the most efficient low-cost system that can control home appliances in the largest range. In the process, he made a system that can switch 15 appliances from a single remote location. The system also includes a GSM modem that will notify the owner of the relationship between the current switch ON or switch OFF state of the appliance and its predefined specific mobile phone number.

III. Prototype Design and Methodology:

This research aims to perform the performances analysis of two Home Automation Systems one is Internet based and second is GSM based and make comparison of two systems. It mainly focuses on monitoring and controlling household appliances through the Internet and GSM cellular networks. The system consists of two main parts: a hardware interface module and a software communication module. The first part consists of: Arduino UNO microprocessor, Wi-Fi module, GSM module and relay module. The microprocessor is the central device that connect the Wi-Fi module and GSM module, and receives instructions to monitor and control the home electrical appliances. The server and GSM cellular network handles the communication between the end-user and microprocessor, thus monitoring and controlling the appliances remotely. The software communication module uses a webpage as the frontend, which serves as an interface to the user to communicate with the microprocessor. It presents a list of home appliances with which the user can interact.

Arduino and server program for Internet based HAS:

The software communication part also contains Arduino IDE programming with Internet network to communicate with cayenne server. The program is make

with Token number given by server when we create account on server. The server is connected with the system through commands in command prompt.

Arduino and GSM module program for GSM based HAS:

Arduino IDE programming with GSM module to communicate on GSM cellular network. The GSM module works on AT commands for example to make call, AT command for call is ATD+92XXXXXX. This +92XXXXX shows the number which you want to call from GSM module. According to these different AT command we set a program in Arduino IDE to make communication possible of Arduino and GSM module.

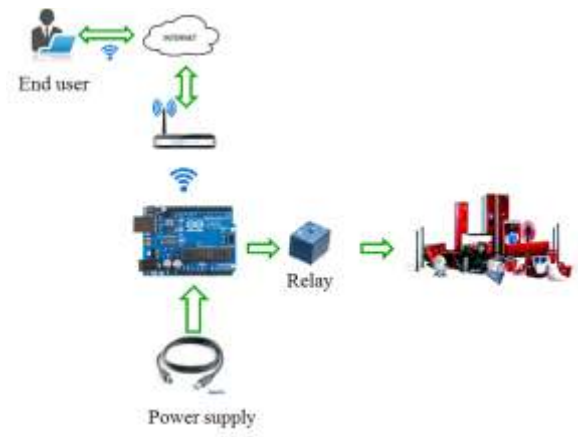

Figure 2a. Internet based HAS Architecture

Figure 2a shows the architecture of Internet based Home Automation System. In which it show that end user is connected with Cayenne (server) through Internet by server URL. After the connection with end user and Cayenne server is established successfully. Now program the Arduino with Token given by Cayenne server and then connect the Arduino serially with ESP8266 Wi-Fi module so as to Arduino communicate with Internet.

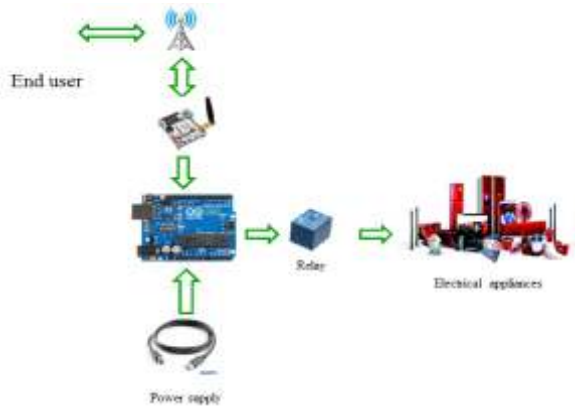

Figure 2b. GSM based HAS Architecture

Figure 2b shows the architecture of GSM based Home Automation System. In which it show that end user is connected with GSM Cellular network with phone. Now to communicate Arduino to GSM Cellular network, we used A6 GSM module and connect serially through RX and TX pins. A6 GSM module works on AT commands so in order to program Arduino we use different AT commands to set program for controlling appliances with Arduino microcontroller on GSM cellular network.

Arduino and Relay connection and programming:

In this case, the electrical equipments that are going to be controlled are LED lights and Fan. Arduino UNO is firstly programmed to communicate with the relay. It is designed as a controller to control the relay that act as a switch. The relay is used in this circuit because it is an electric switch that can be directly connected to the output. Relay switch connections are usually marked as Command (COM), Normally Closed (NC) and Normally Open (NO). In switched ON state, the circuit will be connected to COM and NC. On the other hand, the circuit will be connected to COM and NO in switched OFF condition.

IV. Results and Comparison:

Two systems (GSM and Internet Based HAS) were proposed to test and determine the accuracy of the prototype.

The prototypes were tested in different parameters.

1. ON/OFF status of Home Appliances
2. Sensors data
    a. PIR Motion sensor
    b. LM35 Temperature sensor

1. ON/OFF status of Home Appliances:

Following bar graphs show the ON/OFF trialed data taken from GSM and Internet based Home Automated systems.

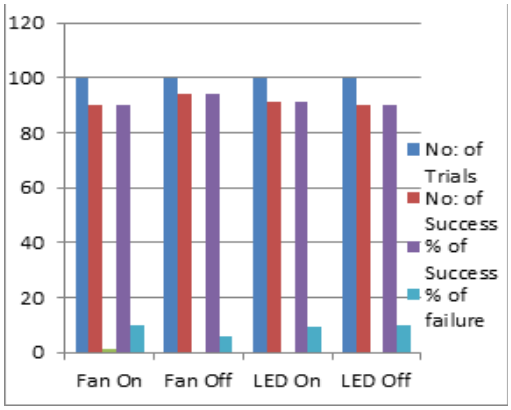

Figure 3. ON/OFF comparison of Internet system

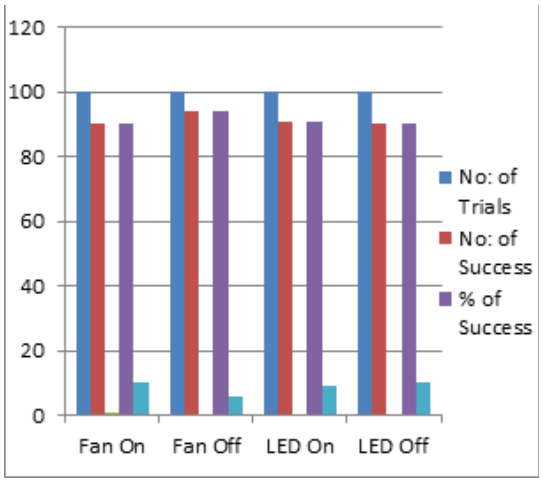

Figure 4. ON/OFF comparison of GSM system

Figure 3,4 shows ON/OFF comparison of electrical appliances(Fan and LED lights). On right side of graphs shows the graphs of Internet bas HAS and on left the graph of GSM based HAS. In which blue bars show the number of trials(initially 100 trials are taken). Whereas red and purple color bars show the number and percentage of success respectively. It can be observed that the average ON/OFF percentage out of 100 trials in Internet based Home Automation system(HAS) is 90.75%, while in GSM based HAS it is 94% for the same number of trials (100 trials).

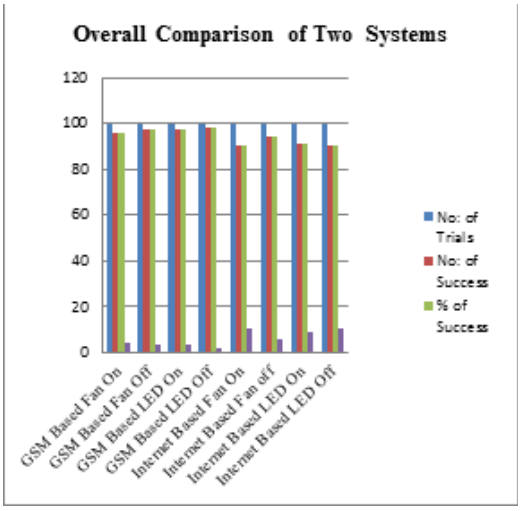

Figure 5.Overall comparison of Internet and GSM based systems

Figure 5 shows the overall comparison of GSM and Internet Based Home Automation system. In which blue color bars show number of trials for ON/OFF of Fan and LED lights. Results are based on 100 trials out of which ON/OFF percentage of Home appliances are taken. Whereas red color bars show number of success of LED lights and Fan ON. Green color bars show the percentage of successively switched ON of Fan and LED lights. It can be observed that the average percentage of success for GSM is 94% which is better than percentage of Internet based HAS which is 90.75%.

Table 1. Cost comparison table of Internet based HAS

Internet Based HAS	
COMPONENTS	COST(Rupees)
Arduino UNO	600
ESP8266 WiFi Module	400
2 Channel Relay	100
PIR Motion Sensor	250
LM35 Temp: Sensor	80
LED	100
Fan	120
Bread Board	100
Battery 9V	30
Jumper Wires	100
Net Package(Per Month)	500
TOTAL	2380

Table 2. Cost comparison table of GSM based HAS

GSM Based HAS	
COMPONENTS	COST(Rupees)
Arduino UNO	600
GSM Module	1800
2 Channel Relay	100
LED	100
Fan	120
Bread Board	100
Battery 9V	30
Jumper Wires	100
SMS Package(Per Month)	100
TOTAL	2950

Cost comparison for both Internet and GSM based HAS is given Table 1 and Table 2 respectively. It is clearly observed from Table 1 and Table 2 that the cost of GSM based HAS is higher than Internet based HAS but the running cost per month of GSM based HAS is lower than Internet based HAS.

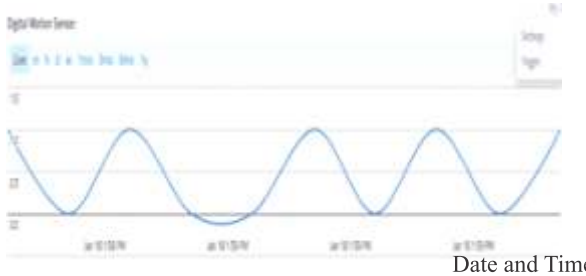

Figure 6. PIR motion sensors

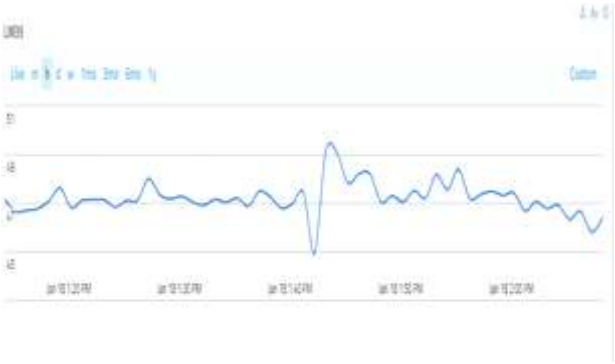

Figure 7. LM35 Temperature sensors

Figure 6,7 show graphs of PIR Motion sensor and LM35 Temperature sensor whose data is continuously been uploaded on web server (cayenne). Readings are taken during the day time on 18 Jan 2018. Readings of PIR Motion sensor goes to 0 when it detect no motion, whereas, PIR Motion sensor reading goes to 1 as it detects motion. LM35 Temperature sensors senses the temperature which is 45 degrees Fahrenheit approx. X-axis shows the Date and time on the graphs of PIR motion and LM35 Temperature sensors respectively, whereas Y-axis indicates the motion and temperature values of both PIR motion and LM35 temperature sensors respectively. We used these two sensors data and upload it on web server for real time monitoring and status of Home. With the help of this, Home appliances are also been controlled according to the environment of Home.

Figure 8. GUI of Internet based system

F

Figure 8 shows the GUI of Internet based HAS and Figure 9 shows GUI of GSM based HAS. GUI of Internet based HAS shows simple and user understandable buttons of Fan and LED lights. Whereas GUI of GSM based HAS only shows the SMS format for (ON/OFF) of Fan and LED lights which is neither user friendly GUI nor simple and do not provide fast switching like Internet based HAS.

Table 3: Performance Comparison of GSM and Internet Based HAS

HAS	Cost	Security	Real Time monitoring and status	Availability	GUI	Performance
GSM	Low	High	Low	High	No	Low
Internet	High	Fair	High	Fair	Yes	High

Table 3 shows the performance parameters of both systems(GSM and Internet based HAS). Table 3 clearly shows that although GSM based HAS is low in cost and have high security but it lacks in real time monitoring, no GUI and overall performance is also low as compared to that of Internet based HAS.

V. Conclusion and Future Work:

In this research, we have successfully tested both GSM and Internet based HAS hardware and have also performed comparative analysis of both the systems. Arduino is integrated with two sensors (PIR motion and LM35 temperature) and uploaded their data to web server to check environment of home and to control home appliances according to home environment. It is clearly seen from Figures, Graphs and Tables that the Internet based HAS is more innovative and meets with the requirements of today's Home Automated System as compared to GSM based HAS is more secure but it is not capable of providing real time monitoring. The designed system can be implemented in Home to monitor real time status of home environment and control Home appliances according to environment changes. Designing and implementation of such kind of systems can improve the outcomes of automated systems. For the testing purpose initially the system is based on two appliances (FAN and LED) however, more appliances can be added into the system and is left as future work and results can be analyzed accordingly.

Acknowledgment:

This research work is carried on at IoT Laboratory, Dept. of Telecommunication of Mehran University of Engineering and Technology, Jamshoro, Sindh, Pakistan

References:

[1] Alkar, Ali Ziya, and Umit Buhur. "An Internet based wireless home automation system for multifunctional devices." *IEEE Transactions on Consumer Electronics* 51, no. 4 (2005): 1169-1174.

[2] Elkamchouchi, H., and Ahmed ElShafee. "Design and prototype implementation of SMS based home automation system." In *Electronics Design, Systems and Applications (ICEDSA), 2012 IEEE International Conference on*, IEEE, (2012). pp. 162-167.

[3] D.V.Shinkar , Pallavi B. Bhole , Pratiksha R. Giram , Reshma Y. Kale , Harshada V. Patil. " A Comparative Study and Implementation of Smart Home Automation and Security. " *International Journal of Innovative Research in Computer and Communication Engineering* , Vol. 5, Issue 2, February (2017).

[4] Behera, Amiya Ranjan, Jyoti Devi, and Deepta Sundar Mishra. "A comparative study and implementation of real time home automation system." In *Energy Systems and Applications, 2015 International Conference on*, IEEE, 2015. pp. 28-33.

[5] Yuksekkaya, Baris, A. Alper Kayalar, M. Bilgehan Tosun, M. Kaan Ozcan, and Ali Ziya Alkar. "A GSM, Internet and speech controlled wireless interactive home automation system." *IEEE Transactions on Consumer Electronics* 52, no. 3 (2006).pp. 837-843.

[6] Sarkar, Anirban, Sadia Sultana, and Md Habibur Rahman. "A Smart Control System of Home Appliances using SMS." *Global Journal of Research In Engineering* (2017).

[7] Kotiyal, Bandanawaz. "Web Server Based Home Automation." In *Electrotechnical Conference,* (2015).

[8] Pawan Singh, Krupa Chotalia, Sanket Pingale, and Sandhya Kadam. "A Review Paper on Smart GSM Based Home Automation System." *International Research Journal of Engineering and Technology (IRJET),* (2016).

[9] David, Nathan, Abafor Chima, Aronu Ugochukwu, and Edoga Obinna. "Design of a home automation system using arduino." *International Journal of Scientific & Engineering Research* 6, no. 6 (2015).pp. 795-801.

[10] Shah, Jalpa, Bhavik Modi, and Rohit Singh. "Wireless home appliances controlling system." In *Electronics and Communication Systems (ICECS), 2014 International Conference on*, IEEE, (2014). pp. 1-6.

Multi-Agent Surveillance and Threat Evaluation for Indoor Environment

Ali Nasir, Adeel Arif
Electrical Engineering Department University of Central Punjab Lahore, Pakistan

Abstract

This paper discusses a hierarchical multi-agent architecture for implementing semi-automated surveillance in the indoor environment. Specifically, a scientific lab environment is considered for demonstration purposes. A three-layered multiagent architecture of the surveillance system is presented with local intelligence, global intelligence, and human supervision. The internal architectures, models, and algorithms for local and global intelligence agents are presented and discussed in the context of surveillance of a scientific laboratory. Possible issues in practical implementation, scaling, and advancement of the proposed approach are also discussed in the paper.

Keywords

Multiagent systems; hierarchical decision making; video surveillance

I. Introduction

The trend of video surveillance has grown rapidly due to the increasing threats to public safety. In this regard, millions of security cameras have been installed in different countries. Pakistan government is also realizing the importance of video surveillance and in this regard, more than 1800 surveillance cameras have been installed recently in Islamabad under the "safe city" project. Thousands of cameras are to be installed in other major cities of Pakistan as well. We are past that point where we discuss whether we should have surveillance cameras or not. The major question to ask right now is how to make the surveillance system efficient and effective.

The traditional way of surveillance where guards watch live footage on screens in a control room is no longer feasible. For example 1800 cameras in Islamabad require 450 guards to monitor (assuming 1:4 ratio for cameras versus guards). Ideally, 1800 screens are also required but if the view is split screened, maybe 450 screens could be used (4 views per screen). Even then, each guard has to take a small five to ten minute break in each hour for maintenance of health. Timely response and identification of threat is difficult in such circumstances. Therefore aid of technology (especially artificial intelligence) is required to assist traditional surveillance system.

Fortunately there has been plenty of work on video surveillance in different areas e.g. object detection, object tracking, behavioral analysis, and event detection [5][6]. Surveillance in particular has acquired the attention of researchers for a long time now. Most of the literature on surveillance is on surveillance of public places and outdoor environment [1][2]. Specifically, surveillance problem using drones (quadrotors or fixed wing unmanned aerial vehicles) has been addressed by [1][2][4] and many others. Multiagent surveillance with distributed intelligence has been proposed by [7] where one major point to ponder is whether the information from various cameras shall be merged by each of the "agents" or only some agents. Furthermore, which agent should use which information (or whether all agents should use all information) is an important issue to address especially when the available memory and computational power is limited. This issue is somewhat addressed in [7] by classifying information to be communicated as "relevant" and "irrelevant". But there is another systematic way of addressing the issue of information handling and that is to have a supervisory agent with superior computational and data storage capability.

In this paper, we propose a novel idea and algorithms for indoor video multiagent surveillance. The novelty in the approach is in the use of three-layer architecture resulting in hierarchical multiagent surveillance system. Furthermore, the approach is tailored for the requirements and constraints of indoor environment as opposed to much generic approach found in existing literature. Major benefit of focusing on indoor problems is that the space of possibilities is much more limited as compared to an open or public area. Due to this, we can afford to use tools in artificial intelligence that are computationally expensive and hard to implement on problems with large state space.

II. The Proposed Architecture

A. System Level Architecture

The problem of surveillance in general is too broad to be addressed in one paper. There are many aspects of surveillance that form proper research areas such as activity analysis, object (or face) detection and identification, object (or human) tracking, camera calibration and multi-camera topology definition [6]. Most of the algorithms involved in such research involve image processing and artificial intelligence. This paper is concerned with the artificial intelligence part of the problem where inference about the situation (or scene) is drawn based on the processed image data. Specifically, we propose a multiagent approach for autonomous surveillance. A multiagent approach has been discussed in the past [3].

Approach in [3] presents a more generic perspective and the use of multiagent is mainly to distribute the intelligence and hence the computational burden. The approach we propose however is intended for more than just distribution of intelligence, we also divide the intelligence into two hierarchical levels i.e. local

intelligence and global intelligence. Fig. 1 shows the basic architecture of the surveillance system that represents the proposed hierarchical multiagent intelligence. Fundamentally, the decision making and intelligence in the proposed system is at three levels where two levels are autonomous and the highest level is manual involving human security officials. This is one other unique feature of our proposed approach i.e. the intelligence involved is not entirely that of computerized software. Having security officials can save complex decisions and remove uncertainties which otherwise would be hard to deal with. The proposed surveillance system works in the following manner. Image or raw data is gathered by the cameras. The data is converted into digital form and forwarded to the local intelligence algorithms for further processing. The local intelligence agents inspect the data for presence of any of the predefined features of interest. All information obtained at local agents is forwarded to the global agent where rigorous analysis is performed to correlate information and determine the overall situation. After processing the local information, the global agent generates alarms or warnings for the security officials and low level processing commands for the local agents. Low level processing commands are intended for further elaboration on a specific feature of interest. The security officials act according to the alarms and warnings and update the global agent about the situation e.g. threat taken care of or threat found to be nonexistent. Global agent can also learn based on the feedback from the security officials in response to specific alarms and warnings.

Fig. 1: Surveillance System Overview

The concept of hierarchical multiagent surveillance described above has certain advantages over the conventional surveillance and the multiagent system proposed in [3]. For example due to the hierarchy, the computation at the local agents is simplified because each agent has to process information obtained by its own designated sensors only. This is useful advantage since each local agent may not have infinite backup power and it is usually not feasible to install big computing devices at each local agent location. On the other hand, global agent could be a state of the art computer placed in the control room with ample backup power to ensure uninterrupted operation of the system. Furthermore, since all agents communicate with one global agent, the communication equipment required to implement the system is also simplified. Finally the involvement of human intelligence layer saves the global agent from complex detailed analysis that is difficult to do using the limited information obtained from the local agents. It is relatively easier for a computerized agent to detect an ambiguity whereas determination of the exact nature of ambiguity may not be easy to find in all situations. In such cases, the global agent can generate a warning and the human security officials can confirm or reject the presence of a threat. Based on human feedback, the global agent can learn about various situations thus improving the efficiency of the system.

B. Agent Level Architecture

At the agent level, we propose the use of three-tier computational intelligence architecture [8] with some modifications to suit the surveillance application. The original three-tier is intended for spacecraft operations with three layers called the controller, the sequencer, and the deliberator. In surveillance, we need different architectures for local and global agents. For the local agents, the computational layers are the object detection, object identification, and the activity analysis layer. Fig. 2 shows the three-tier architecture for local agent. Note that each agent may have different routines specific to the detection of various objects. Similarly, object identification and activity analysis may be done using more than one scheme. Purpose of having multiple methods is that not all objects and activities can be identified using a single algorithm.

Fig. 2: Local Agent Architecture

Having the three tier architecture proposed above fits smoothly with the surveillance system presented in Fig. 1. Specifically, the commands to the local intelligence shall determine which object detection, identification, and activity analysis algorithms shall be processed. For the global agent, the three-tier architecture is shown in Fig. 3. Note that the three layers here are different i.e. correlation analysis, threat evaluation, and calculation of alarms and commands. Correlation analysis in the global agent is performed to determine the consistency between the states of the cameras with overlapping or adjacent fields of view. Once the correlations analysis is performed, the evaluation of threat is performed. Different threats are evaluated using different algorithms (hence the multiple blocks of threat evaluation).

Finally, the alarms are generated for the threats that are fairly certain (and warnings could be generated for ambiguities). Also generated at the top layer in the global agent are the commands for the local agent to perform a targeted analysis of certain objects or activities.

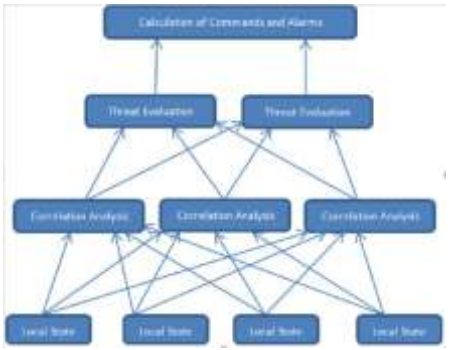

Fig. 3: Global Agent Architecture

III. Modeling and Algorithms

Before developing algorithms to carry out the tasks involved in different layers presented in the previous section, it is required to develop a mathematical model of the environment. There can be infinitely many possible ways to model an environment. Furthermore a model can be as complex as one desire. But here we stick to a simplest possible model that suffices two objectives. First is the detection of an intruder, and the second is the evaluation of a threat. We assume that the surveillance is to be done inside a research lab. We further assume that all officials working in the lab are known and the timings of the lab are also known. Based on the above assumptions, we consider the following variables in the model for a local agent

$$
\begin{aligned}
&S = \{S_1, S_2, ..., Sq\}\\
&S_j = \{O_j, P_j, i_j, w_j, b_j\}\\
&O = \{o_1, o_2, ..., o_n\}\\
&o_k \in \{0,1,2\},\ k \in \{1,2,...,n\}\\
&P = \{p_1, p_2, ... p_m\}\\
&p_k \in \{0,1\} k \in \{1,2...,m\}\\
&i \in \{0,1,2,3\}\\
&w \in \{0,1,2,3\}\\
&b \in \{0,1,2,3\}
\end{aligned}
\qquad (1)
$$

In above equation, S represents the set of states of the environment. Each element of the set is a unique combination of the values of all the variables in the model. In our model for a local agent, there are five variables. Variable O is a vector of objects (equipment, furniture etc.) in the lab. Each object o_j can either be missing ($o_j = 0$) or found at its designated place ($o_j = 1$) or found misplaced in the lab ($o_j = 2$). Next variable P is also a vector that represents staff and researchers working in the lab. Each staff member can either be present in the lab ($p_j = 1$) or not present in the lab ($p_j = 0$). Next variable i represents how many (if any at all) intruders are detected in the lab. Note that we have assigned four possible values to the variable i. The intention is to differentiate between no intruder ($i = 0$), one or two intruders ($i = 1$), a few intruders (i=2), and many intruders (i=3). The exact value (or range) of the number of intruders corresponding to "a few" and "many" can be assigned by the user. Next variable in the model is w that represents the presence of weapons. The values assigned to w are to signify type of weapon e.g. small, large, firearm, steel knife etc. In this paper, w = 0 means there are no weapons detected in the lab. Other values of w represent whether the weapon detected in a knife or pointy metal (w = 1), a pistol or small size firearm (w = 2) or any large size firearm (w = 3). Final variable in the model is b representing the kind of activity that might be taking place in the lab. As usual b = 0 represents no activity is taking place. Other values of b represent whether normal lab research is taking place (b = 1), or there is a hostage situation (b = 2), or physical beating (b = 3) is going on (or just occurred).

A combination of the variables described above forms local state or state of the environment as far as the local agent is concerned. The state for the global agent has to include information from all local agents and the requests or updates from the security officials. Hence the state can be formulated as

$$
\begin{aligned}
&S = \{s_1, s_2, \dots, s_r\}\\
&s_j = \{s_{1j}, s_{2j}, \dots, s_{kj}, G_j\}\\
&s_{vj} = \{O_{vj}, P_{vj}, i_{vj}, w_{vj}, b_{vj}\}\\
&v \in \{1,2, \dots, k\}, j \in \{1,2, \dots, r\\
&G = \{g_1, g_2, \dots, g_f\}\\
&g_l \in \{0,1,2\}, l \in \{1,2, \dots, f\}
\end{aligned}
\qquad (2)
$$

Most of the variables in the state of a global agent are the same as those in the local agent states. Vector G is set of variables used to identify requests and information from the security officials. Vector G can expand or shrink as the agent learns more situations or is to forget about some situation. Each variable in vector g can have three possible values corresponding to no information about an event (g = 0), a certain event been in hostile situation (g = 1) or a certain event been in a nonthreatening situation (g = 2). We assume f built-in (or anticipated) events for example: presence of a potential terrorist in the lab, occurrence of a fight in the lab, harmful spill in the lab, presence of weapons in the lab and so on. Note that g = 0 is an indication of request for more information on a certain event. Note that the set of alarms that a global agent can trigger is not in the state space. One could have those in the set of action space.

Now we present general algorithms for local and global agents that use the information from the model and perform actions that are required to update the information of the variables involved in the model. Fig. 4 shows algorithm for the local agent. Inputs to the algorithm are the digital image data acquired by the associated camera and the command from the global agent. Local agent is assumed to have a built-in library of

images including the images of the lab equipment, lab staff, the placement of the equipment in the lab, possible weapons that could be brought into the lab, and other images that might help in detecting features of interest from the current image acquired. First of all, the local agent addresses any command that is issued by the global agent. This command could be to identify or confirm an intruder or a weapon or it could be to confirm a missing or misplaced equipment etc. The purpose of the command is to perform rigorous image processing on the past and current images in order to identify some feature that is hard to identify or could have been missed by routine algorithms of image processing. This is realistic because routine image processing needs to be fast and to complete a task faster usually requires reduced computations which may lead to some errors in judgement. Since these errors are not frequent, it is worthwhile to have a separate deep search algorithm which executes on demand only.

If there is no specific command from the global agent, the local agent identifies (or updates) the features of the local state using routine algorithms each dedicated for a specific task. For example the compare_image function is for comparing the current image of the lab (or a specific part of the lab) with relevant library images to determine if all objects are present or any (or some) of the objects are missing (or misplaced). If an object of the lab is not supposed to be in the field of view of a certain camera, then it is by-default assumed to be in-place by the local intelligence associated with that camera. To elaborate, let us suppose that a lab has three shelves and three cameras (one for each shelf). If camera 1 does not have any item of shelf 2 and 3 on its image, then local agent 1 will assume that those items are placed on their corresponding shelves whereas local agents 2 and 3 may or may not agree based on what is on their corresponding images. Function for staff detection simply would tell the global agent about which member is in which area of the lab. For instance if a member is not visible to one camera, he/she is absent from lab according to the local intelligence but some camera (assuming that the lab does not have a camera-blind spot) ought to detect that staff member and hence the global intelligence would know about the presence of the same

```
function Local Intelligence (digital_image, Command) returns local
state
inputs: digital_image, Command
static: liberary_images, image_history

if Command not null then do
s ← deep_search (Command, digital_image, liberary_images,
image_history)

else if digital_image not null then do
O ← compare_image (liberary_images, digital_image)
P ← detect_staff (digital_image, liberary_images)
i ← detect_intruder (digital_image, liberary_images)
w ← detect_weapon (digital_image, liberary_images)
b ← detect_activity (digital_image, image_history)
s ← (O, P, i, w, b)
return s
```

Fig. 4: Local Agent Algorithm

The remaining functions can be codded to work in a similar manner. For instance, the intruder detect function can mark the presence of a non-member of the lab as intruder. When this information reaches the global agent, the threat associated with the intruder can be evaluated using predefined algorithms at the global level and by requesting feedback from the security officials (which of course do not have to do any image processing and hence can tell rather quickly just by looking at the live feed whether a person detected as an intruder is worth worrying about or not). Similar intelligence can be used for weapon detection. Note that both intruder detection and weapon detection functions use the image library that includes template images of possible weapons and maybe intruder outfits (or outfits that rule out a person being intruder e.g. a guest badge or sweeper uniform etc.). Finally, the activity detection function serves two purposes. First is to detect activities of any intruders (if any). Second is to detect the activities of the staff and non-intruder personnel. This function is important for a staff member can pose a threat (or someone who may be disguised as one of the staff members or sweeper).

Algorithm for the global agent is shown in Fig. 5. There are three built-in functions in the global agent. Before we discuss the functions, it is important to understand the information contained in the variable (vectors) *camera_topology* and *threat_vector*. The topology vector includes information about the field of views of the local agents or overlap, if any, in the information obtained. This information helps in increasing confidence in the information (assuming that the information is matching rather than conflicting). Topology information also helps avoiding double count of any intruder or weapon. The threat vector is for keeping track of the kinds of threat e.g. unusual activity, presence of weapons or intruders etc. The reason why this vector is a static variable is that a weapon or an intruder cannot just disappear in a flash. So if the local information shows unexpected change, this change can be considered as a threat itself.

```
function Global Intelligence (local_states, security_data) returns
alarms and commands
inputs: local_states, security_data
static: camera_topology, threat_vector

threat_vector ← update_threat_vector (threat_vector, local_states,
camera_topology)
alarms ← generate_alarms (security_data, threat_vector)
for j = 1 to k do
commands(j) ← generate_local_commands (alarms, security_data,
camera_topology)

return alarms, commands
```

Fig. 5: Global Agent Algorithm

The function to update the threat vector is used to determine the changes in the security situation of lab as per new information obtained from all the local agents. This updated threat vector is then used in the alarm generation function that incorporates the security related information obtained from the human officials. The reason to use security data in the alarm generation is to incorporate any inaccuracies in the automated threat evaluation due to image processing errors or other

anomalies or special circumstances such as some rehearsal or renovation going on in the lab or presence of armed guards in case of a visit by a high profile person e.g. a minister or a high rank army officer. Finally, the command generation function alarms, security data, and camera topology to determine tasks to be performed by the local agents in case there are any discrepancies, conflicts, or doubts in the information obtained.

IV. Practical Issues and Advancements in the Proposed Approach

In this section we discuss important issues that can offer nontrivial challenges while implementing our proposed surveillance approach. We also discuss how to advance the architecture in terms of functionality and better adaptability to the ever changing scenarios.

A. Computational Complexity

First we discuss the computational complexity of the problem. As far as the local agents are concerned, most of computations involve image processing but is it really so? The algorithm in Fig. 4, requires the local agent to assign values to each of the state variables. In order to assign one of the possible values, in worst case, the associated function of the algorithm may have to check for possibility of each of the value being true. This means that the larger the domain space of each variable, the larger is the number of computations required to assign its value. Fortunately, since each variable is assigned its value independent of the other variables, the complexity is additive in terms of all variables i.e. the complexity of the local agent is given by

$$C_L = 3^n + 2^m + 4 \times 3 \quad (3)$$

Here n is the number of objects in the lab and m is the number of staff members. Take an example of the lab with 10 staff members and 50 equipment items. This leads the factor 3^{50} as the decisive value of complexity this value is definitely above the capability on the other hand 3^{10} or 3^{12} is marginally tractable. This means that one camera should not be held responsible for more than 10 to 12 items. Similarly, lab staff cannot exceed a similar limit. This means that in order to keep the complexity of the local agent below the threshold of the technological capability, more agents are to be installed.

Now for global agent, the problem is contradicting because as we increase the number of local agents, the complexity of the global agent increases since the complexity of the global agent is given by

$$C_G = k \times C_L + 3^f \quad (4)$$

Above equation assumes no correlation between the agents and in such case, the number of agents contribute linearly to the complexity. But if the agents are correlated, then the complexity becomes exponential. For example, assume that out of k local agents, k1 are correlated, then the complexity becomes

$$C_G = (C_L)^{k1} + (k - k1) \times C_L + 3^f \quad (5)$$

Let us assume we have five local agents (five cameras) and there are 10 events about which the security officials may provide feedback/request to the global agent. First we assume all five local agents to be independent, then the complexity contribution from the local agent and global agent is only different if 3^f factor exceeds 3^n in the C_L. In this situation, as long as the number of events to be handled is small enough, there are no computational problems expected. On the other hand, if three of the agents are correlated, then the complexity due to local agents becomes 3^{3n}. This indeed can create significant problems and computational delays in the surveillance loop.

Therefore, in order to keep the complexity in the global agent tractable, one need to confine the number of events within a certain limit and also correlation between the agents has to be minimized. Notice here that, the correlation between local agents is useful in terms of robustness in the system and having to avoid correlation to reduce complexity is a tradeoff.

One possible solution to the complexity problem is to have multiple global agents (or to have pseudo-global agents). The idea is to have each pseudo-global agent be assigned a subset of local agents only (or a subset of security-related events only). We leave this idea to be explored in future research on this topic.

B. Scalability

Scalability is important for the approach to be practically usable. Since the paper discusses the approach only for one lab, whereas in real world, there may be tens of labs in a facility. Also there are corridors and lobbies and meeting rooms. Theoretically, if each room or each lobby is secured individually, then the whole building can be considered as secured. But practically, there are certain issues such as exchange of critical information (between global agent of a room and that of a lobby) and the information about who is allowed to access which places.

In principal, the extension of the proposed approach does require nontrivial working in terms of modeling, algorithms, and architecture. On the other hand, the proposed hierarchical approach, the model, and the algorithms serve as a basis for such extensions. The additional features would be required on top of the proposed architecture to facilitate the security of a multi-lab building. For instance, the consideration of which person is among the employees in the building and which member is not. Furthermore, which member belongs in which lab and what equipment belong in which lab. Also, there could be information about restricted versus public areas within the building. The concept of larger scale architecture is shown in Fig. 6. Here bidirectional arrows indicate two way information exchange and each block labeled as surveillance system comprises of the local and global intelligence agents as in Fig. 1.

Fig. 6: Expansion over the Architecture in Fig. 1

C. *Online Learning and Updates*

Online learning and updates in the image liberary and threat vector are key ingredients for a long term surveillance solution.

It is not possible to know *all* possible threat types and the images of *all* possible weapons or intruder outfits etc. Many of these things are learnt over time with "experience". Therefore, a natural extension of the proposed architecture is to add learning algorithms in the local and global intelligence agents. Most common form of learning in multiagent systems is reinforcement learning [9]. For the proposed surveillance system, learning can be incorporated at local and global intelligence levels. The local agent can learn to identify the state with better accuracy by using the feedback from human security officials and adding more images to the library of images (or maybe replacing images in some cases). The global agent can learn new threat types and can also learn to add or remove from the set of alarms. Furthermore, the accuracy of alarm generation can be improved through learning that may use feedback from the security officials.

V. Conclusions

Implementation of intelligent surveillance in general is a problem that cannot be addressed in a single research paper. An attempt has been made to discuss a specific part of the problem i.e. indoor surveillance. In this context, a three-layered multiagent architecture is presented that involves artificial intelligence as well as human supervision. Through the example of a scientific laboratory, it has been demonstrated how the proposed system can be designed. The implementation of the proposed system however is not straight forward for large or medium sized buildings. Most important issue is that of computational complexity. Some ways have been proposed to avoid complexity problems using the insights of the proposed approach. Still a lot of work is to be done in order to mature the idea for practical use. Some directions in this regard have been discussed in the paper.

References

[1] Kingston, Derek, Randal W. Beard, and Ryan S. Holt. "Decentralized perimeter surveillance using a team of UAVs." *IEEE Transactions on Robotics* 24.6 (2008): 1394-1404.

[2] Varga, Maja, et al. "Evaluation of control strategies for fixed-wing drones following slow-moving ground agents." *Robotics and Autonomous Systems* 72 (2015): 285-294.

[3] Kariotoglou, Nikolaos, et al. "Multi-agent autonomous surveillance: a framework based on stochastic reachability and hierarchical task allocation."*Journal of dynamic systems, measurement, and control* 137.3 (2015): 031008.

[4] Leahy, Kevin, et al. "Persistent surveillance for unmanned aerial vehicles subject to charging and temporal logic constraints." *Autonomous Robots*(2015): 1-16.

[5] Dee, Hannah M., and Sergio A. Velastin. "How close are we to solving the problem of automated visual surveillance?." *Machine Vision and Applications* 19.5-6 (2008): 329-343.

[6] Wang, Xiaogang. "Intelligent multi-camera video surveillance: A review."*Pattern recognition letters* 34.1 (2013): 3-19.

[7] Remagnino, Paolo, A. I. Shihab, and Graeme A. Jones. "Distributed intelligence for multi-camera visual surveillance." *Pattern recognition* 37.4 (2004): 675-689.

[8] Gat, Erann. "On three-layer architectures." *Artificial intelligence and mobile robots* 195 (1998): 210.

[9] Wahab, Matthew. "Reinforcement learning in multiagent systems." *McGill university School of computer Science* (2003).

Analysis of Stability Radius of Inverted Pendulum on a Cart System

Jawad Khalid Qureshi[1], Ali Nasir[2], M. Awais Arshad[3], Adeel Ahmad[4]

[1,2,3]University of Central Punjab, 1-Khayaban-e-Jinnah, Johar Town, Lahore, Pakistan

[4]University of Lahore, Lahore Pakistan

Abstract:

This paper discusses the concept of stability radius and presents an evaluation of the same for inverted pendulum on a cart system. In a system, robustness can be calculated or determined by using stability radius. It is shown through example that the usual margins (gain and phase margins) may not always present an accurate measure of stability robustness. Simulation results indicate that some parameters in the system may affect the stability radius more than the others. The results also indicate the effect of simultaneous changes in system parameters on the stability radius may be highly nonlinear and non-monotonic. Finally, a design guideline for inverted pendulum mass to length ratio has been derived from the results.

Keywords:

Stability Radius, Parameter Variation Analysis, Inverted Pendulum on a Cart

1. Introduction

Stability is one of the major concerns in control systems. A good amount of research has been done on achieving stability in multiple systems. In nonlinear inverted pendulum system, the pendulum rod is stabilized in its upward direction by moving the attached cart. This is one of the benchmarks for research in control systems.

Inverted pendulum structure is a platform in which cart can only move in horizontal direction and pendulum rod (initially facing downwards) is attached with cart. Hence the rod is in its stable equilibrium state.

The purpose of this research paper is to analyze stability of inverted pendulum by varying either the rod's mass or rod's length or varying both simultaneously. Among the existing work, robustness analysis is done using fractional PID controller on ADAMS-MATLAB co-simulation using recursive least squares method in [1]. There is extensive literature on robustness testing of dynamic systems. But the method proposed is different in that it uses the concept of stability radius rather than usual concepts of gain and phase margins. In [2], linear matrix inequality (LMI) tool is used to test the robustness of system that is modeled using combination of Particle Swarm Optimization (PSO) and Takagi Sugeno (T-S) fuzzy control approach. In [3], analytical study of inverted pendulum system has been done using high frequency harmonic excitations. Larger the intensity of stochastic excitation or strength of frequency perturbations, larger is the Lyapunov exponent which destabilizes the system. Neural networks propose to behave more robust controller but in absence of disruptive effects over performances in perturbed conditions when balancing non-linear inverted pendulum system[4][5][6]. In[7], controller are designed to stabilize inverted pendulum in upright position using feedback by checking if sampling time delay was not large enough, controller keeps the system stabilized. Adaptive control schemes for inverted pendulum have been discussed in [8][9] where [8] presents the neural network based approach whereas sliding mode controller based approach has been explored in[9].

As the cart can move only in horizontal track and pendulum rod can move w.r.t a single angle, the dynamics of the system can be described as pendulum angle θ, pendulum angular velocity $\dot{\theta}$, card position x and cart velocity $\dot{x}$. This system also has some constraints like the cart can move up to a finite limited length and pendulum rod can move up to some finite limited angle on which the cart can move and steer back the pendulum rod to stabilize. Beyond that angle, the rod cannot be stabilized in its upright position. The pendulum rod in its upright position is in unstable equilibrium state when $\theta=0$ (vertically upward), some control method is needed to be applied to maintain the stability of the system.

Research has been done earlier on stabilization of inverted pendulum by using feedback controller response or by using fixed feedback. Stability of the system can also be analyzed with respect to variations in the mass of pendulum rod or in pendulum rod's length so that controller can behave more robust against external uncertainties. In this paper, we have made some variation in pendulum original mass and rod's length and analyzed the system stability. Major difference of the approach used in this paper from the existing work is that we have made use of the knowledge of stability radius for our analysis as opposed to conventional tools such as root locus Bode plot or Nyquist plot.

2. The Concept of Stability Radius:

The concept of stability radius is presented in [10]. Stability radius is defined as the radius of the smallest circle centered at the critical point $(-1 + 0j)$ that touches the Nyquist plot of the open loop transfer function of the feedback control system. In order to clearly understand the definition, consider the feedback control system shown in Figure 1.

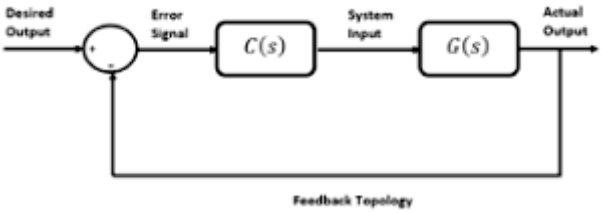

Figure 1: Feedback Control System

The loop transfer function for the above system is given by

$$L(s) = C(s)G(s) \quad (1)$$

The Nyquist plot of this loop transfer function is used to depict closed loop stability, gain margin and phase margin. The methods of finding the stability and the margins are in every control systems text book e.g. [11]. Stability radius is however a different concept as illustrated in Figure 2. As defined earlier, it is the radius of the circle touching the Nyquist plot of the open loop transfer function L/(s). In order to understand the importance of stability radius, one has to understand the importance of sensitivity function given by

$$S(s) = \frac{1}{1 + L(s)} \tag{2}$$

The sensitivity function imposes many constraints on the closed loop performance [11]. Specifically, larger the value of sensitivity, more prone is the system performance to external disturbances. The way gain and phase margins are defined, it is possible to have a system with infinite gain margin and a good ($> 60^0$) phase margin and yet poor stability due to high value of sensitivity function.

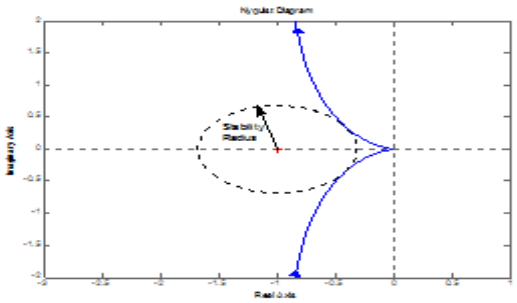

Figure 2: Example of Stability Radius

For example, in the system of Figure 2 *(L(s)=1/S²+s))* gain margin is infinite and phase margin is 51.8^0 yet sensitivity value is high for a range of frequencies. This tells us that it is important to analyze the stability radius of the systems. In this paper, we have done such analysis for an inverted pendulum because it is a benchmark system. Similar analysis can be performed on other systems in order to study the stability radius as a function of changes in system parameters. Such study can help in designing more robust and disturbance tolerant systems.

3. Inverted Pendulum Model

In figure 3, rod and cart system is shown on which force is being applied. Force on cart is represented as *N* in horizontal direction. Force on rod is represented as *P* in vertical direction.

From forces in horizontal direction (for the cart), the equation below can be obtained

$$M\ddot{x} = F - f\dot{x} - N \tag{3}$$

where.

F = Force being applied on cart
x = Horizontal position of cart
f = damping coefficient
N = Force exerted on the cart in horizontal direction due to motion of the pendulum
M = mass of the cart

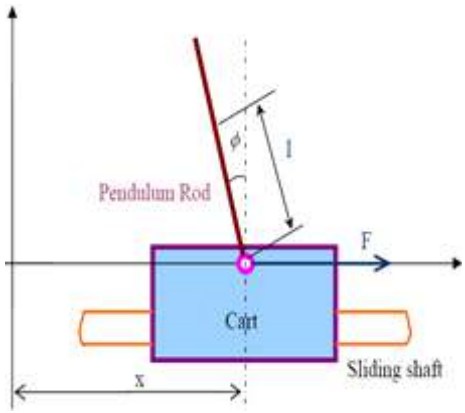

Figure 3: Inverted Pendulum on a Cart System

From the force acting on the rod in horizontal direction we get

$$N = m\frac{d^2}{dt^2}(x - l\sin\phi) \tag{4}$$

l=length of the pendulum rod
ϕ= Angle of the rod
m=mass of pendulum rod
Equation (4) can be written as,

$$N = m\ddot{x} - ml\ddot{\phi}\cos\theta ml\dot{\phi}^2\sin\phi \tag{5}$$

Substituting equation (5) into equation (3), first equation for non-linear system obtained is

$$(M+m)\ddot{x} + f\dot{x} - ml\ddot{\phi}\cos\phi + ml\dot{\phi}^2\sin\phi = F$$

Similarly, combining the forces acting on the rod in vertical direction, we obtain second equation of motion

$$(I + ml^2)\ddot{\phi} - mgl\sin\phi = ml\ddot{x}\cos\phi \tag{6}$$

Linearization of equations (5) and (6) about the equilibrium point $[x \quad \dot{x} \quad \phi \quad \dot{\phi}]^T = [0 \quad 0 \quad 0 \quad 0]^T$ results in the following state space equation in matrix form.

$$\begin{bmatrix} \dot{x} \\ \ddot{x} \\ \dot{\phi} \\ \ddot{\phi} \end{bmatrix} = \begin{bmatrix} 0 & 1 & 0 & 0 \\ 0 & \frac{-(I+ml^2)b}{I(M+m)+Ml^2} & \frac{m^2gl^2}{I(M+m)+Ml^2} & 0 \\ 0 & 0 & 0 & 1 \\ 0 & \frac{-mlb}{I(M+m)+Ml^2} & \frac{mgl(M+m)}{I(M+m)+Ml^2} & 0 \end{bmatrix} \begin{bmatrix} x \\ \dot{x} \\ \phi \\ \dot{\phi} \end{bmatrix} + \begin{bmatrix} 0 \\ \frac{I+ml^2}{I(M+m)+Ml^2} \\ 0 \\ \frac{ml}{I(M+m)+Ml^2} \end{bmatrix} u \tag{7}$$

where $u = F$ and the output equations can be written as,

$$y = \begin{bmatrix} x \\ \phi \end{bmatrix} = \begin{bmatrix} 1 & 0 & 0 & 0 \\ 0 & 0 & 1 & 0 \end{bmatrix} \begin{bmatrix} x \\ \dot{x} \\ \phi \\ \dot{\phi} \end{bmatrix} + \begin{bmatrix} 0 \\ 0 \end{bmatrix} u$$

By using equation (5), we can form

$$\begin{bmatrix} \dot{x} \\ \ddot{x} \\ \dot{\phi} \\ \ddot{\phi} \end{bmatrix} = \begin{bmatrix} 0 & 1 & 0 & 0 \\ 0 & \frac{a_1}{b} & \frac{a_2}{b} & 0 \\ 0 & 0 & 0 & 1 \\ 0 & \frac{a_3}{b} & \frac{a_4}{b} & 0 \end{bmatrix} \begin{bmatrix} x \\ \dot{x} \\ \phi \\ \dot{\phi} \end{bmatrix} + \begin{bmatrix} 0 \\ \frac{b_1}{b} \\ 0 \\ \frac{b_1}{b} \end{bmatrix} u \quad (8)$$

$$y = [0 \quad 0 \quad 1 \quad 0] \begin{bmatrix} x \\ \dot{x} \\ \phi \\ \dot{\phi} \end{bmatrix}$$

$$SI - A = \begin{bmatrix} s & -1 & 0 & 0 \\ 0 & s - \frac{a_1}{b} & \frac{-a_2}{b} & 0 \\ 0 & 0 & s & -1 \\ 0 & \frac{-a_3}{b} & \frac{-a_4}{b} & s \end{bmatrix} \quad (9)$$

$$\det(SI - A) = s\left(\left(s - \frac{a_1}{b}\right)\left(\frac{-a_4}{b}\right) - \left(\frac{-a_2}{b}\right)\left(\frac{-a_3}{b}\right) + s\left(\left(s - \frac{a_1}{b}\right)s\right)\right)$$

$$\det(SI - A) = s\left(\frac{-(bs - a_1)(a_4)}{b^2} - \frac{a_2 a_3}{b^2} + s^2\left(\frac{bs - a_1}{b}\right)\right)$$

$$Adj(SI - A) = \begin{bmatrix} A_1 & A_2 & 0 & 0 \\ 0 & A_3 & A_4 & 0 \\ 0 & 0 & A_5 & A_6 \\ 0 & A_7 & A_8 & A_9 \end{bmatrix}^T$$

$$Adj(SI - A) = \begin{bmatrix} A_1 & 0 & 0 & 0 \\ A_2 & A_3 & 0 & A_7 \\ 0 & A_4 & A_5 & A_8 \\ 0 & 0 & A_6 & A_9 \end{bmatrix}$$

$$A_1 = \frac{1}{b}[(a_1 - bs)(a_4) - a_2 a_3 + s^2(bs - a_1)]$$

$$A_2 = 0$$

$$A_3 = \frac{s}{b}[bs^2 - a_4]$$

$$A_4 = \frac{a_2 s^2}{b}$$

$$A_5 = \frac{s^2}{b}(bs - a_1)$$

$$A_6 = \frac{s}{b}(bs - a_1)$$

$$A_7 = \frac{s^2 a_3}{b}$$

$$A_8 = \frac{1}{b^2}[a_4 s(bs - a_1) + a_2 a_3]$$

$$A_9 = \frac{s^2}{b}(bs - a_1)$$

Now, we have achieved the values for the system matrix for which we are going to analyze by changing length and mass to test the robustness of the system.

4. Stability Radius Analysis

In control systems, one of the dominant issue is to obtain robustness and stability. One of the main problem in analysis of robustness is to confirm that the system under study is able to maintain the stability under certain (defined/variable) conditions. Stability radius can be considered as the distance to instability. A system can be termed as natural robust if it has covered distance from point of instability to point of stability by keeping same dimensions. In different industry scenarios, it is conveniently easy to deal with polynomials of closed loop system e.g. for a system with single output or for with single inputs. One of the fundamental property of a system in closed loop analysis is to achieve or obtain the roots on a complex plane. If all the roots lie with stability region, the system (polynomial within complex variable) will be termed as stable.

All simulations are carried out using constant mass of the cart that is 0.792 kg. Increasing the length of the pendulum rod does not have much effect on stability radius as shown in Figure 4. The stability radius is changing in a little fraction with increase in pendulum rod's length as shown in Figure 5 (length variation from 0.304 m to 10 m in intervals of 0.8 m). Although the change in stability radius with respect to length is not very significant but reaching to a conclusion that increasing or decreasing the length does not affect stability would be too soon at this point. Therefore further analysis has been performed using the mass to length ratio in order to determine more realistic effect of change in length on the stability of the system. In practice, increasing the length does increase the overall mass of the system.

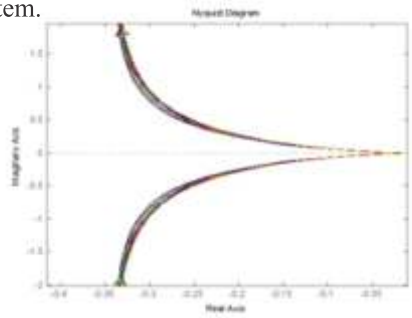

Figure4: Nyquist Diagram for variation of length

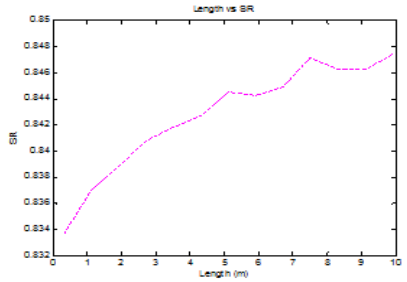

Figure5: Length vs Stability Radius

Now if we vary the mass on pendulum rod, the response and change in stability radius is decreasing. The response is shown in Figure 6 and Figure 7 (mass variation from 0.231 kg to 10 kg in intervals of 0.8 kg). Figure 6 shows that the Nyquist plot corresponding to various values of pendulum mass differ significantly. Comparing Figure 6 with Figure 4, the effect of variation in mass on stability is higher than that of length. But as stated earlier, variation in length does involve variation in mass. If we change both mass and length simultaneously, stability radius behavior shows abrupt decrease as shown in Figure 8 (mass over length ratio variation from 0.01 kg/m to 100 kg/m in intervals of 0.05 kg/m). This result indicate that the selection of mass to length ratio of inverted pendulum should be selected below 20 or 15 i.e. mass (in kilograms) should not be more than 20 times the length (in meters) for reasonable stability robustness. Such a conclusion is difficult to obtain from conventional root contour method and is very important for designing a robust stable system.

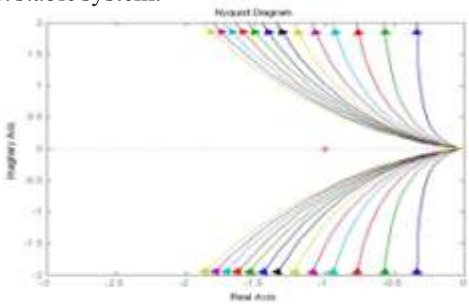

Figure6: Nyquist plot for variation of pendulum rod mass

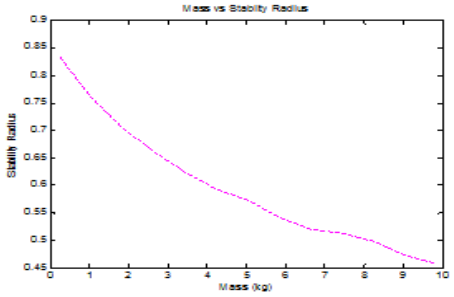

Figure7: Mass vs Stability Radius

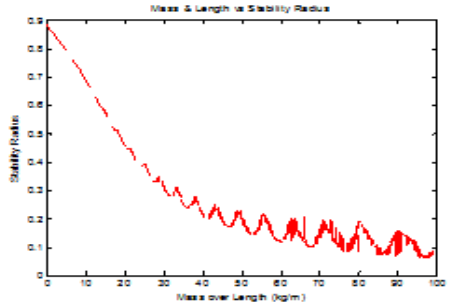

Figure8: Mass and length variation vs Stability Radius

1. Conclusions

Variations in the stability radius are shown for an inverted pendulum on a cart system as function of variations in mass and length of the rod. The results show that there is nontrivial variation in the stability radius when both parameters are changed simultaneously. It is also shown that the length alone does not affect the stability radius by a great amount. From these results, the motivation for the readers is to do such analysis on the systems to be controlled and identify parameters that affect the stability radius more than the others. Such analysis can help in achieving closed loop stability that is robust to parameter changes.

References:

[1] Viola, J., and L. Angel. "Fractional control and robustness analysis of an inverted pendulum system." *Automatic Control (CCAC), 2015 IEEE 2nd Colombian Conference on*. IEEE, 2015.

[2] Yu, Gwo-Ruey, and Shun-Min Wang. "Robust fuzzy control for inverted pendulum with model uncertainty and output constraint via LMI stability analysis." *Fuzzy Theory and it's Applications (iFUZZY), 2012 International Conference on*. IEEE, 2012.

[3] Zhi-Long, Huang, Jin Xiao-Ling, and Zhu Zi-Qi. "Stability analysis of an inverted pendulum subjected to combined high frequency harmonics and stochastic excitations." *Chinese Physics Letters* 25.9 (2008): 3099.

[4] Vicentini, Federico. "Stability Analysis of Evolved Continuous Time Recurrent Neural Networks that Balance a Double Inverted Pendulum on a Cart." *Neural Networks, 2007. IJCNN 2007. International Joint Conference on*. IEEE, 2007.

[5] S. Jung and S.S. Kim, 2008. Control experiment of a wheel-driven mobile inverted pendulum using neural network. *IEEE Transactions on Control Systems Technology*, *16*(2), pp.297-303.

[6] J. Khalid, A. Nasir, U. Shami, A. Baig, "Using Denoising Autoencoders to Predict Behavior of an Inverted Pendulum on a Cart System", *Technical Journal UET Taxila*, Vol 22, Issue 1, 2017 pp 30-40

[7] Landry, Maria, et al. "Dynamics of an inverted pendulum with delayed feedback control." *SIAM Journal on Applied Dynamical Systems* 4.2 (2005): 333-351.

[8] Z. Li and C. Yang, 2012. Neural-adaptive output feedback control of a class of transportation vehicles based on wheeled inverted pendulum models. *IEEE Transactions on Control Systems Technology*, *20*(6), pp.1583-1591.

[9] R.J. Wai and L.J. Chang, 2006. Adaptive stabilizing and tracking control for a nonlinear inverted-pendulum system via sliding-mode technique. *IEEE Transactions on Industrial Electronics*, *53*(2), pp.674-692.

[10] *A First Graduate Course in Feedback Control*, J. S. Freudenberg, University of Michigan, 2009

[11] *Modern control engineering*, Ogata, Katsuhiko, and Yanjuan Yang (1970).

Automatic Number Plate Recognition System Based on Discrete Wavelet Transform and Bounding Box Technique

Sara Saboor[1], Dr. Imran Touqir[2], M. Riaz Mughal[3]

[1]Department of Electrical Engineering Military College of Signals,
[2]Director Image Processing Centre , Military Collrge
National University of Sciences and Technology. Rawalpindi, Pakistan.

[3]Professor, Computer System Engineering, Mirpur University of Science and Technology,
Mirpur, Azad Jammu Kashmir, Pakistan.

Abstract

Automatic Number Plate Recognition (ANPR) technique occupies a significant importance as an intelligent management and monitoring system in real time. It acts as an essential part in a large portion of the vehicle monitoring systems, for example, activity administration, auto stopping/outstay control, tracking and identification of unauthorized vehicle in highly secure regions. An extensive variety of research on ANPR frameworks are accessible in writing. But these existing algorithms become inadequate due to changing illumination level and background conditions. Non-standard design of number plates in Pakistan make it even harder for the existing systems to show promising results. This paper concentrates on a productive framework to design an efficient ANPR system by applying Two-Dimensional Discrete Wavelet Transformation. Haar wavelet is being proposed due to its simplicity and being computationally convenient among all wavelet. The experimental result of this algorithm demonstrates that combining Wavelet transformation along with bounding box method results in a better performance in edge detection and character recognition.

Keywords

Discrete wavelet Transform; RBFNN; Haar and Optical Character Recognition.

I. Introduction

Nowadays security and safety has turned into a noteworthy issue for even the most secure nations. With the increase in terrorist activities and advancement in their methods. It is necessary to deploy systems to ensure that security is withstand. Terrorist activities are mostly carried out near crowded spaces and secured buildings with the help of stolen or un-registered vehicle. Therefore, system to automatically monitor the number plate was a requirement. In theory, there are an extensive variety of ANPR systems. Different algorithms were applied to come up with an effective system by keeping security in mind. However, some algorithms were good enough for certain environment whereas show inadequate results for others. Processing time of these algorithms make it even impossible to be used for monitoring in real time with Tera bytes of high resolution images being captured in a span of one day.

ANPR systems based on wavelet transform promises an efficient system. The Two-Dimensional Discrete Wavelet transform compresses the high-resolution image into multiple sub-bands i.e., LL, LH, HL and HH. The lower LL sub-band is the average component whereas the LH, HL and HH comprises of the detailed information. The Low-Low sub-band can be further divided into 4 sub-bands. This high resolution multi-level decomposition of DWT is used in image processing to detect edges. As 2D DWT can detect three kinds of edges at a time as compared to the traditional edge detection filters, thus making the process efficient. 2D DWT enables ANPR system to process the algorithm quickly and helps the system with low computational and storage load.

II. Related Work

The most common techniques used are: correlation based, neural network and Discrete Wavelet Transformation. There are number of different algorithms despite those mentioned above that gives promising result. In [1] Kalman filter for the recognition of number plate was suggested. The algorithm observes the frames of input video for the number plate recognition. Y.C. Chung et al [2] proposed color edge method along with fuzzy training for plate recognition. In their method Jobin et al [3] proposes a programmed number plate recognition framework with the help of Stroke Width Transform [4]. The mean shift algorithm was used by Jia et al. [5]. In which the color images were segmented into candidate region with the aid of mean shift hence defining it as either number plate or not. A definite overview on the best in class methods for number plate recognition framework can be found in [6]. Psoroulas [7] present algorithm for still images and video sequence. Singh Gurjinder et al [8] used image processing methodology for the identification of number plate system. The system has gained a lot of popularity recently with the rapid increase in crimes with the aid of stolen vehicle. Munno et al. [9] can work on the preliminary stages of number plate recognition system. He explains the sizing, normalization as well as the orientation of detection and recognition system. In his work Ibrahim, et al. [10] states that the efficiency of the

system depends on the quality of the images captured. Bing-Fei Wu et al. [11] proposed a system centered on support vector machine and HOG. Jian [12] proposed that the impact of binary image positioning enhances the precision and proficiency of the framework. P.Vijayalakshmi et al. [13] introduces a Generic algorithm capable of operating at two level for the vehicle detection, plate localization and character recognition.

A. *Number Plate Detection using Radial Basis Function Nueral Network (RBFNN)*

The radial basis work as far as numerical displaying is a counterfeit neural system. It utilizes radial basis functions as its enactment capacities. The yield of the procedure is a direct yield.

$$Ri(x_k)=EXP(-\|x_k-c_i\|^2/2\sigma_i^2)$$

$$y_k=\Sigma W_{ki}Q_i-Q_k \quad (1)$$

Wang et al [14] utilizes approach of line development and multilevel RBFNN. The consequence of the line development and qualities of the course of action of tag character is utilized to localize the plate. Adaptive binarization is used locally to refine the localization process. Reliable and accurate results are thus achieved by applying multi-level RBFNN on the feature vector input. However, the system has a lower recognition rate for some characters. Yilmaz in [15] utilizes picture connection and Neural system alongside Learning Vector Quantization (LVQ) that guarantees an expansion likelihood of acknowledgment of characters. The system has a 100%-character segmentation capability thus removing all unwanted regions, however, as the characters are being recognized by correlation and then feed into neural network there is the possibility of erroneous character recognition at the correlation stage.

B. *Number Plate Detection using Template Matching*

One approach to deal with interpretation issues on an image is by utilizing Template matching technique. The intensities of the pixels are analyzed by utilizing the SAD (Sum of absolute differences) measure. A pixel in the image with directions (xs, ys) has force Is (xs, ys) and a pixel in the layout with directions (xt, yt) has power It (xt, yt). Hence the total distinction in the pixel powers is characterized as:

$$Diff(x_s,y_s,x_t,y_t)=|I_s(x_s,y_s)-I_t(x_t-y_t)|$$

$$SAD(x,y)=\sum_{i=0}^{Trows}\sum_{j=0}^{Tcols}Diff(x+i,y+j,i,j) \quad (2)$$

In [16] the character segmentation is made possible by the V/H projection with the removal of unwanted regions and enhancement of segmented characters. Character recognition process is carried by Optical character recognition (OCR) method. The OCR method works on the concept of correlation, the most hits defines the character. However, the system fails if the plate contains multiple fonts and unclear background. Kanagapushpava et al. [17] in his work describe a four stage ANPR system. The procedure starts with the conversion of RGB picture into a dim scale and binary image picture. Morphological operators are then applied on the input image. Histogram equalization method has been adopted for the pre-processing of plate. Resultant of character segmentation is fed to OCR for the recognition stage. The process shows promising result; however, it gives wrong result in case of confusing and identical characters like 2 and Z.

III. Methodology

The proposed methodology is based on Discrete Wavelet Transformation (HAAR Wavelet) along with bounding box method and Template Matching. The methodology aims to achieve a computationally efficient and effective system. Haar wavelet provides more PSNR and comparison ratio in contrast to DCT. A better picture quality can be achieved with a greater PSNR. Both the techniques give a well-structured directional edge. However, with Haar wavelet we achieve adaptively quantized high frequency sub-band with a better resolution.

For character recognition, a wide range of techniques are available in literature. Template matching is an accurate and efficient method due to its low level of complexity.

The algorithm used not only improves the efficiency of the system but also achieve better performance for the following prospects: [18]

- Detection of three kind of edges at a time, which a traditional edge detector is inadequate to do so.
- Reduction in computational load and processing time.
- Lossless compression of high resolution images captured in a real-time scenario.
- Reduction in the complexity.

A Block diagram in Fig. 1 shows how the algorithm works. The algorithm is divided into three stages: Pre-processing, Number plate detection, character segmentation and recognition. Pre-processing stage involves conversion of the image captured in real time scenario into binary form. Filtering and smoothing of the subject image is done followed by two level wavelet decomposition which helps in separation of coarse information. Plate detection stage involves the use of Haar wavelet for effective and efficient edge detection. Once the plate is being localized; morphological operators help in smoothing the edges and removal of noise, followed by the segmentation and recognition of characters carried out by Bounding Box method and Template Matching respectively. [19]

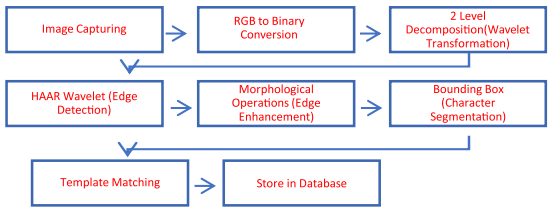

Fig. 1. Result and Simulations

IV. Results and Simulations

Variety of ANPR system exist in literature but they become inadequate considering Pakistani non-standard design of number plates. However, the algorithm proposed successfully extracted information from number plate belonging to different region of Pakistan with change in background and foreground design.

To compare the results of different techniques; number of images are tested in MATALB (R2010b). Simulation is carried out on four test images and their results are compiled in figures below.

Fig. 2, 3, 4 and 5 shows the comparison of simulation result of the traditional and Haar wavelet technique.

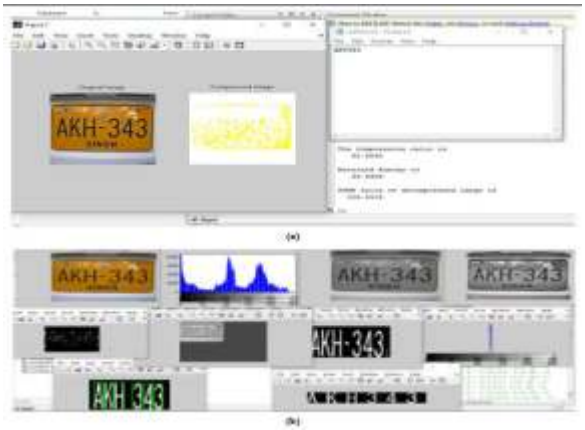

Fig. 2. (a) Traditional ANPR system (b) Proposed Algorithm.

Both the system successfully extracts the information from number plate. However, algorithm in (b) gives a detailed information of the process carried out.

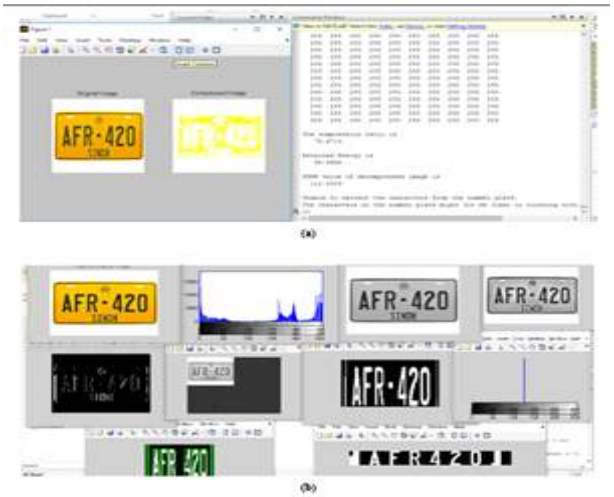

Fig. 3. (a) Traditional ANPR system (b) Proposed Algorithm.

Due to variation in illumination level traditional ANPR is inadequate to extract the information from number plate. Whereas the proposed algorithm was successful in determining the information.

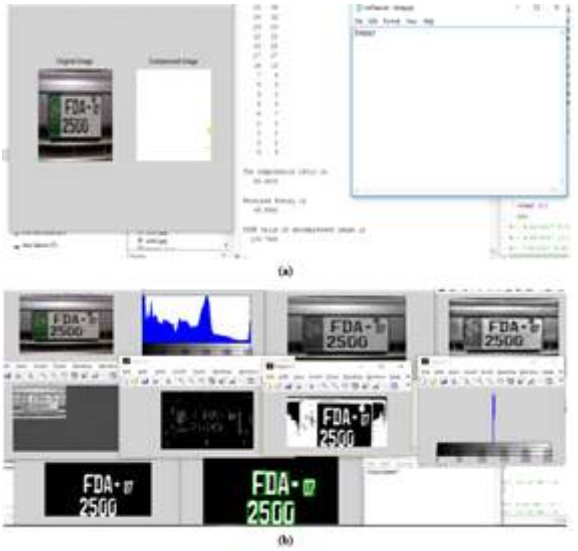

Fig. 4. (a) Traditional ANPR system (b) Proposed Algorithm.

The test image contains white background and green foreground. New feature of year of registration is also marked in the number plate. Due to which traditional ANPR system fails to extract correct information. Whereas the proposed algorithm was successful in determining the information.

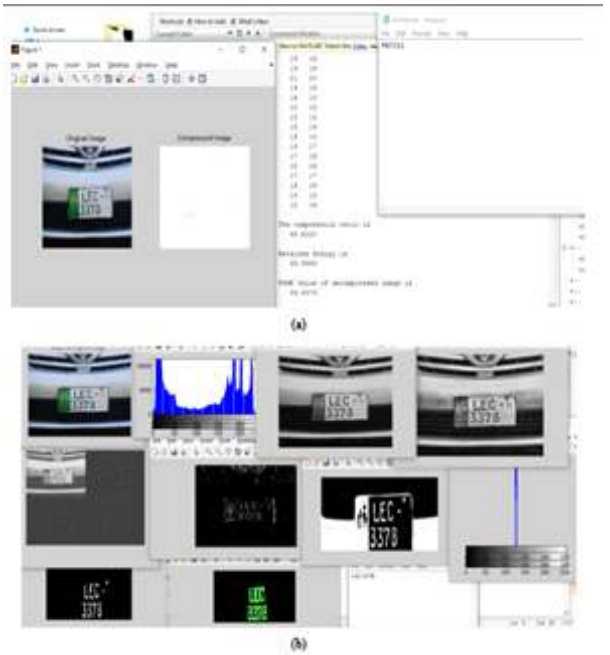

Fig. 5. (a) Traditional ANPR system (b) Proposed Algorithm.

The test image contains white background and green foreground. New feature of year of registration is also marked in the number plate. Due to which traditional ANPR system fails to extract correct information. However proposed algorithm successfully extracts the information.

Figure 6 shows the comparison drawn for test images between the accuracy achieved for traditional edge detectors and Haar wavelet.

Image	Traditional Algorithm	Proposed Algorithm
Test (1)	81.2%	96.5%
Test(2)	19.5%	95.4%
Test (3)	11.34%	93.5%
Test (4)	14.6%	85.4%

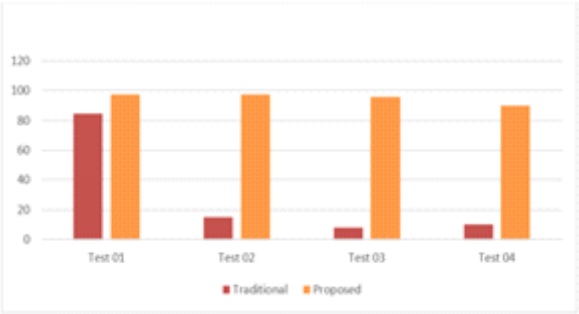

Fig. 6. Accuracy (%)

Figure 7 shows the comparison between the processing time taken by the traditional edge detectors and Haar wavelet techniques.

Image	Traditional Algorithm (sec)	Proposed Algorithm
Test 01	1.003	0.143
Test 02	1.00	0.1343
Test 03	1.254	0.154
Test 04	1.00	0.254

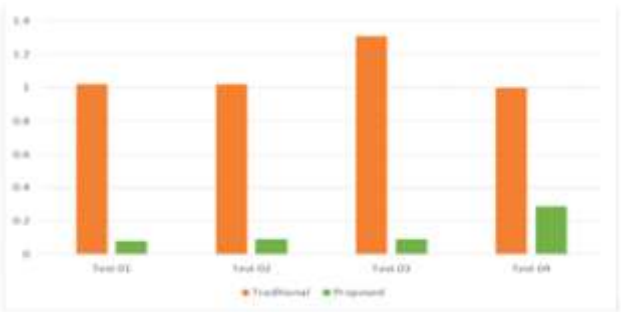

Fig. 7. Processing Time (sec)

Fig. 8 exhibits result compiled after taking opinion from the group of people. The graph shows the mean opinion score

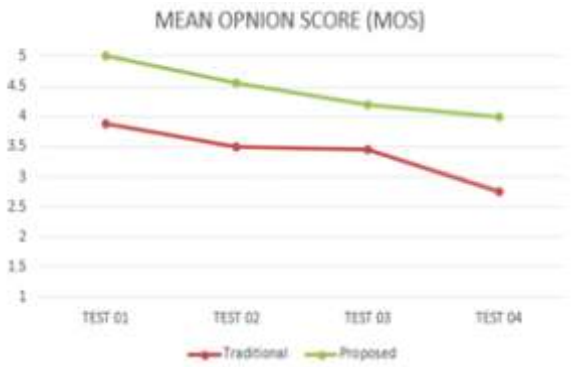

Fig. 8. Mean Opinion Score

v. Conclusion

An efficient ANPR system is the requirement of hour to meet security needs. The proposed algorithm successfully identifies the number plate; it reduces the computational load and complexity; processing time is minimized and accurate results are achieved. Haar wavelet along with morphological operators and bounding box technique is used for better performance of edge detection and character recognition.

Considering the real-time scenario noisy background can disrupt the output. Therefore, the future work focuses on the edge enhancement of noisy edges. For a noisy background; Haar wavelet performance degrade exponentially with the level of decomposition. Cleaning and refinement techniques for edge must be cascaded. Haar wavelet in fusion with the fuzzy logic and morphological operators can be focused to suppress the noises effectively.

References

[1] F. Limberger and C. Arth: 'Real-time license plate recognition on an embedded dsp-platform', IEEE Transaction on Intelligent Transportation Systems, vol. 1, no. 4, pp: 34–54, 2007.

[2] Y. Chung, S.L. Chang, L.S. Chen, and SW Chen: 'Automatic license plate recognition', IEEE Transaction on Intelligent Transportation Systems, vol. 5, no. 2, Pp: 42–52, 2004.

[3] Jobin K.V, Jiji C.V, Anurenjan P.R: 'Automatic Number Plate Recognition system using modified Stroke Width Transform', INSPEC: 14181809, IEEE Xplorer, 2014.

[4] B. Epshtein, E. Ofek and Y. Wexler: 'Detecting Text in Natural Scenes with Stroke Width Transform', IEEE Conference on Computer Vision and Pattern Recognition (CVPR), pp: 2963–2970, 2010.

[5] H. Zhang, W. Jia, and M. Piccardi: 'Mean shift for accurate license plate localization', IEEE Conference on Intelligent Transportation Systems (ITSC), vol. 1, no. 1, pp: 566–571, 2005.

[6] S. Du, Ibrahim M., Shehata M., Badawy W: 'Automatic License Plate Recognition (ALPR): A State-of-the-Art Review' IEEE Transactions on Circuits and Systems for Video Technology, Volume: 23, Issue: 2, pp: 311–325, 2013.

[7] C. E. Anagnostopoulos, I. E. Anagnostopoulos, I. D. Psoroulas, V.Loumos and E. Kayafas: 'License Plate Recognition From Still Images and Video Sequences: A Survey', IEEE Transaction on Intelligent Transportation, 2015.

[8] G.P. Singh and N. Bawa: 'License Plate Recognition using Hopfield Neural Networks', International Journal of Modern Trends in Engineering and Research (IJMTER), Volume 02, Issue 03, 2015.

[9] Cosmo H.Munuo, Dr. M. Kisangiri: 'Vehicle Number Plates Detection and Recognition using improved Algorithms: A Review with Tanzanian Case study', International Journal Of Engineering And Computer Science ISSN: 2319-7242 Volume 3 Issue 5, pp: 5828-5832, 2015.

[10] M. Ibrahim, M. Shehata: 'Automatic License Plate Recognition (ALPR):A State-of-the- Art.Review', IEEE Transactions On Circuits And Systems For Video Technology, Vol. 23, No. 2, 2013.

[11] B.F. Wu, H.Y. Huang, T.T. Lee, C.J. Chen: 'Degraded License Plate Recognition System for Town Buses on Highway', IEEE doi:978-1-4673-5200-0/13, 2013.

[12] J. Yang, B. Hu, J.H. Yu, J. An and G. Xiong: 'A License Plate Recognition System Based on Machine Vision', IEEE, doi:978-1-4799-0530-0/13, 2013.

[13] P.Vijayalakshmi and M.Sumathi: 'Design of Algorithm for Vehicle Identification by Number Plate Recognition', IEEE, doi: 978-1-4673-5584-1/12, 2012.

[14] T.Wang and J.Fei: 'Adaptive RBFNN fuzzy sliding mode control for active power filter', IEEE International Conference on Mechatronics and Automation, pp: 6 - 11, 2016.

[15] K. Yilmaz, 'A Smart Hybrid License Plate Recognition System Based on Image Processing using Neural Network and Image Correlation', IEEE International Symposium on Innovations in Intelligent Systems and Applications, doi: 10.1109/INISTA.2011.5946087, pp:148-153, 2011.

[16] S. Kumar, S. Agarwal & K. Saurabh: 'License Plate Recognition System for Indian vehicles', International Journal of Information Technology and Knowledge Management, Volume 1, No. 2, pp:311-325, 2008.

[17] D.R. Devi and D.K Ui: 'Automatic License Plate Recognition', IEEE, pp:75-78, 2011.

[18] Y.S. AL-HALABI and H. JONDI: 'New Wavelet-Based Techniques For Edge Detection', Journal of Theoretical and Applied Information Technology, 2015.

[19] Monika and R. Bala: 'Image Edge Detection using Discrete Wavelet Transform', International Journal of Innovative Research in Computer and Communication Engineering, Vol. 4, Special Issue 4, August 2016.

Gain Enhancement of Membrane Antenna Utilizing Dielectric Lens for Millimeter Wave Applications

Muhammad Kamran Saleem and Muhammad Saadi
Electrical Engineering Department, University of Central Punjab, Lahore 54000, Pakistan,

Abstract

The design, configuration and simulation results of a membrane antenna integrated with homogenous hemispherical dielectric (Teflon) lens is presented. The membrane antenna consists of six layers and a homogenous extended hemispherical dielectric lens, which is placed over the top layer of membrane antenna. The longitudinal rectangular slot etched in the SIW ground plane is utilized to excite the microstrip patch antenna (MPA). The membrane antenna gain is enhanced by integration of a homogenous extended hemispherical dielectric lens. The proposed antenna operates in millimeter wave band and having bandwidth of 6 GHz (90 - 96 GHz). Furthermore, the antenna gain is found to be above 15 dB.

Keywords:

Millimeter Wave, Membrane Antenna, Substrate Integrated Waveguide, Homogenous Extended Hemispherical Dielectric Lens, 94 GHz

I. Introduction

The millimeter wave region especially, the W-band window having center frequency of 94 GHz is in focus due to its elite property of high transmission through atmospheric obstructions like clouds, fog, thin dielectrics and smoke [1],in addition to for the development of ultra broadband wireless communications systems and high resolution imaging applications [2]. Furthermore, due to the small wavelength at millimeter wave (mmW) region, fabrication of compressed structures for various modern communication systems such as radio astronomy, remote sensing, compact sensors [3], automotive collision warning radar [4], cloud radar and point to pointmulti GBPS communications is possible. The basic requirements for mmW antennas includes high antenna gains, wide operating bandwidth, high radiation efficiency, compatibility and easy integration with other communications modules. Furthermore, To convert a non-planar structure to its equivalent planar structure [8], the SIW [5-7] is currently the best possible candidate in the structure of family of Substrate Integrated Circuits (SICs).Utilizing SIW benefits of a rectangular waveguide such aselectrical shielding, high Q-factor and high power handling can be attained. In the SIW geometry metallic viasholes are placed in close proximity through which radiation leakage is minimized and metallic rectangular waveguide like propagation properties are achieved [9]. Due to these advantages the SIW in utilized in proposed antenna design to mitigate high metallic losses in mmW operation. The implementation of SIW based structures can be made by employing conventional PCB process [10, 11], multi-layer PCB process [12], photo-imageable thick film technology [13] and LTCC technique.

In this article the design, configuration and simulation results of a membrane antenna integrated with a homogenous extended hemispherical dielectric lensare presented. As found in literature addition of dielectric lens can be utilized to enhance antenna gain [14]. It will be shown that integration of homogenous extended hemispherical dielectric lens with membrane antenna will result in 7 dB increase in overall gain of antenna. The available flexible pyralux TK copper clad laminate and FR-4 dielectric substrates are exploited in proposed antenna. Furthermore, the ANSYS HFSS is utilized for modelling and optimization of proposed antenna.

In section 2 antenna design and configuration is shown. Where as in section 3 the results of membrane antenna with and without the homogenous extended hemispherical dielectric lens are presented. The conclusion is presented in section 4.

II. Antenna Design and Configuration

The proposed membrane antenna (6 layers) integrated with homogenous hemispherical dielectric lens is shown in Fig. 1. The proposed design comprises of two substrates i.e. FR4 substrates having $\varepsilon_r = 4.4$ and pyralux substrate with $\varepsilon_r = 2.5$. The dielectric losses are included in simulation by keeping loss tangent ($\tan\delta$) = 0.002 and 0.02 for the pyralux and FR4 substrates respectively. In Fig. 1(a) the 3D layered model of proposed antenna geometry is shown. The top layer contains a rectangular microstrip patch antenna. The patch is etched below the top pyralux substrate. The FR4 substrate having a rectangular air gap constitutes the second layer of membrane antenna. This FR4 layer is integrated into design to support the patch antenna above the SIW. The SIW geometry is constructed in bottom three layers. To excite the patch antenna on top layer the rectangular slot is etched on the SIW top ground plane. This slot antenna in SIW excites the patch through the air cavity present in FR4 substrate. The main advantage of the SIW utilization

in the design is to reduce inherent high metallic losses present in the millimeter range. The homogenous extended hemispherical dielectric lens is placed over the top layer, through which gain of membrane antenna is enhanced. The proposed membrane antenna structure integrated with homogenous extended hemispherical dielectric lens is shown in Fig. 1(b).The homogenous extended hemispherical dielectric lens consists of Teflonmaterial ($\varepsilon_r = 2.1$). The height of cylinder is H = 3.2 mm whereas the diameter and radius of top sphere is 4.8 mm and 2.4 mm respectively. The copper clad in proposed membrane antenna have thickness of 18 μm, whereas the thickness of dielectric substrates i.e. FR4 and pyralux are taken to be 100 μm and 50 μm respectively. The overall thickness of membrane antenna is 0.218 mm.

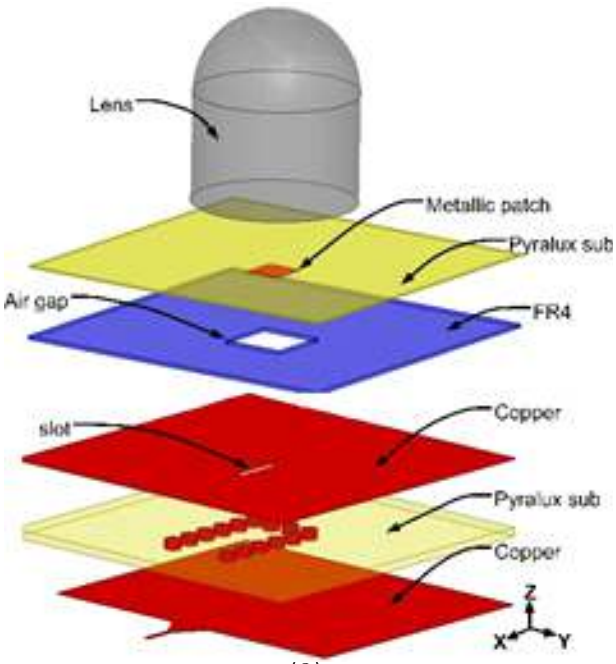

(a)

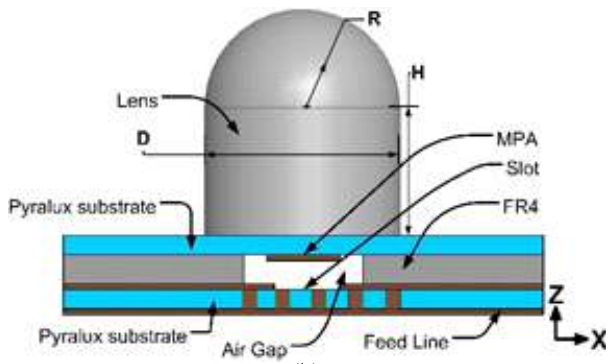

(b)

Fig. 1. Geometry of proposed 6-layered membrane antenna integrated withhomogenous extended hemispherical dielectric lens. (a). 3-D layered model. (b). 2-D side view.

The cut off frequency of SIWis determined by the spacing between two parallel rows of metallic via holes engraved in dielectric medium (substrate). Generally, TM modes are not supported by SIW and dominant mode of SIW is TE_{n0} mode. The broad side dimension of SIW i.e. $a_d$is foundby

$$a_d = \frac{a}{\sqrt{\varepsilon_r}}$$

Where, dielectric constant of substrate is represented by ε_r and dimensions of a i.e. width of SIW is from standard WR-10 waveguide (2.54mm). The following expression is utilized to calculate the distance among the two parallel rows of metallic via holes in SIW geometry i.e. a_s

$$a_s = a_d + \frac{d^2}{0.95p}$$

'd'in above expression is the diameter of metallic via holes joining the lower and upper metallic layers of the substrate (pyralux). The initial dimensions of metallic via diameter is chosen by $d = \lambda_g/5$. Furthermore, the SIW 'pitch' dimension is taken by $p<2d$.

In Fig. 2 the top view of the proposed antenna and placement of rectangular longitudinal slot is emphasized. The recommended distance from the SIW short-circuited end to the center of longitudinal slotd_{off2} is usually multiple of quarter of the guided wavelengths. However, this distance is takento be three quarter of the guided wavelength. The slot offset i.e. d_{off1} is adjusted for coupling of H-field from the longitudinal slot to excite the patch antenna. The initial length for longitudinal slot is calculated from the expression given as below.

$$L_s = \frac{\lambda_o}{\sqrt{2(\varepsilon_r + 1)}}$$

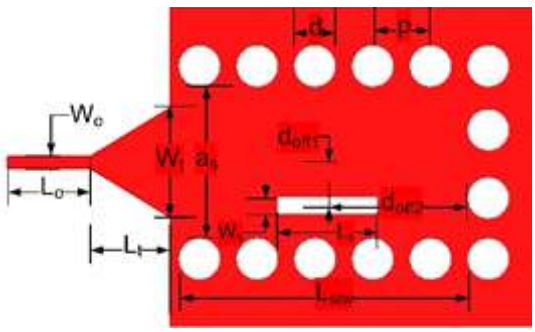

Fig. 2. Microstrip feed SIW slot antenna with rectangular slot and triangular transition.

The FR4 substrate is utilized to support the patch antenna. The air cavity of 1.8 × 1.8 mm in FR4 substrate is utilized to efficiently couple the H-field from the longitudinal slot. The optimum measurements for microstrip patch antenna are found to be 1.115 × 0.985 mm. The homogenous extended hemispherical dielectric lensis placed over the top layer. The center of dielectric lens is aligned with the center of MPA as can be observed in the Fig. 3. The overall antenna size is 10 × 10 × 5.88 mm. The membrane antenna is feed by a50 Ω microstrip line.

To avoid impedance mismatch between the SIW and microstrip feed a tapered microstrip (triangular) transition is utilized. The various important antenna parameters are shown in Fig. 3. Whereas, the optimum dimension after tedious simulations carried out in ANSYS HFSS to achieve required results are as following. $W_t = 1.335, W_o = 0.144, L_o = 1, d = 0.5, L_t = 0.91, a_s = 1.49, p = 0.7, L_s = 1.225, W_s = 0.201, d_{off1} = 0.55, L = 3.5, d_{off2} = 1.4125, L_a = 1.849, W_p = 1.05, W_a = 1.849, L_p = 1.151$, L= 10 and W= 10, (all dimension in "mm").

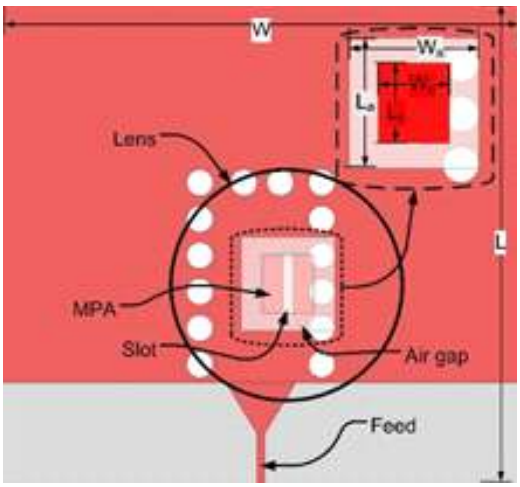

Fig. 3. Membrane antenna integrated with homogenous extended hemispherical dielectric lens (top view).

III. Results and Discussion

The membrane antenna integrated with dielectric lens is simulated and optimized using Ansys High Frequency Structure Simulator (HFSS©).

The reflection coefficient (S_{11}) of two cases i.e. with and without the dielectric lens is shown in Fig. 4. The two resonances are achieved. These are due to existence of patch and slot in antenna geometry. The both resonances are merged together to achieve widerbandwidth. The antenna operating bandwidth is found to be 6 GHz (90-96 GHz). Itcan be easily observed that with integration of homogenous extended hemispherical dielectric lensthe impedance bandwidth is also slightly improved.

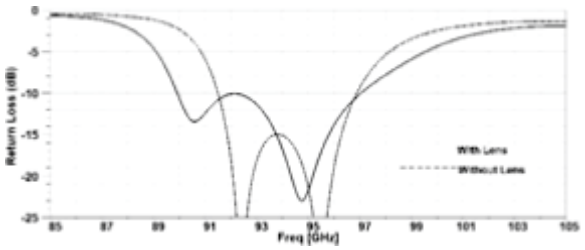

Fig. 4. Simulated return loss of membrane antenna with and without homogenous extended hemispherical dielectric lens.

The 2D radiation pattern in E and H plane is shown in Fig 5a and Fig5b respectively. It can be easily observed that antenna beamwidth is narrowed with integration ofhomogenous extended hemispherical dielectric lens.The gain enhancement of approximately 7 dB by integration of homogenous extended hemispherical dielectric lens can also be observed.The 3D radiation pattern of membrane antenna alone and with integration of homogenous extended hemispherical dielectric lens is shown in Fig 6 for a better understanding of antenna radiation pattern characteristics.

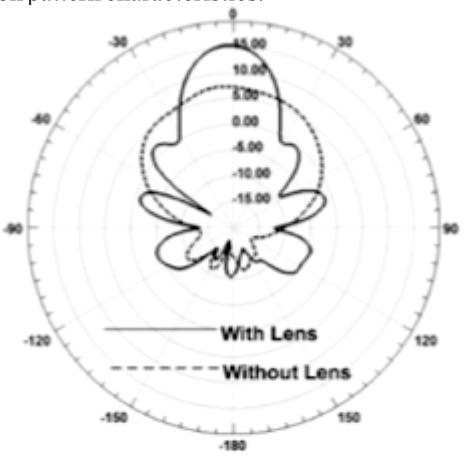

(a)

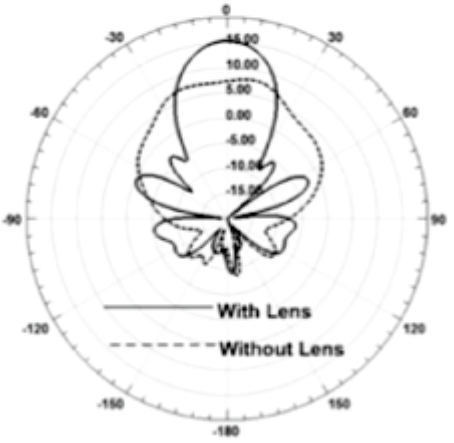

(b)

Fig. 5. Comparison of simulated 2D radiation pattern for membrane antenna alone and membrane antenna integrated withhomogenous extended hemispherical dielectric lens. (a). E-plane. (b) H – plane.

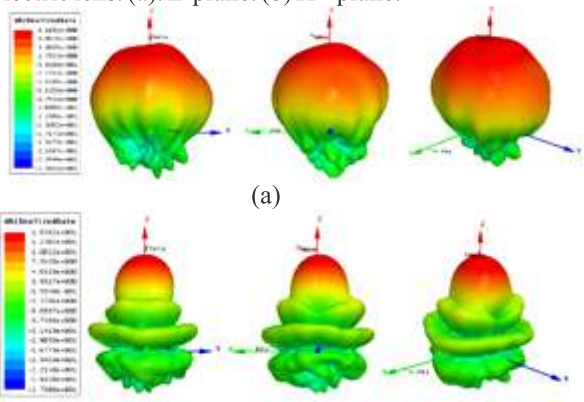

(a)

(b)

Fig. 6. 3D radiation pattern of proposed antenna. (a). Membrane antenna alone. (b). membrane antenna integrated with homogenous extended hemispherical dielectric lens.

The comparison of antenna realized gain for membrane antenna with and without homogenous extended hemispherical dielectric lens is shown in Fig. 7. The gain enhancement of more than 7 dB can be clearly observed. Furthermore, the advantage of utilizing SIW in antenna structure can be seen in Fig. 8, where it is clearly seen that the the E-filed in well confined inside the proximity of SIW.

The performance comparison of membrane antenna alone and membrane antenna integrates with homogenous extended hemispherical dielectric lens is given in table 1 for a better understanding.

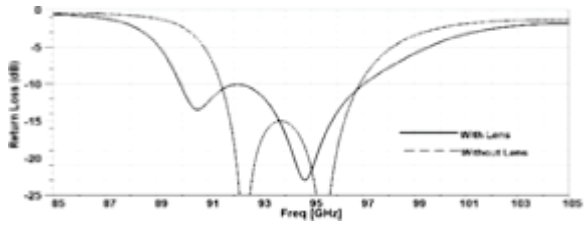

Fig. 7. Comparison of Simulated gain of membrane antenna alone and membrane antenna integrated with homogenous extended hemispherical dielectric lens.

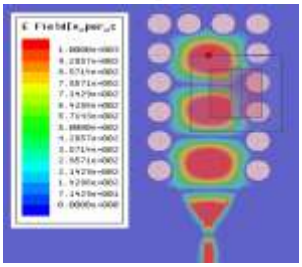

(a)

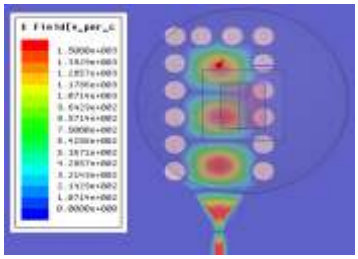

(b)

Fig. 8. Electric field distribution inside SIW (a). Membrane antenna alone. (b). membrane antenna integrated with homogenous extended hemispherical dielectric lens.

	Membrane Antenna alone	Membrane Antenna with lens
Brandwidth	6.5 GHz	7 GHz
Realized Gain	7.9 dBi	15.33 dBi
Beamwidth E-Plane	60°	28°
Beamwidth H-plane	60°	28°

Table. 1: Performance comparison of membrane antenna alone and membrane antenna integrated with homogenous extended hemispherical dielectric lens.

IV. Conclusion

The design and simulation results of a 6 layer membrane antenna integrated with homogenous extended hemispherical dielectric lens is presented. The antenna is operating at center frequency of 94 GHz and a wide impedance bandwidth of approximately 6 GHz is achieved. The gain enhancement of more that 7 dB is achieved by integration of homogenous extended hemispherical dielectric lens. Furthermore, the SIW is effectively incorporated in theproposed antenna geometry for mitigating inherent metallic losses present in the mmW region.

References

[1] E. S. Roseblum, “Atmosphere absorption of 10-400 KMQS radiation: summary and biography up to 1961,” Microwave Journal, vol.4, pp.91-96, March, 1961.

[2] Ke. Wu, Yu Jian Cheng, Tarek Djerafi and Wei, Hong, "Substrate-Integrated Millimeter-Wave and Terahertz Antenna Technology," Invited paper, Proceeding of the IEEE, vol. 100, no. 7, July 2012.

[3] M. Kamran Saleem, M. Abdel-Rahman, A. R. Sebak, Majeed Alkanhal, "A Cylindrical Dielectric Resonator Antenna-Coupled Sensor Configuration for 94 GHz Detection," International Journal of Antennas and Propagation, 2014.

[4] M. Kamran Saleem, Hamsakutty Vettikaladi, Majeed A. S. Alkanhal and Mohamed Himdi, "Integrated Lens Antenna for Wide Angle Beam Scanning at 79 GHz for Automotive Short Range Radar Applications, " IEEE Transactions on Antenna and propagations, vol. 65, issue, 4, pp. 2041 – 2046, 2017.

[5] J. Hirokawa and M. ando, "Single layer feed waveguide consisting of posts for plane TEM wave excitation in paralllel plates," IEEE Trans. Antennas Propag., vol. 46, pp. 625-630, 1998.

[6] D. Deslandes and K. Wu, "Single substrate integration technique of planar circuits and waveguide filters," IEEE Trans. Microw. theory Tech., pp. 595-596, 2003.

[7] D. Deslandes and K. Wu, "Accuarte modeling, wave mechanisms, and design considerations of a substrate integrated waveguide," IEEE Trans. Microw. theory Tech., pp. 2516-2526, 2006.

[8] K. Wu, D. Deslandes, and Y. Cassivi, "The substrate integrated circuits - A new concept for high frequency electronics and optoelectronics," in Proc. 6th Int. conf. telecommun. Modern Satellite Cable Broadcast Service, Oct. 2003, vol. 1, pp. 3-5.

[9] M. Bozzi, A. Georgiadis and K. Wu, "Review of substrate integrated waveguide circuits and antennas," IET Microwave, Antenna and propagation, Vol. 5, pp. 909-920, 2011.

[10] L. Yan, W. Hong, G. Hua, J. Chen, K. Wu and T. J. Cui, "Simulation and experiment on SIW slot array antennas," IEEE Microw. Wirless Compon. Lett., Vol. 14, pp. 446-448, Sep. 2004.

[11] W. Hong, B. Liu, G. Q. Luo, Q. H. Lai, J. F. Xu, Z. C. Hao, F. F. He and X. X. Yin, "Integratged microwave and millimeter wave antennas based on SIW and HMSIW technology," Proc. IEEE int. Workshop Antenna Tech. Small Smart Antennas Metamaters. and Applicat., (iWat), pp. 69-72, March. 2007.

[12] H. Nakano, R. Suga, Y. Hirachi, J. Hirokawa and M. Ando, "60 GHz post wall waveguide aperture antenna with directors made by multilayer PCB process," Proc. EuCAP, Italy, April. 2011.

[13] D. Stephens, P. R. Young and I. D. robertson, "W band substrate integrated waveguide slot antenna," Electron. Lett., vol. 41, no. 4, pp 165-167, Feb. 2005.

[14] M. Kamran Saleem, Majeed A. S. Alkanhal, A. Fattah Sheta, M. Abdel Rahman, M. Himdi "Integrated Lens Antenna Array with Full Azimuth Plane Beam Scanning Capability at 60 GHz," Microwave and Optical Technology Letters,.vol. 59, no. 1, 2017.

Design and Analysis of Slotted Microstrip Patch Antenna using High Frequency Structure Simulator (HFSS)

Hafiz Zaheer Ahmad, Kamran Ezdi[1]
[1]Assistant Professor, Faculty of Engineering, University of Central Punjab, Lahore

Abstract

Microstrip patch antennas are mostly recognized for their flexibility in terms of possible geometries that make them applicable for many different situations. The light weight construction and suitability for integration with microwave integrated circuits are two further advantages. Typically, patch antennas have low directivity. This limits their range of propagation. Therefore, directivity enhancement is an important issue in the design of patch antennas. This paper presents a rectangular microstrip patch antenna operating at 5GHz that has slots cut over the patch to enhance the directivity. The antenna is assumed to be a cavity resonator operating in the Transverse Magnetic (TM33) mode. Moreover, a few slots are cut over the patch and these slots behave like tiny aperture antennas, which increase the directivity. HFSS is utilized for simulation of the antennas. These antennas are directional antennas and their applications can be found in automobiles, aircraft and spacecraft etc.

Index Terms

Microstrip Patch Antenna, Directivity, Antenna Power, Aperture Antenna, Directional Antenna, Transverse Magnetic Mode

1. Introduction

With the widespread proliferation of wireless communication technology in recent years, the demand for compact, low profile, broadband, and higher gain antennas has increased significantly. To meet these requirements, a lot of research over the microstrip patch antenna has been conducted [1][2][3]. However, conventional microstrip patch antenna suffer from very low directivity, typically about 3-6 dBs [4]. This poses a design challenge for the microstrip antenna designers. There are several well-known methods to increase the directivity of the patch antennas, such as the use of thick substrates, cutting a resonant slot inside the patch, the use of low dielectric substrates, multi-resonator stack configurations [5], the use of various impedance matching and feeding techniques, and the use of slot antenna geometry, etc.

In this research paper, we propose a microstrip patch antenna that behaves like a dielectric loaded cavity resonator and operates at 5GHz. Moreover, the antenna has a directivity as high as 10.23dBs and a VSWR less than 2.

I. Methodology

TM33 Mode

Microstrip patch antennas greatly resemble dielectric loaded cavities [6]. Dielectric loaded cavities exhibit different Transverse Electric and Transverse Magnetic Modes. Figure 1 shows the field configuration modes for a rectangular microstrip patch antenna

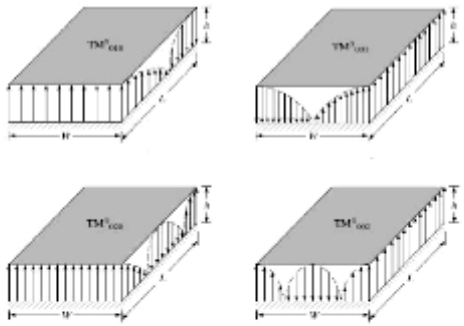

Figure 1: Field configuration modes for rectangular microstrip patch antenna

From the basic knowledge of patch antennas it is known that there are various current maxima at different locations of the patch, and the number of current maxima and their location varies according to the mode of designs.

It can be assumed that if the slots are cut over the exact current maxima points, these slots behave like tiny aperture antennas, and by finding the exact dimensions of the slots, resonance can be achieved. Resultantly, the maximum gain/directivity from a single patch antenna can be attained.

In this paper the TM033 mode based rectangular microsrip patch antenna is proposed. Figure 2 shows that such a design has 9 resonant points over the patch. The exact location and dimensions of the slots will turn these points into tiny aperture antennas and maximum directivity from a single patch can be found.

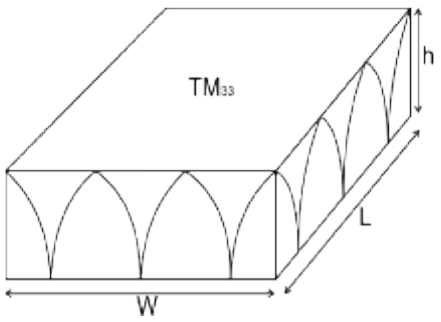

Figure 2: TM033 Configuration

II. Mathematical Analysis

The equation which describes the TM modes of the cavity resonator is given below: [7]

$$(f_r)_{mnp} = \frac{v_o}{2\pi\sqrt{\varepsilon_r}}\sqrt{\left(\frac{m\pi}{h}\right)^2+\left(\frac{n\pi}{L}\right)^2+\left(\frac{p\pi}{W}\right)^2} \quad (1)$$

Since the antenna is to be designed over TM033 configuration, so m=0 and the above equation reduces to

$$(f_r)_{mnp} = \frac{v_o}{2\pi\sqrt{\varepsilon_r}}\sqrt{\left(\frac{n\pi}{L}\right)^2+\left(\frac{p\pi}{W}\right)^2} \quad (2)$$

This shows that the height is zero. However, practically the height of the antenna can never be zero.

Hence,

$(f_r)mnp$ = resonant frequency at which the antenna operates

L= length of the patch

W= Width of the patch

v_o =speed of light in free space

ε_r= relative permittivity of the substrate

III. Un Slotted Antenna Design

Initially, an unslotted antenna is designed to analyze its parameters. The design variables are as under

$(f_r)mnp$ = 5GHz

h = 0.5 mm (height cannot be zero)

W = 90 mm

L = 39.09 mm

ε_r=2.1 (teflon)

X1 = 0.5 mm

X2 = 12.9375 mm

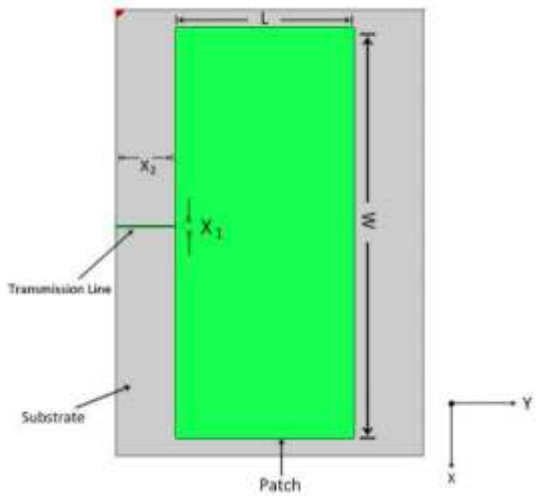

Figure 3: Unslotted Patch Antenna

A. Antenna Parameters

The antenna parameters of the un slotted antenna are as under

TABLE I

Antenna Parameters

Quantity	Value
Max U	0.523909 W/sr
Peak Directivity	**9.763867**
Peak Gain	9.029039
Peak Realized Gain	6.583790
Radiated Power	0.674301 W
Accepted Power	0.729179 W
Incident Power	1.000000 W
Radiation Efficiency	0.924740

B. Current Pattern

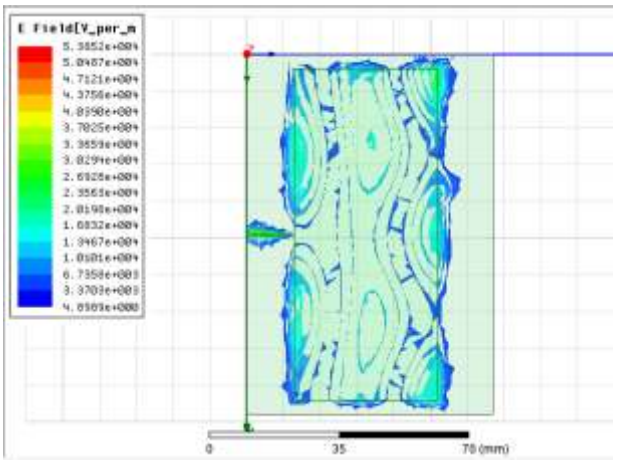

Figure 4: Electric Field Radiation Plot of the Unslotted Patch Antenna

The electrical field radiation plot of the figure above shows that the antenna is behaving like a cavity resonator as 9 maxima points can be seen.

C. VSWR analysis

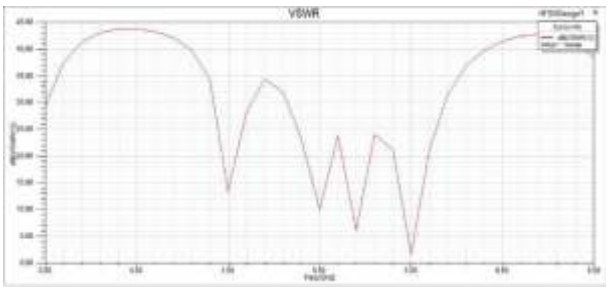

Figure 5: VSWR Plot of Unslotted Patch Antenna

We have assumed the height to be 0 in our calculations. However, in practice, the height can never be 0, so a little mismatch was expected and the antenna resonates at 5.5GHz.

D. S11 Parameters

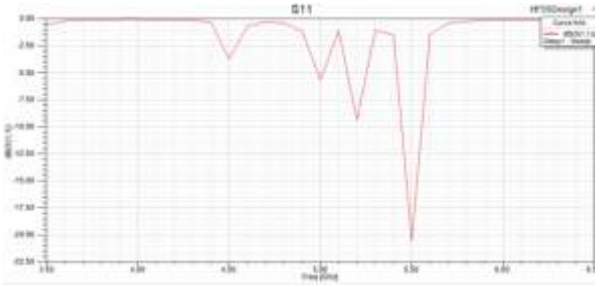

Figure 6: S11 Parameters of Unslotted Patch Antenna

As stated earlier, since the height of the antenna is assumed to be zero, the S11 parameters shift from from 5GHz to 5.5GHz. Moreover, attempting to match the line with the patch results in a degradation of the directivity.

E. 3D Radiation Pattern

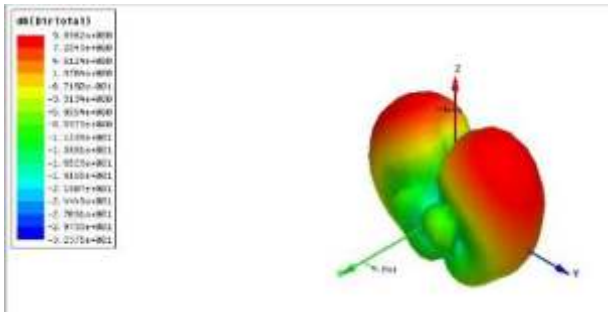

Figure 7: 3D Radiation pattern of Unslotted Patch Antenna

The 3D radiation pattern exhibits two lobes. This indicates that the antenna has a different current maxima scheme over the patch as compared to the conventionally designed antennas. Moreover, there is a slight mismatch between the line and the patch.

F. 2D Radiation Patterns

Moreover, the 2D radiation patterns for phi 0 degree and phi 90 degree for the antenna are as follows

Phi 0 Degree

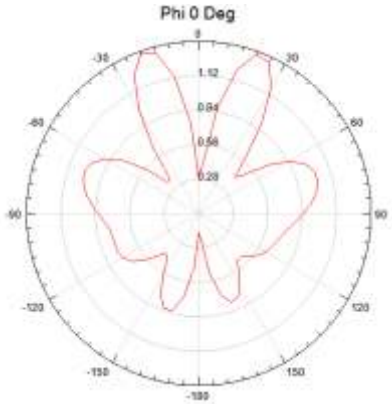

Figure 8: 2D Radiation pattern at phi 0 degree of Unslotted Patch Antenna

Phi 90 Degree

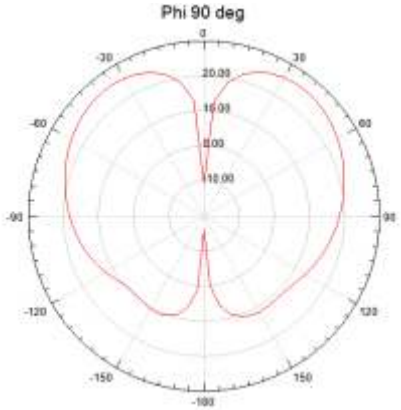

Figure 9: 2D Radiation pattern at phi 90 degree of Unslotted Patch Antenna

IV. Slotted Antenna Design

$(f_r)mnp = 5GHz$

h = 0.5 mm (height cannot be zero)

W = 90 mm

L = 39.09 mm

Ɛr=2.1 (teflon)

X1 = 0.5 mm

X2 = 12.9375 mm

Y1 = 2 mm

Y2 = 4.6 mm

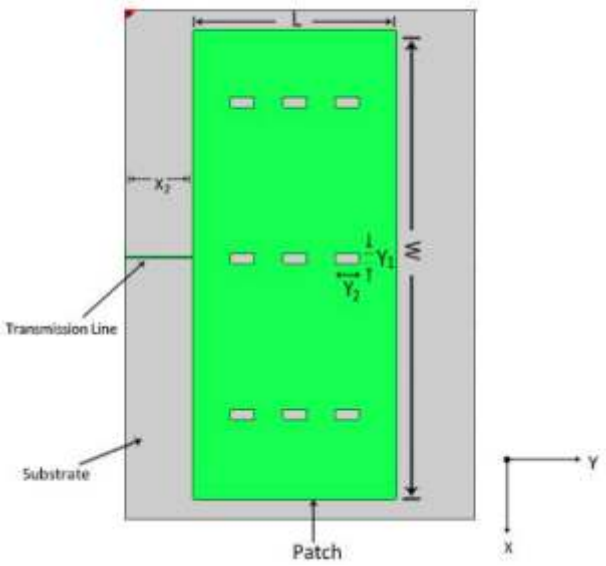

Figure 8: Slotted Patch Antenna

The slots, having dimensions of 2 mm by 4.6 mm, are symmetrically cut over the previously-discussed antenna (utilizing the optimetrics tool of HFSS).

A. Antenna Parameters

Following are the antenna parameters of the slotted antenna

TABLE 2

Antenna Parameters for the Slotted Antenna

Quantity	Value
Max U	0.595875 W/sr
Peak Directivity	**10.222119**
Peak Gain	9.387455
Peak Realized Gain	7.488167
Radiated Power	0.732545 W
Accepted Power	0.797678 W
Incident Power	1.000000 W
Radiation Efficiency	0.918347

The directivity of the antenna increases from 9.763867 dB to 10.222119 dB, which is almost 5% enhancement in the directivity. This validates our design technique of utilizing the TM033 mode based microstrip antenna.

B. Current Pattern

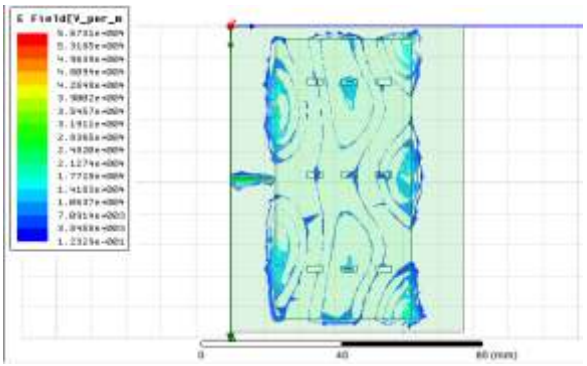

Figure 10: Electric Field Pattern Patch Antenna

The electrical field radiation plot exhibits that the slots behave like aperture antennas. The increase in directivity is a result of this phenomenon.

C. VSWR analysis

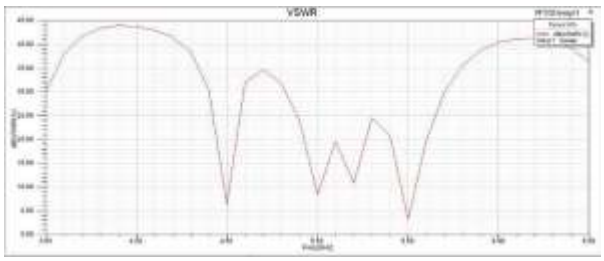

Figure 11: VSWR Plot of the Patch Antenna

Again, due to the zero height assumption, we see a mismatch between the transmission line and the patch. This can be thought of as a design tradeoff between impedance matching and directivity.

D. S11 Parameters

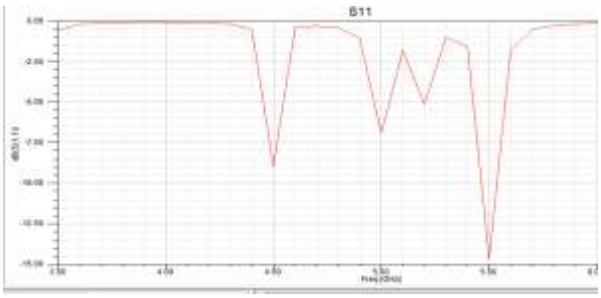

Figure 12: S11 Parameters of the Patch Antenna

The S11 parameters of the slotted antenna show that the antenna is a narrowband antenna (approximately 100 MHZ), and that there is a mismatch between the line and the antenna.

E. 3D Radiation Pattern

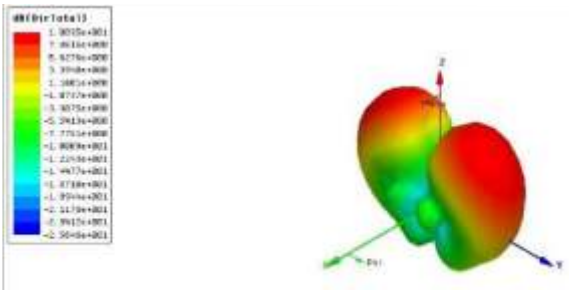

Figure 13: 3D Radiation pattern of slotted Patch Antenna

Once again, the 3D Radiation pattern exhibits two lobes, proving that the antenna has current maxima, as well as a minor mismatch.

F. 2D Radiation Plots

Similarly the 2D radiation plots for Phi at 0 degree and phi at 90 degree showing the same results are as under

Phi 0 Degree

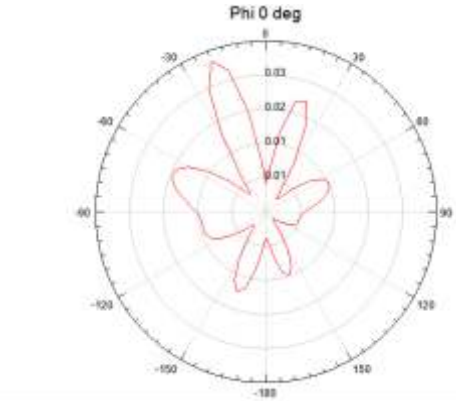

Figure 14: 2D Radiation pattern at phi 0 degree of slotted Patch Antenna

Phi 90 Degree

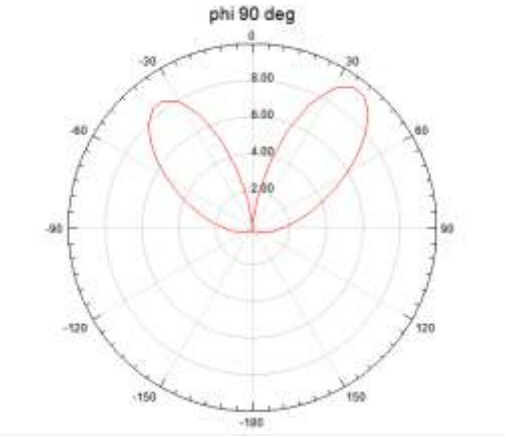

Figure 15: 2D Radiation pattern at phi 90 degree of slotted Patch Antenna

V. Conclusion

It appears from the present work that the microstrip patch antenna has a great deal of similarity with dielectric loaded cavities. Assuming the height of the antenna to be zero, the antenna can be designed at the TM033 mode configuration. In that particular configuration, there are 9 current maxima points over the patch, and cutting the slots turns these points into tiny aperture antennas. This results in increasing the maximum directivity from a single patch antenna. This leads to an important method for designing the highly directive microstrip patch antennas. Moreover, this analysis method depends upon theoretical calculations, which assist in predicting the possibilities for enhancing the directivities from a single patch antenna.

Acknowledgment

The author would like to thank the Dean FOE, University of Central Punjab, as well the all the members of the Post Graduate committee for their support, guidance and help.

References

[1] T. Garg, "Hexagonal Shaped Slotted Microstrip Patch Antenna", *International Journal of engineering science and computing, (IJESC)*, DOI:10.4010/2016.525, 2016

[2] Tarun Kumar Kanade, Alok Kumar Rastogi, Sunil Mishra, "Design, Simulation and Experimental Investigation of Microstrip Patch Antennas and its Feed Line", *International*

Journal of Engineering Research & Technology (IJERT), Vol. 4 Issue 02, February-2015.

[3] Shailendra Kumar Dhakad, Dr. Neeraj Kumar, Keshav Kumar, Joshi G. B., Ashwani Kr. Yadav, "Slotted Microstrip Patch Antenna for Dual Band and UWB Applications", *ICCCT'15,* September 25-27, 2015, Allahabad, India.

[4] Deepender Dabas, Abhishek, "Design of Circular Micro strip Patch Antenna with different Slots for WLAN & Bluetooth Application", *International Journal of Engineering Research & Technology (IJERT),* Vol. 2 Issue 9, September - 2013

[5] Ajay Kumar Sharma, B.V.R Reddy, Ashok Mittal, "Fan Blade Shaped Slotted Patch Antenna for Wideband Circular Polarization", *International Conference on Computer and Computational Sciences (ICCCS),* 2015

[6] Mohammad A.A., Subhi H., Ahmad A. K. and Juma S. M., "Cavity model analysis of rectangular microstrip antenna operating in TM03 mode" *0-7803-9521-2/06/$20.00 $2006 IEEE*

[7] C. A. Balanis, *Antenna Theory*, *3rd edition*, John Wiley, New York, 2005.

List of International Referees

1) **Dr. Tariq Masood**
Associate Editor, IEEE Access
Email:T.Masood.Dr@bath.edu

2) **Dr Dil Akbar Hussain**
Associate Professor
Aalborg University, Esbjerg
Denmark
E-Mail: akh@et.aau.dk

List of Local Referees

1) **Prof Dr Bhawani Shankar Chowdhry**
Distinguished National Professor
Dean FEECE, MUET
Email:Id dean.feece@admin.muet.edu.pk

2) **Dr.Badar Munir**
Assistant Professor
Telecommunication Engineering
MUET,Jamshoro,Pakistan
badar.muneer@faculty.muet.edu.pk

3) **Engr.Prof Dr.Hyder Abbas Mussavi**
Dean FEST, Indus University, Karachi
E-Mail:dean@indus.edu.pk

4) **Prof Dr. Muktiar Maher**
Electrical Engineering Dept MUET
EMail: mukhtiar.mahar@faculty.muet.edu.pk

5) **Engr.Prof Dr. Irfan Ahmad Halepota**
Associate Professor
Dept. of Electronics Engineering
MUET Jamshoro, Sindh
E-Mail: irfan.halepota@faculty.muet.edu.pk

6) **Dr. Faisal Khan**
Dean
Engineering computer Science
BUITEMS
E-Mail: faisal.khan@buitms.edu.pk

7) **Dr. Sammer Zai**
Asstt Professor Computer Systems Engineering
MUET
Email Id: sammer.zia@faculty.muet.edu.pk

8) **Dr. Imtiaz Kalwar**
Associate Professor
DHA SUFA University, Karachi.
E-Mail: imtiaz.kalwar@gmail.com

Notes

Notes

Time-Line for Papers Processing for IEEEP Quarterly Journal "New Horizons"

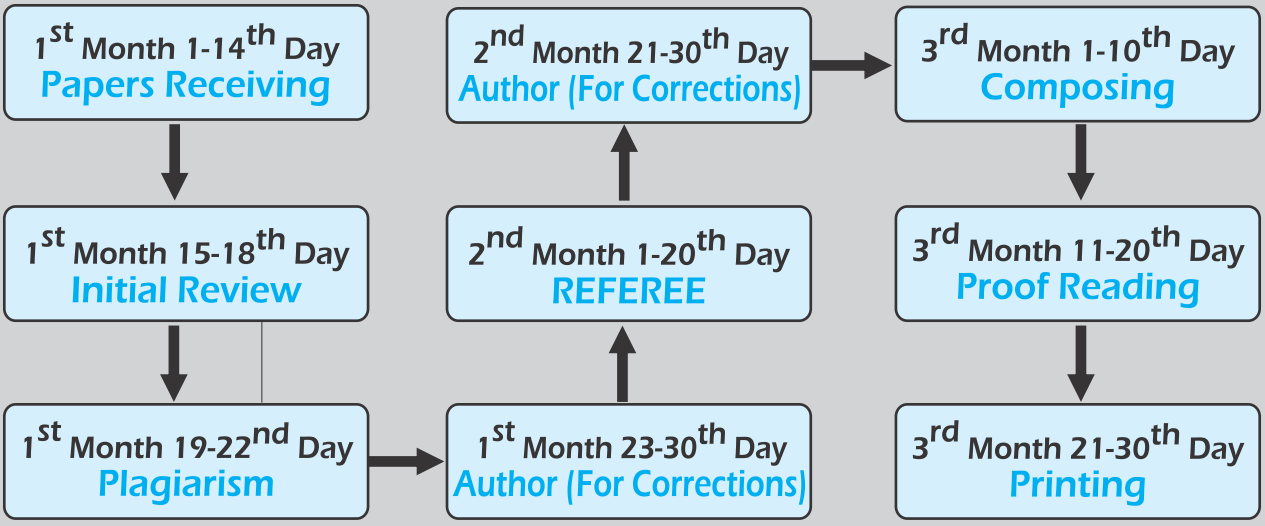

CALL FOR RESEARCH PAPERS FOR "NEW HORIZON"

Research Papers from engineers in the disciplines of Electrical, Electronics (Including Information Technology and Telecommunications), Controls, Mechatronics, Avionics, Computers and Medical Engineering are invited for publication in "New Horizons", HEC recognized Y-Category, quarterly research journal of the Institution of Electrical & Electronics Engineers Pakistan. A soft copy of the paper may please be sent to ieeep1969@gmail.com or info@ieeep.org.pk in the following format:-

1. The research paper should be prepared in MS Word Software in Two-Column Format.
2. Select A-4 size, 1 inch margins on all four sides, 1.0 line spacing, Times New Roman Font with size 12 and justification on both sides.
3. All headings should be in capital bold letters.
4. All figures and diagrams must be properly numbered and labeled.
5. All diagrams, tables, graphs and photograph must be black outlined with white back ground.
6. All text within diagrams must be bold enough for readable clarity.
7. The papers must not contain more than 6 pages.
8. Complete references must be provided at the end of the paper.
9. Reference should be as per international standard. Format for one of the references is given below as a sample.

   N.E. Nilsson and J. Mercurio "Synchronous generator capability curve testing and evaluation" IEEE. Trans. Power. Del., Vol: 9, no:1 , pp 414. 424, Jan 1994.

PLEASE NOTE: You are requested to provide a brief Resume of yourself and of the co-authors (if any) alongwith the paper(s). Also please provide contact numbers and email addresses of all authors. Kindly note that papers/material as PDF Files will not be accepted.

LATEST INVENTIONS IN ENGINEERING WORLD

Countless inventors have created amazing technologies that have completely changed the way we live. Today there are thousands of individuals and companies across the globe who are working hard to develop alternative energy solution. IEEEP, in its newsletter, tries its best to keep you up to date with the recent most inventions.

A paper battery powered by bacteria
made of paper and fueled by bacteria -- Commercial batteries are too wasteful and expensive, and they can't be integrated into paper substrates best solution is a paper-based bio-battery has a shelf-life of about four months inexpensive, disposable, flexible and has a high surface area.

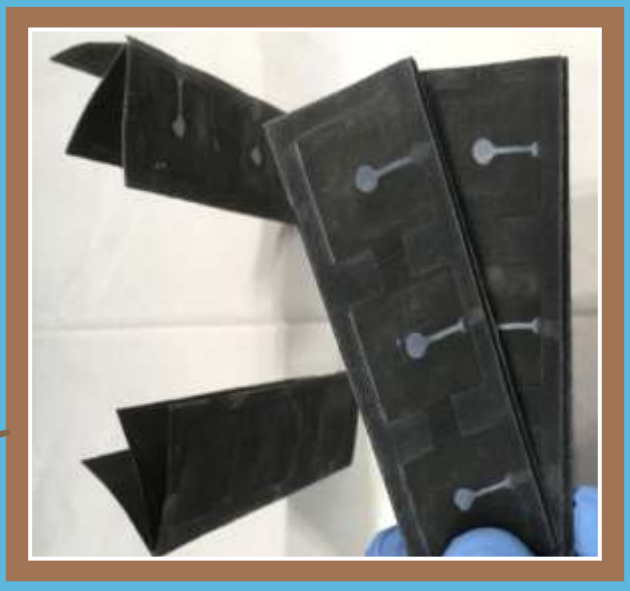

Popcorn-Powered Robots
Popcorn's unique qualities can power inexpensive robotic devices that grip, expand or change rigidity

Since kernels can expand rapidly, exerting force and motion when heated, they could potentially power miniature jumping robots

Just need to apply voltage to get the kernels to pop, so it would take all the bulky and expensive parts out of the robots

The Institution of Electrical and Electronics Engineers Pakistan Ph: +92 (42) 36305289 Fax: (042) 36360287
4 Lawrence Road, Lahore-54000, Pakistan. Email:ieeep1969@gmail.com Website: www.ieeep.org.pk